Redox Reactions of NOx (x = 1, 2) with First Row Transition Metal Complexes

A dissertation submitted to the
Indian Institute of Technology Guwahati as
Partial fulfillment for the degree of
Doctor of Philosophy in Chemistry

Submitted by

Kuldeep Gogoi

(Roll No. 126122009)

Supervisor

Prof. Biplab Mondal

Department of Chemistry

Indian Institute of Technology Guwahati

December, 2017

Dedicated to My Parents
&
Teachers

STATEMENT

I hereby declare that this thesis entitled "**Redox Reactions of NOx (x = 1, 2) with First Row Transition Metal Complexes**" is the outcome of research work carried out by me under the supervision of Prof. Biplab Mondal in the Department of Chemistry, Indian Institute of Technology Guwahati, India.

In keeping with the general practice of reporting scientific observations, due acknowledgements have been made wherever the work described is based on the findings of other investigators.

December, 2017

Kuldeep Gogoi

Indian Institute of Technology Guwahati

भारतीय प्रौद्योगिकी संस्थान गुवाहाटी
INDIAN INSTITUTE OF TECHNOLOGY GUWAHATI
North Guwahati, Assam – 781039, India

Prof. Biplab Mondal
Department of Chemistry

Phone : + 91-361-258-2317
Fax: + 91-361-258-2349
E-mail: biplab@iitg.ernet.in

Certificate

This is to certify that **Mr. Kuldeep Gogoi** has been working under my supervision since July, 2012 as a regular Ph.D. student in the Department of Chemistry, Indian Institute of Technology Guwahati. I am forwarding his thesis entitled "**Redox Reactions of NOx (x = 1, 2) with First Row Transition Metal Complexes**" being submitted for the Ph. D. degree.

I certify that he has fulfilled all the requirements according to the rules of this Institute regarding the investigations embodied in his thesis and this work has not been submitted elsewhere for a degree.

December, 2017 **Biplab Mondal**

Acknowledgements

First and foremost I would like to express my sincere gratitude to my supervisor Prof. Biplab Mondal. I appreciate all his invaluable time, guidance and encouragement to make my Ph.D experience productive and exciting. The joy and enthusiasm he has for his research was quite motivational for me, even during tough times in the pursuit. His attitude of living every moment as it comes, making serendipitous observation and converting them to new possibilities, correlating ideas and understanding the obvious has helped me come a long way and will always guide me in future.

My doctoral committee has guided me through all these years giving their valuable inputs during the evaluation process. I would like to thank chairman of the committee Prof. B. K. Patel and members Dr. Debasis Manna and Dr. A. S. Achalkumar for their valuable suggestions and advices. Also I would like to thank all the faculty and staff members of the Department of Chemistry for their consistent help and support. I acknowledge Central Instruments Facility (CIF) and Department of Chemistry for providing instrument facilities. Due acknowledge to IIT Guwahati for financial support and all the facilities.

I would like to acknowledge all the teachers I learnt from since my childhood, I would not have been here without their guidance, blessing and support.

I am indebted to my lab seniors who have taught me the lab culture and have lived by example to make me understand the hard facts of life. I am very thankful to Hemanta Da, Somnath Da, Apurba da, Pankaj Da, Aswini Da, Kanhu da, Viksah Da for their help, support and motivation. My heartfelt thanks to Soumen, together with whom I started and finishing my Ph.D. journey and to my juniors Baishakhi, Dibyajyoti Da, Rakesh for always being there and bearing with me the good and bad times. I had the pleasure of working with several project students during the course of my work, thank to them as well. The memory of the moments we spent together will always remind me how wonderful the life with you was.

I would also like to thank all my friends at IITG, Hiranya, Jugal, Nilutpol, Dipjyoti, Sourav, Silaj, Manas, Soham, Kesab, Halder, Rajendra, Wajid, Uday, Arvin…… my seniors and juniors from Department of Chemistry, for all the love and support that they have

showered upon me. I would like to acknowledge my other friends for their moral support and motivation, which drives me to give my best. Devajit, Mrinmoy, Polash, Dipom, Partha, Mukunda, Mridu, Satya, Jitu, Pallav, Pobitro, Suraj, Rituporna, Ritu, Santanu, Lakhi, Chetry, David, Joy, Debajit, Kiran Da, Ananta, Ajit, Simanta…..the list is endless…..thanks to one and all.

The journey would not been initiated without some wonderful persons that come across my life. I am very grateful to the family members of Mrinmoy, for their affection and constant belief on me. My heartiest thanks to Gayatri, it was her companion and encouragement which help me to deal with the challenges that came across the journey and to proceed with more enthusiasm.

I owe it all to the Almighty God for granting me the wisdom, health and strength to undertake this research task and enabling me to its completion.

Finally, I would like to acknowledge the people with whom the source of my life energy resides: my parents and brothers. I have an amazing family, unique in many ways and it is their unconditional support and sacrifices which made it possible for me to be at IITG pursuing my Ph.D. I am always grateful to the family members of my parent's relatives for all the love and blessings. The kind of support and encouragement from my mamas' and mahi's are some of the most beautiful things in my life. I wished all of them to be with us to celebrate the success of this journey together, but still I am sure wherever they are, they will feel proud of this moment and shower me with blessings. I am also thankful to all my well-wishers whose blessings and encouragements to pursue higher studies are always there to guide me through the right path. I would like to thank all others who are associated with my work directly or indirectly at IIT Guwahati for their help.

Kuldeep Gogoi

Indian Institute of Technology Guwahati

Contents

Synopsis

The thesis entitled, "**Redox Reactions of NOx (x = 1, 2) with First Row Transition Metal Complexes**" is divided into five chapters.

Chapter 1: Introduction

Nitric oxide (NO) has attracted enormous interest from chemists and biochemists since it has been discovered as a signaling agent in humans.[1] It is also known that NO plays diverse roles in biological processes such as vasodilatation, muscle contraction, etc. when produced in low concentration.[2,3] However, in micromolar concentration, it stimulates the reactive nitrogen species (RNS) and causes carcinogenesis and neurodegenerative disorders.[1-4] Most of these roles played by NO in biology are attributed to the formation of nitrosyl complexes of the metallo-proteins, mainly iron or copper.[5] In literature, the number of examples of metal nitrosyls including iron and copper are large owing to their biological relevance. Understanding of the versatile reactivity or decomposition pathways of these nitrosyl complexes has attracted enormous scientific research and the quest is still going on. On the other hand, NO reactivity of other first row transition metal ions have not been studied to that extent.[6-8]

NO reacts rapidly with different reactive oxygen species (ROS) to result in the generation of powerful secondary nitrating and/or oxidizing agents, like nitrogen dioxide (NO_2) and peroxynitrite.[9] NO_2 is believed to be the key intermediate for protein tyrosine nitration.[10] Hence, the reactivity of NO_2 with metal ions will be of interest with a goal of elucidating the redox transformations between various NOx complexes. In this context, reactions of NO_2 with iron porphyrin models were described by Kurtikyan *et al.*[11] Reactions of nitrosyls of cobalt with various ROS have demonstrated by Nam and co-workers with N-tetramethylatedcyclam derived ligands.[12]

Metal-nitrite species are known to involve in the oxo-transfer reactions from coordinated nitro-groups in transition metal complexes to appropriate oxygen acceptors, which can serve as important routes for oxidation of various substrates.[13-15] Thus, interaction of NOx with transition metal complexes and their redox behavior is always an interesting field of research from coordination as well as bioinorganic chemistry perspective.

This thesis is originated from our interest to study the redox reaction of NOx assisted by Fe, Cu and Co complexes. In this context, oxo transfer reactivity of copper(II)-nitrito and cobalt(III)-nitro complexes are discussed in the second and third chapters, respectively. Chapter four describes the dioxygenation of a $\{CoNO\}^8$ species and its mechanism whereas the final chapter discusses the unusual decomposition of a $\{FeNO\}^7$ species to a $\{Fe(NO)_2\}^9$ DNIC and a ferric complex.

Chapter 2: Nitrogen Dioxide Reactivity of a Copper(II) Complex

Mononuclear complex **2.1**, $[Cu^{II}(L1H)(O_2CCH_3)_2]$ of ligand **L1H** [L1H=4,6-di-*tert*-butyl-2-((2-picolyl(isopropyl)amino)methyl)phenol] was prepared by stirring a mixture of copper(II) acetate monohydrate with equivalent quantity of **L1H** in acetonitrile. X-ray single crystal structure of **2.1** reveals a distorted square pyramidal geometry around Cu(II) center in the mononuclear unit. Two acetate anions are coordinated to the metal center and balance the charge of the metal ion (Figure S1).

Addition of equivalent amount of NO_2 to the dry and degassed methanol solution of **2.1** resulted in the change of color from brown to light yellow. In the UV-visible spectral monitoring, the absorption bands at 470 nm (ε/M^{-1} cm^{-1}, 600) and 676 nm (ε/M^{-1} cm^{-1}, 400) disappeared (Figure S2a). EPR study revealed that the solution became EPR silent after addition of NO_2. These are attributed to the reduction of Cu(II) by NO_2 to Cu(I) (Scheme S1).

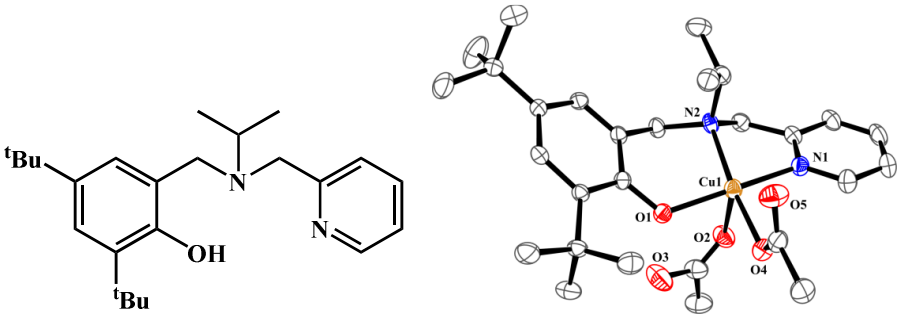

(a) **(b)**

Figure S1. (a) Ligand **L1H** and (b) ORTEP diagram of complex **2.1** (35% thermal ellipsoid plot; H atoms are not shown for clarity).

Addition of equivalent amount of NO_2 to the dry and degassed methanol solution of **2.1** resulted in the change of color from brown to light yellow. In the UV-visible spectral monitoring, the absorption bands at 470 nm (ε/M^{-1} cm^{-1}, 600) and 676 nm (ε/M^{-1} cm^{-1}, 400) disappeared (Figure S2a). EPR study revealed that the solution became EPR silent after addition of NO_2. These are attributed to the reduction of Cu(II) by NO_2 to Cu(I) (Scheme S1).

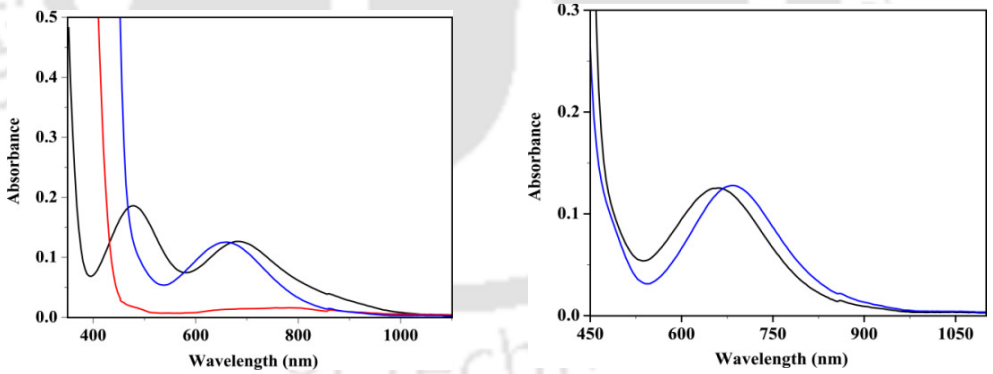

(a) **(b)**

Figure S2. (a) UV-visible spectra of complex **2.1** before (black), after purging 1 equivalent (red) and 2 equivalents (blue) of NO_2 in methanol. (b) UV-visible spectra of **2.2** before (black) and after purging NO_2 (blue) in methanol.

In ^{1}H-NMR spectroscopy, the broad signals of paramagnetic complex **2.1** became well-resolved after addition of equivalent amount of NO_2 suggesting the formation of

diamagnetic species (Figure S3). The reaction also resulted in simultaneous release of the tertiary butyl cation confirmed by GC-mass analysis.

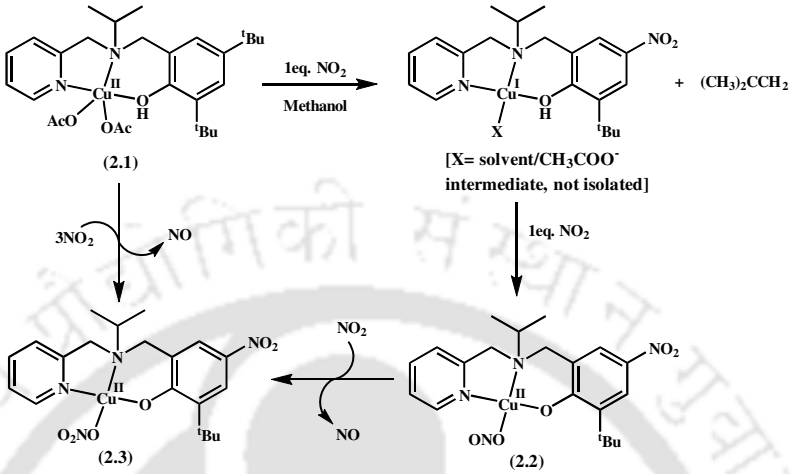

Scheme S1. Reaction of complex **2.1** with NO_2.

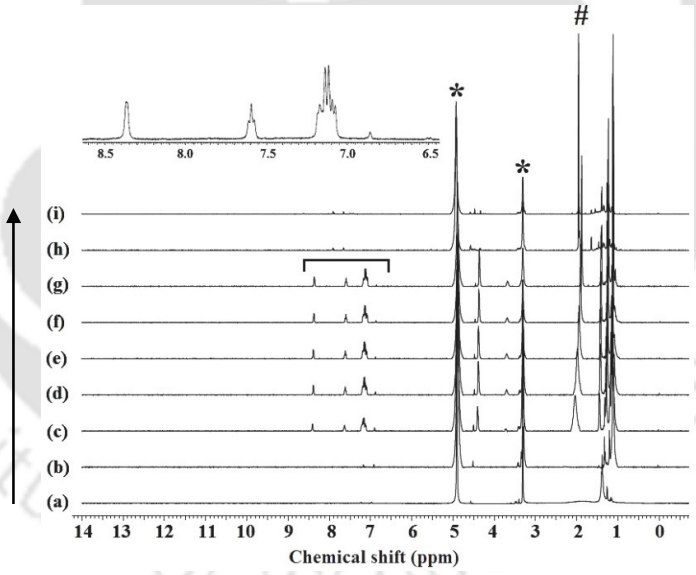

Figure S3. ^{1}H-NMR spectra of complex **2.1** before and after purging NO_2 in CD_3OD. (a) **2.1**. (b–i) Complex **2.1** after the addition of 0.1, 0.2, 0.3, 0.5, 0.75, 1.0, 2.0 equiv and excess NO_2, respectively. (inset) The aromatic region of (g) is expanded. The * marked signals are for solvent and # marked signal indicates the formation of $(CH_3)_3COD$.

To the reaction mixture, addition of one more equivalent of NO_2 resulted in the appearance of a new *d–d* band at 660 nm (ε/M^{-1} cm^{-1}, 340) along with a charge transfer band at 386

nm (ε/M^{-1} cm^{-1}, 17890) (Figure S2a). The appearance of the *d–d* band is presumably because of the formation of the corresponding intermediate [Cu^{I}-NO_2] complex, which can be considered as [Cu^{II}-NO_2^-]. In EPR study, the signals characteristic of Cu(II) appeared. In ^{1}H-NMR, the signals became broadened. The isolation of the intermediate and structural characterization, indeed, revealed the formulation as [Cu^{II}–NO_2^-]. The ORTEP diagram of **2.2** is shown in figure S4a. In FT-IR spectrum, it shows a new band at 1275 cm^{-1} which is assigned to the symmetric N–O stretching of NO_2^-.

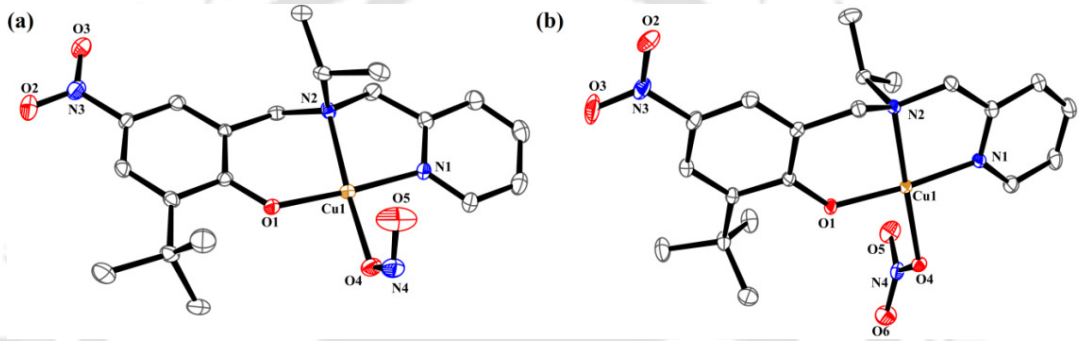

Figure S4. ORTEP diagrams of complexes (a) **2.2** and (b) **2.3** (35% thermal ellipsoid plot; H atoms are not shown for clarity).

Further addition of NO_2 in the methanol solution of **2.2** leads to the shift of λ_{max} from 660 to 685 nm in UV-visible spectroscopy (Figure S2b). In FT-IR studies, the NO_2^- stretching at 1275 cm^{-1} disappeared with the appearance of a new intense stretching frequency at 1384 cm^{-1}. Isolation and structural characterization of the product revealed the formation of corresponding Cu(II) nitrate complex, **2.3**. The ORTEP diagram of **2.3** is shown in figure S4b. In **2.3**, the NO_3^- ion is O-coordinated in monodentate fashion. Thus, the reaction of **2.2** with NO_2 in methanol resulted in the oxo transfer leading to the formation of corresponding NO_3^- complex, **2.3**, and formation of NO is expected as side product. The release of NO was confirmed by spin trapping using iron(II)diethyldithiocarbamato complex.

The FT-IR spectral studies with ^{18}O labeled NO_2 confirmed that O-atom transfer takes place from free NO_2 to the N-atom of Cu(II)–O–NO moiety.

Chapter 3: Oxo Transfer Reaction in Cobalt(III)-nitro Complexes

This chapter describes the oxo transfer reactivity of cobalt(III)-nitro complexes with tetradentate (**L2H$_2$**, **L3H$_2$**) and pentadentate (**L4H$_2$**) ligands. All the complexes were synthesized, characterized by spectral analyses and by their single crystal structure determination except for **3.2** (Figure S5).

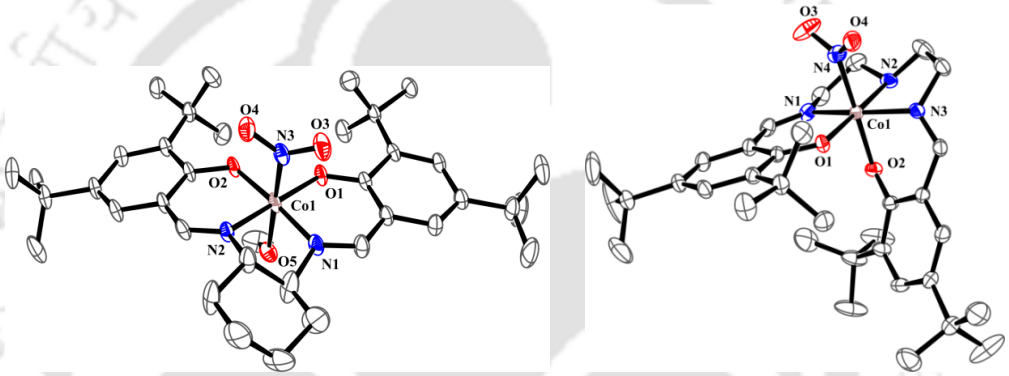

(a) **(b)**

Figure S5. ORTEP diagrams of complexes (a) **3.1** and (b) **3.3** (35% ellipsoid probability; H atoms and solvent molecules are not shown for clarity).

In the UV-visible spectroscopy, complexes **3.1** and **3.2** in methanol solution show *d-d* transitions at 690 nm (ε/M^{-1} cm^{-1}, 237) and 650 nm (ε/M^{-1} cm^{-1}, 300), respectively. Complex **3.3**, in methanol solution absorbs at 510 nm (ε/M^{-1} cm^{-1},110). All the three complexes are EPR inactive in X-band EPR spectroscopy confirming the presence of Co(III) centre.

Addition of dimethyl sulfide (DMS) solution to dry and degassed methanol solution of **3.1** and **3.2** at room temperature resulted in the formation of **3.4** and **3.5**, respectively. The color of the solutions changed to reddish brown from light red in course of the reaction.

In UV-visible spectroscopy, the absorption bands at 690 nm and 650 nm for **3.1** and **3.2**, respectively, diminished upon addition of DMS.

In the FT-IR spectroscopy, N-O stretching of coordinated NO_2^- groups at 1358 and 1361 cm^{-1} for **3.1** and **3.2**, respectively, were found to diminish after addition of DMS and new stretching frequencies at 1650 and 1659 cm^{-1} appear, respectively (Figure S6). These frequencies are assignable to the coordinated NO group.

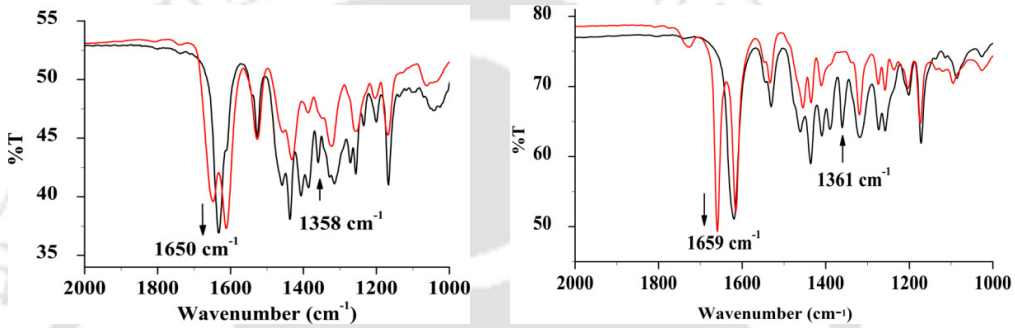

Figure S6. FT-IR spectra of complexes (a) **3.1** (black) and after addition of DMS (red), (b) **3.2** (black) and after addition of DMS (red).

Both the complexes **3.4** and **3.5** were characterized structurally. Single crystal structures of both **3.4** and **3.5** (Figure S7) reveal that the cobalt is coordinated by four N-atoms from the ligand and one axial NO group in a distorted square pyramidal geometry.

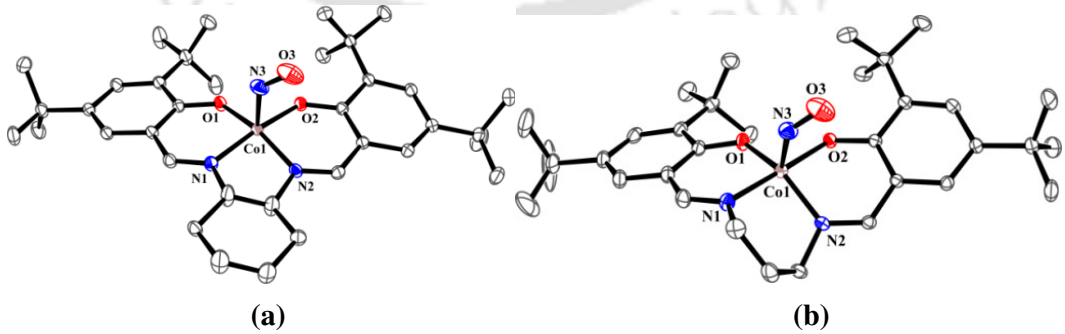

Figure S7. ORTEP diagrams of complexes (a) **3.4** and (b) **3.5** (35% ellipsoid probability; H atoms and solvent molecules are not shown for clarity).

The conversion of nitro group of **3.1** and **3.2** to corresponding nitrosyl moieties presumably proceeds *via* an oxo transfer mechanism. The reaction was initiated by the addition of DMS and thus it expected to result in the formation of dimethyl sulfoxide (DMSO). GC-mass analysis of the headspace gas of the reaction mixtures shows the presence of unreacted DMS, while analysis of the solution part suggests the presence of DMSO. However, complex **3.3** was found to be inert towards oxo transfer reactivity in similar reaction condition. No change was observed in spectroscopic studies after addition of DMS.

Chapter 4: Dioxygenation Reaction of a Cobalt-nitrosyl: Putative Formation of a Cobalt-peroxynitrite *via* a {Co(NO)(O_2^-)} Intermediate

The bubbling of NO gas to the degassed methanol solution of the ligand **L5H** followed by the addition of an equivalent amount of cobalt acetate tetrahydrate resulted in the precipitation of the Co(II)-nitrosyl complex, [(L5)Co(NO)(OAc)] (**4.1**). Single crystal X-ray structure determination revealed that the cobalt center is coordinated by the three N-atoms from the ligand, one acetate and one NO group in a distorted square pyramidal geometry (Figure S8a).

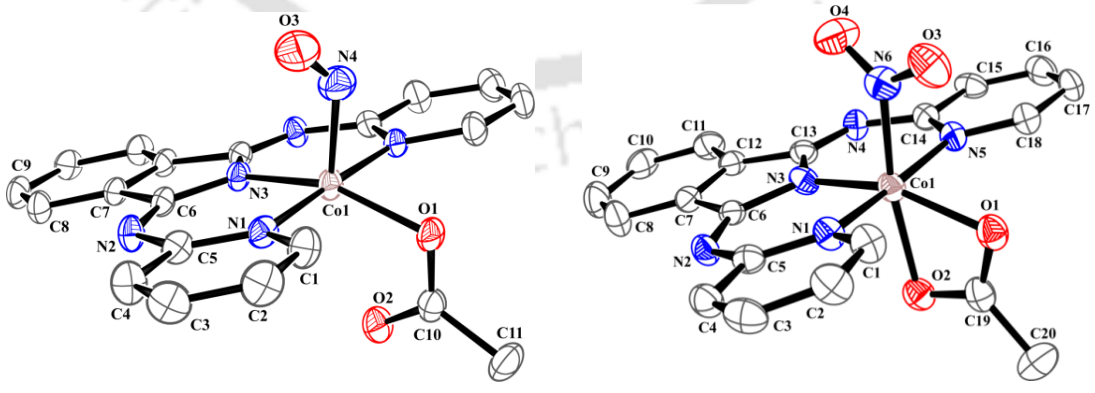

(a) **(b)**

Figure S8. ORTEP diagrams of complexes (a) **4.1** and (b) **4.2** (35% ellipsoid probability; H atoms and solvent molecules are not shown for clarity).

In the UV-visible spectroscopy, dichloromethane solution of **4.1** absorbs at 467 nm (ε/M^{-1} cm^{-1}, 6230) and 348 nm (ε/M^{-1} cm^{-1}, 12400). The addition of O_2 gas to the degassed dichloromethane solution of **4.1** resulted in the appearance of bands at 477 nm and 450 nm, respectively (Figure S9a).

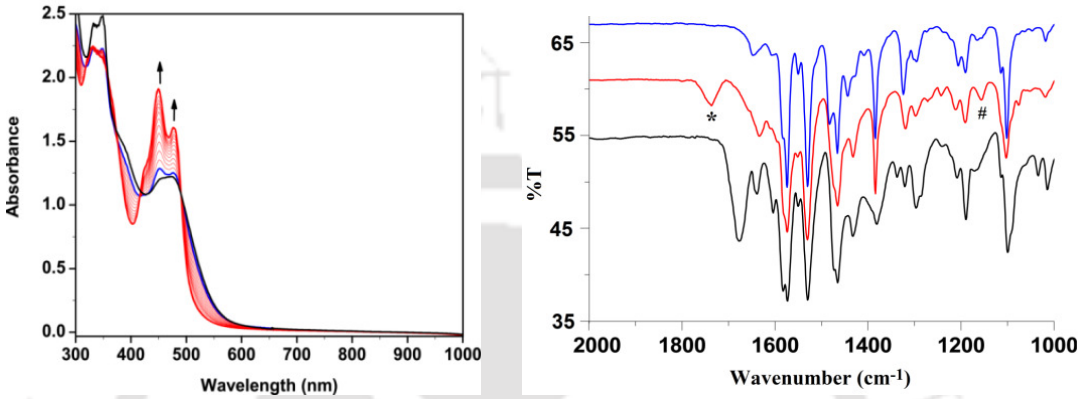

(a) **(b)**

Figure S9. (a) UV-visible spectra of complex **4.1** (black) and after addition of O_2 (blue; immediately after addition and red traces) in CH_2Cl_2 at -20 °C. (b) FT-IR spectra of complex **4.1** (black); immediately after addition of O_2 (red) and after 1 h of addition of O_2 (blue) in CH_2Cl_2.

The compound corresponding to this final spectrum was isolated as solid and characterized as **4.2** [(L5)Co(NO_2)(OAc)]. The complex **4.2** was further confirmed by structural characterization (Figure S8b). The kinetic studies revealed that the reaction rate of **4.1** with O_2 depends on the concentration of the added O_2 suggesting the involvement of an associative mechanism.

In FT-IR spectrum, the addition of O_2 gas to the degassed dichloromethane solution of **4.1** resulted in the disappearance of the NO stretching frequency at 1675 cm^{-1}, while new band appeared at 1740 cm^{-1}. This band was assigned to the NO stretching of the resulting intermediate, **4.1a** (Figure S9b and Scheme S2). On the other hand, in addition to the 1740 cm^{-1} band, a new stretching frequency at 1155 cm^{-1} was observed in the FT-IR spectrum (Figure S9b). This frequency was sensitive to the

$^{18}O_2$ and found to shift to 1116 cm^{-1}. The observed stretching frequency at 1155 cm^{-1} is suggestive to the formation of a metal-bound superoxide (O_2^-).

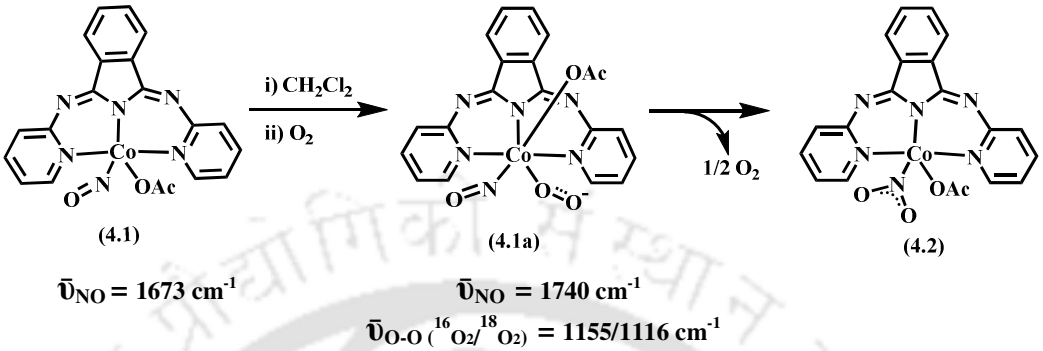

Scheme S2. Reaction of complex **4.1** with O_2 in CH_2Cl_2.

Hence, the formulation of the intermediate **4.1a** as $[(L5)Co^{III}(NO)(O_2^-)]^+$ is logical (Scheme S2). Both the 1740 and 1155 cm^{-1} bands disappeared with time and the appearance of two stretching frequencies at 1322 and 1297 cm^{-1} assignable to the N-bound NO_2^- group in **4.2** (Scheme S2) were observed. The labelling experiment with $^{18}O_2$ resulted in the shift of these characteristic frequencies to 1290 and 1271 cm^{-1}, respectively suggesting the incorporation of ^{18}O-atom into the **4.2**.

The decomposition of the intermediate **4.1a** to **4.2** presumably proceeds *via* the formation of an $ONOO^-$ intermediate, though no indication was observed in UV-visible studies. We sought chemical evidence for the formation of $ONOO^-$ intermediate. When the oxygenation reaction of **4.1** was carried out in presence of 2,4-di-*tert*-butylphenol, the formation of corresponding nitro-phenol with an appreciable yield was observed. Though, it is expected that the $ONOO^-$ intermediate will afford quantitative conversion of the phenol to nitrophenol, the parallel decomposition of the intermediate to **4.2** resulted in the formation of nitrophenol with a less yield.

Chapter 5: Disproportionation of a $\{FeNO\}^7$ Species into $\{Fe(NO)_2\}^9$ and Ferric Complex

A dinitrosyl iron(I) complex, **5.1**, [Fe(L5)$(NO)_2$], of the tridentate N-donor ligand, **L5H** has been synthesized from the ferrous precursor. The complex **5.1** was characterized by single crystal X-ray structure determination. Single crystal structure of **5.1** revealed the presence of Fe(I)-dinitrosyl, $\{Fe(NO)_2\}^9$ moiety where Fe(I) is coordinated by three N-atoms from the ligand and two NO groups in a trigonal bipyramidal geometry (Figure S10a).

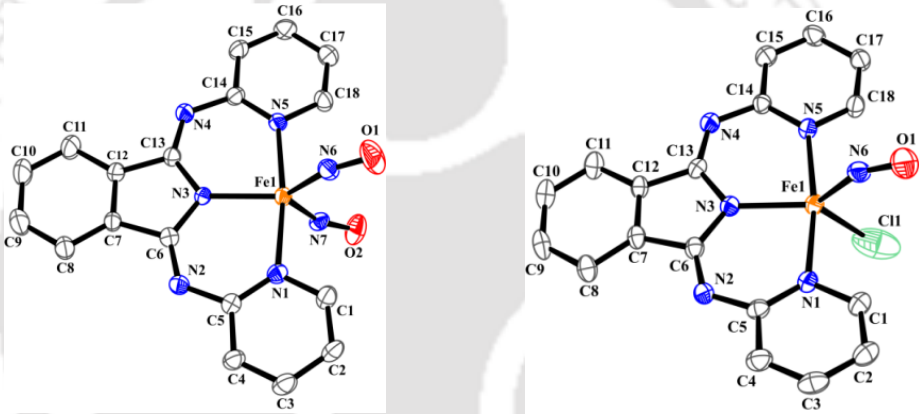

Figure S10. ORTEP diagrams of complexes (a) **5.1** and (b) **5.2** (30% ellipsoid probability; H atoms are not shown for clarity).

The reaction was found to proceed through the formation of a green intermediate complex, **5.2**, which gradually decomposed to brown. Isolation and characterization of the complexes from the crude mixture revealed the presence of equimolar amount of **5.1** and **5.3** (Scheme S3).

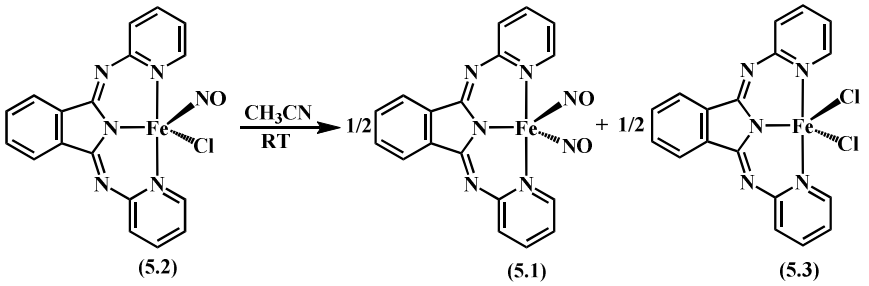

Scheme S3. Decompositionation of complex **5.2** in CH_3CN at room temperature (RT).

The intermediate green complex **5.2** was isolated as solid and characterized by spectroscopic analyses as well as by structure determination (Figure S10b). The single crystal structure of **5.2** revealed the presence of a monomeric $\{FeNO\}^7$ system with Fe(II) center. The three N-atoms from the ligand, one NO group and a Cl atom are coordinated to the Fe(II) center in a distorted trigonal bipyramidal geometry.

In UV-visible spectroscopy, complex **5.2** in acetonitrile solution absorbs at 630 nm (ε/M^{-1} cm^{-1}, 160) in the visible range. But the intensity of band was found to decrease rapidly (Figure S11a). In FT-IR spectrum, a strong stretching frequency was observed at 1795 cm^{-1}. It was attributed to the NO stretching of $\{FeNO\}^7$ complex (Figure S11b).

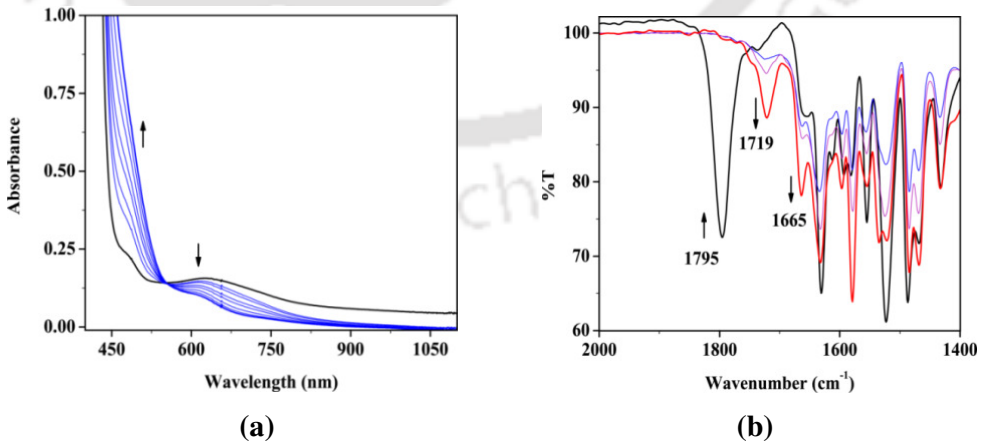

Figure S11. Changes observed in (a) UV-visible spectra and (b) FT-IR spectra of complex **5.2** after dissloving in acetonitrile at room temperature.

The complex **5.2** was found to be unstable in solution at room temperature. FT-IR monitoring of the solution of **5.2** revealed the disappearance of the 1795 cm^{-1} band with a simultaneous appearance of two new stretching frequencies at 1722 and 1665 cm^{-1} (Figure S11b). These two bands are assignable to the NO stretching frequencies of **5.1**. It is attributed to the disproportionation of complex **5.2** to **5.1**.

The concomitant formation of a high-spin Fe(III) complex is expected in this disproportionation mechanism. When the reaction was monitored by EPR spectroscopic studies, the frozen CH_3CN solution of **5.2** displayed signal (g, 5.03 and 1.99) corresponding to the monomeric high-spin $\{FeNO\}^7$ complex. When the spectrum was recorded at room temperature, the intensity of the signal of monomeric $\{FeNO\}^7$ diminished with gradual increase of the intensity of the signal of **5.1** along with signals (g , 14.36, 6.68 and 5.13) assignable to the high-spin Fe(III) complex, **5.3**. Isolation and characterization of **5.3** confirmed this assignment.[16]

References

(1) (a) Furchgott, R. F. *Angew. Chem. Int. Ed.* **1999**, *38*, 1870. (b) Ignarro, J.; *Angew. Chem. Int. Ed.* **1999**, *38*, 1882. (c) Murad, F. *Angew. Chem. Int. Ed.* **1999**, *38*, 1856.

(2) (a) Richter-Addo, G. B.; Legzdins, P. *Metal Nitrosyls* Oxford University Press, New York, **1992**. (b) Feelisch, M.; Stamler, J. S. *Methods in Nitric Oxide Research* John Wiley and Sons, New York, **1996**.

(3) (a) Butler, A. R.; Williams, D. *Chem. Soc. Rev*. **1993**, 233. (b) Jia, L.; Bonaventura, C.; Bonaventura J.; Stamler, J. S. *Nature* **1996**, *380*, 221. (c) Hulse, C. L.; Averill, B. A.; Tiedje, J. M. *J. Am. Chem. Soc.* **1989**, *111*, 232.

(4) Ricciardolo, E. L. M.; Sterk, P. J.; Gaston, B.; Folkerts, G. *Phsiol. Rev.* **2004**, *84*, 731.

(5) (a) Traylor, T. G.; Sharma, V. S. *Biochemistry* **1992**, *31*, 2847. (b) Radi, R. *Chem. Res. Toxicol.* **1996**, *9*, 828.

(6) (a) Gwost, D. G.; Caulton, K. G. *Inorg. Chem.* **1973**, *12*, 2095. (b) Gwost, D. G.; Caulton, K. G. *Inorg. Synth*. **1976**, *16*, 16.

(7) Deka, H.; Ghosh, S.; Saha, S.; Gogoi, K.; Mondal, B. *Dalton Trans.* **2016**, *45*, 10979.

(8) (a) Rhine, M. A.; Rodrigues, A. V.; Urbauer, R. J. B.; Urbauer, J. L.; Stemmler, T. L.; Harrop, T. C. *J. Am. Chem. Soc*. **2014**, *134*, 12560. (b) Rhine, M. A.; Sanders, B. C.; Patra, A. K.; Harrop, T. C. *Inorg. Chem.* **2015**, *54*, 9351.

(9) (a) Schopfer, M. P.; Mondal, B.; Lee, D.-H.; Sarjeant, A. A. N.; Karlin, K. D. *J. Am. Chem. Soc*. **2009**, *131*, 11304. (b) Maiti, D.; Lee, D.-H.; Sarjeant, A. A. N.; Pau, M. Y. M.; Solomon, E. I.; Gaoutchenova, K.; Sundermeyer, J.; Karlin, K. D. *J. Am. Chem. Soc*. **2008**, *130*, 6700. (c) Park, G. A.; Deepalatha, S.; Simona, C. P.; Lee, D.-H.; Mondal, B.; Sarjeant, A. A. N.; Rio, D. Del.; Pau, M. Y. M.; Solomon, E. I.; Karlin, K. D. *J. Biol. Inorg. Chem.* **2009**, *14*, 1301. (d) Kumar, V.; Kalita, A.; Mondal, B. *Dalton Trans*. **2013**, *42*, 16264.

(10) van der Vliet, A.; Eiserich, J. P.; Halliwell, B.; Cross, C. E. *J. Biol. Chem*. **1997**, *272*, 7617.

(11) (a) Kurtikyan, T. S.; Hayrapetyan, V. A.; Mehrabyan, M. M.; Ford, P. C. *Inorg. Chem.* **2014**, *53*, 11948. (b) Kurtikyan, T. S.; Ford, P. C. *Angew. Chem. Int. Ed.* **2006**, *45*, 492.

(12) (a) Kumar, P.; Lee, Y. M.; Park, Y. J.; Siegler, M. A.; Karlin, K. D.; Nam, W. *J. Am. Chem. Soc.* **2015**, *137*, 4284. (b) Kumar, P.; Lee, Y. M.; Hu, L.; Chen, J.; Park,

Y. J.; Yao, J.; Chen, H.; Karlin, K. D.; Nam, W. *J. Am. Chem. Soc.* **2016**, *138*, 7753.

(13) (a) Patra, A. K.; Afshar, R. K.; Rowland, J. M.; Olmstead, M. M.; Mascharak, P. K. *Angew. Chem. Int. Ed.* **2003**, *115*, 4655. (b) Afshar, R. K.; Eroy-Reveles, A. A.; Olmstead, M. M.; Mascharak, P. K. *Inorg. Chem*. **2006**, *45*, 10347.

(14) (a) Goodwin, J. A.; Kurtikyan, T. S.; Zheng, B., Parmley, D.; Howard, J., Green, S.; Walsh, R.; Standard, J.; Mardyukov, A. N. *Inorg. Chem*. **2005**, *44*, 2215. (b) Goodwin, J. A.; Coor, J. L.; Kavanagh, D. F.; Sabbagh, M.; Howard, J. W.; Adamec, J. R.; Parmley, D. J.; Tarsis, E. M.; Kurtikyan, T. S.; Hovhannisyan, A. A.; Desrochers, P. J.; Standard, J. M. *Inorg. Chem*. **2008**, *47*, 7852.

(15) (a) Tovrog, B. S.; Diamond, S. E.; Mares, F. *J. Am. Chem. Soc.* **1979**, *101*, 270. (b) Tovrog, B. S.; Mares, F.; Diamond, S. E. *J. Am. Chem. Soc.* **1980**, *102*, 6618.

(16) Balogh-Hergovich, E.; Speier, G.; Tapodi, B.; Reglier, M.; Giorgi, M. *Z. Kristallogr. NCS* **1999**, *214*, 579.

Chapter 1

Introduction

1.1 General aspect of nitric oxide

Nitric oxide (NO) is a diffusible and short-lived free radical gas with a wide range of functions in both eukaryotes and prokaryotes. It has attracted a considerable research interest since its discovery as a signaling molecule in cardiovascular system.[1,2] For example, it has been found to play the key roles in vasodilatation, muscle contraction, apoptosis facilitation and neurotransmission.[3] The physiological chemistry of NO and other nitrogen oxides (NOx) are believed to be mediated by their interactions with metal centers, especially iron and copper of metalloproteins.[4] In this direction, the best characterized example is the ferro-heme enzyme, soluble guanylyl cyclise (sGC).[5] In sGC, the formation of the nitrosyl complex with Fe(II) leads to labilization of a *trans* axial (proximal) histidine ligand in the protein backbone, and the resulting change in the protein conformation is believed to activate the enzyme for catalytic formation of the secondary messenger cyclic-guanylyl monophosphate (cGMP) from guanylyl triphosphate (GTP). The enzymatic formation of cGMP results into the relaxation of smooth muscle tissue of blood vessels, hence lowering blood pressure.[5]

Another example includes the catalytic cycle of bacterial copper containing nitrite reductase (Cu-NiRs) where a [Cu^{I}-NO^{+} $\leftrightarrow$ Cu^{II}-NO] intermediate is known to involve in the conversion of NO_2^- to NO or, in some cases to N_2O (Scheme 1.1).[6]

NO reacts rapidly with other reactive species such as different reactive oxygen species (ROS). This type of reaction is known to involve in the generation of powerful secondary nitrating and/or oxidizing agents, like nitrogen dioxide (NO_2) and peroxynitrite ($ONOO^-$).[7]

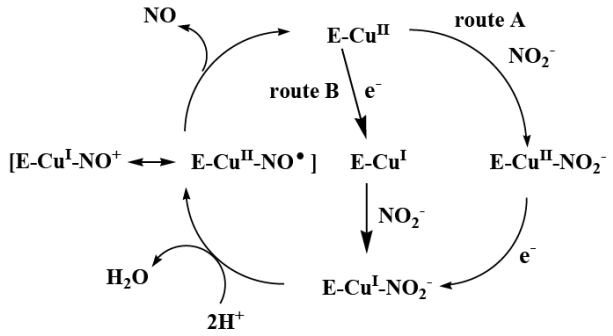

Scheme 1.1. Catalytic cycle of Cu containing nitrite reductase enzyme (Cu-NiRs).

NO_2 is known as the key intermediate for protein tyrosine nitration.[8] Hence, the reactivity of NO_2 with metal ions will be of interest with a goal of elucidating the redox transformations between various NOx complexes. In this context, reactions of NO_2 with iron porphyrin models were described by Kurtikyan *et al.*[9] Spectroscopic analyses revealed that the reaction of small amounts of NO_2 with sublimed thin layers of the [Fe^{II}(Por)] complex [Por = *meso*-tetraphenylporphyrinato dianion, TPP, or *meso*-tetra-*p*-tolylporphyrinato dianion, TTP] resulted in the formation of the corresponding five-coordinate nitrito complexes [Fe(Por)(η^1-ONO)].[9] Further addition of NO_2 led to the nitrato complex [Fe(Por)(η^2-O_2NO)]. Another study from the same group demonstrated the reaction of NO_2 with amorphous layers of Mn(TPP) afforded the corresponding nitrate [Mn(TPP)(η^1-ONO_2)].[10] Thus, interaction of NOx with transition metal complexes and their redox behaviour is always an interesting field of research from coordination as well as bioinorganic chemistry perspective.

In literature, most of the examples of metal nitrosyls include iron and copper owing to their biological relevance. Understanding of the versatile reactivity or decomposition pathways of these nitrosyl complexes have attracted enormous scientific research and the quest is still going on. Other first row transition metal ions have not been explored that much though some of them show interesting reactivity towards NO. For example, cobalt

dinitrosyls nitrosylate alkene double bonds to result in corresponding *bis*-nitroso compounds; they catalyse the disproportionation of NO which is industrially important.[11] Cobalt nitrosyl complex with $\{CoNO\}^8$ configuration has been found to be an potential HNO donor in recent studies.[12]

1.2 Iron and cobalt nitrosyl complexes

Several reports in literature describe the roles of NO as an inhibitor for metalloenzymes such as cytochrome P_{450}, cytochrome oxidase, nitrile hydratase, and catalase, as a substrate for mammalian peroxidases, and as the vasodilator carried by a salivary ferri-heme protein of blood-sucking insects.[13] Heme centers are also involved in the *in vivo* generation of NO by oxidation of arginine catalyzed by nitric oxide synthase (NOS) enzymes.[14] Ferri-heme proteins are known to undergo reduction to ferro-heme in aqueous solution on exposure to NO. These reactions proceed through two distinct steps: (i) formation of iron(III)-nitrosyl adduct; (ii) followed by the pH dependent reduction of Fe(III) to Fe(II) with a simultaneous attack of hydroxide ion to the activated nitrosonium group [Fe^{III}-NO ↔ Fe^{II}-NO^+] leading to the formation of nitrite (NO_2^-).

Recently, the reactivity of several iron(III) porphyrinates containing silanethiolate ligands with NO is reported by Tonzetich group.[15] In the complex [Fe(OMe)(TPP)] and

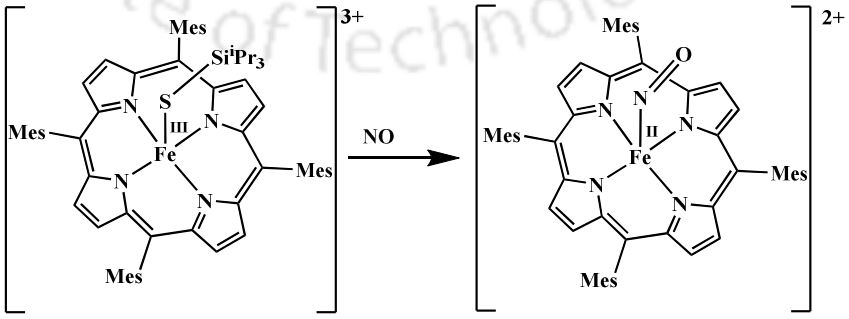

Scheme 1.2. Reaction of Fe(III) complex with NO.

[Fe(OH)(H_2O)(TMP)] (TPP= dianion of mesotetraphenylporphine; TMP = dianion of meso-tetramesitylporphine), Fe(III) centre undergoes reductive nitrosylation to afford the Fe^{II}-NO complex when treated with NO (Scheme 1.2).

It is reported that NO binds reversibly to the Fe(III) complex of a tetra-amido macrocyclic ligand.[16] Upon reaction with NO, the corresponding iron(III) complex results in nitrosyl which is labile and dissociates readily upon purging N_2 (Scheme 1.3).

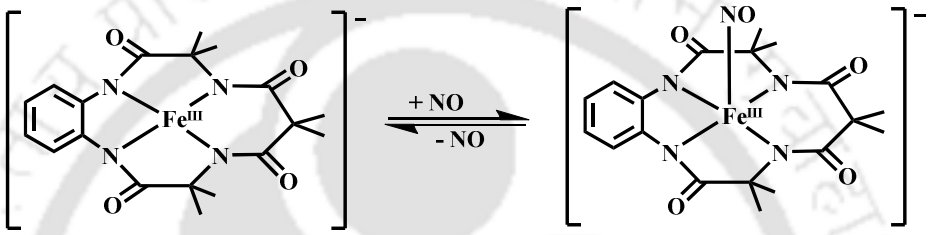

Scheme 1.3. Reversible binding of NO to a ferric complex.

Examples of the diiron dinitrosyl complex of Et-HPTB ligand {Et-HPTB=N,N,N′,N′-*tetrakis*(N-ethyl-2-benzimidazolyl methyl)-2-hydroxy-1,3,diaminopropane}, as a model for the binding of NO to non-heme iron proteins have been reported by the Lippard's group (Scheme 1.4).[17]

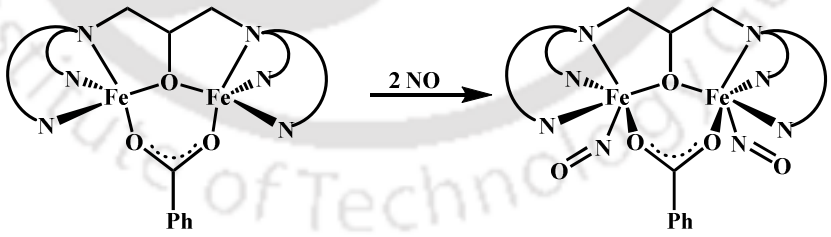

Scheme 1.4. Binding of NO to binuclear non-heme iron complex.

Reaction of bound nitrosyls with dioxygen can result in the formation of either nitrito or nitrato complexes, where the initial step is electrophilic attack of dioxygen on the nitrogen atom. This intermediate could then react with another nitrosyl complex and undergo O–O bond cleavage to form a nitrito complex or could rearrange intramolecularly to generate

the nitrato ligand. Recently, Kim *et al.* has also reported such type of reactivity with bidentate N-donor ligands. Dinitrosyl iron complexes with $\{Fe(NO)_2\}^{10}$ configuration were found to induce phenol ring nitration when exposed to air (Scheme 1.5). This was attributed to the formation of peroxynitrite intermediate which decompose to the corresponding nitrate complexes in absence of phenol substrate.[18]

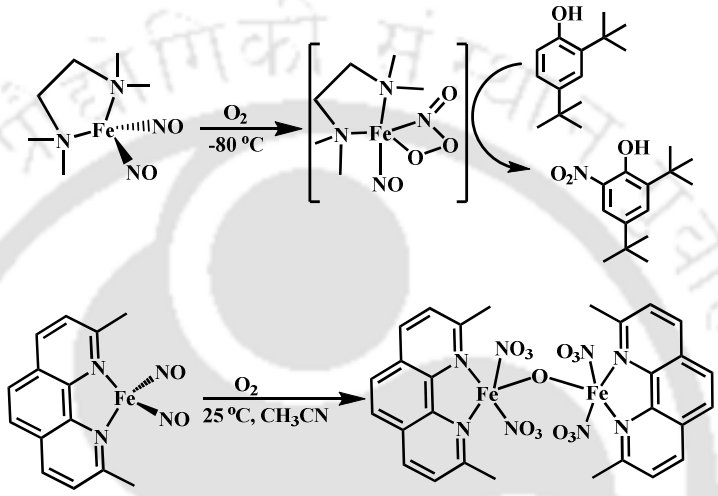

Scheme 1.5. Reaction of iron dinitrosyls with O_2 leading to the formation of $ONOO^-$ intermediate.

Lehnert's group reported the synthetic pathway of a $\{Fe(NO)_2\}^9$ DNIC, $[Fe(DMP)(NO)_2](OTf)$ {DMP = 2,9-dimethyl-1,10-phenanthroline} from a ferrous precursor *via* an unusual pathway, involving disproportionation of an $\{FeNO\}^7$ complex to yield the $\{Fe(NO)_2\}^9$ DNIC and a ferric species, which is subsequently reduced by NO gas to generate a ferrous complex that re-enters the reaction cycle (Scheme 1.6).[19]

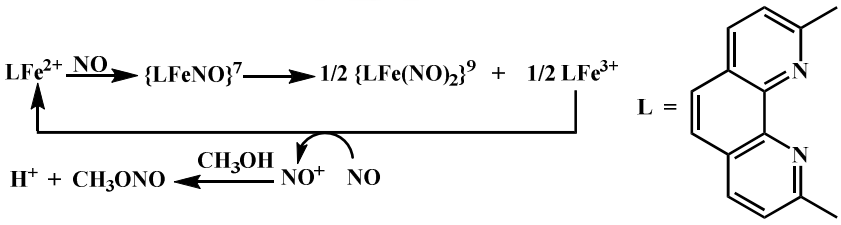

Scheme 1.6. Formation of Fe(I)-dinitrosyl complex from ferrous precursor.

Caulton and co-workers, synthesized $[(TMEDA)Co(NO)_2][BPh_4]$ from the reaction of $CoCl_2$, two equivalents of tetramethylethylenediamine (TMEDA) and NO in dry methanol followed by addition of $NaBPh_4$.[20] Later on, this dinitrosyl was used for synthesis of other cobalt nitrosyl complexes.[21] Lippard's and Hayton's group extensively studied the formation of different type of metal nitrosyl with Fe, Co, Mn, and Ni metal.[22] For example, chemical reduction of dinitrosyl cobalt(I) complex with $\{Co(NO)_2\}^{10}$ configuration afforded corresponding $\{Co(NO)_2\}^{11}$ system (Scheme 1.7).[23]

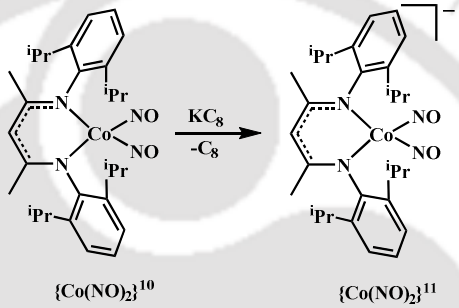

Scheme 1.7. Chemical reduction of $\{Co(NO)_2\}^{10}$ to $\{Co(NO)_2\}^{11}$ species.

Recently, our group has demonstrated the NO reactivity of different cobalt complexes. The complexes differed from each other in terms of the denticity and flexibility of the ligand frameworks (Scheme 1.8).[24]

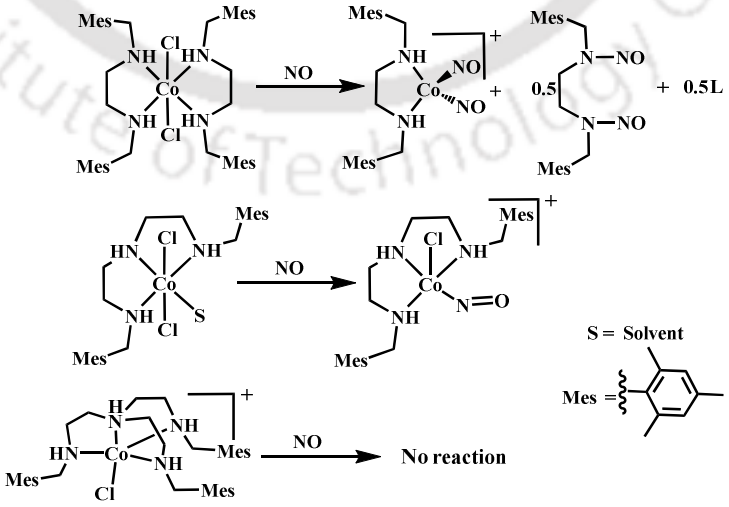

Scheme 1.8. Role of ligand framework in NO reactivity of Co(II) complexes.

Reaction of Co(II)-nitrosyl complex of 12 and 13 membered N-tetramethylated cyclam ligand with superoxide ion have been reported by Nam's group. These reactions were found to afford corresponding Co(II)-nitrite and O_2 *via* a presumed Co(II)-PN intermediate (Scheme 1.9).[25]

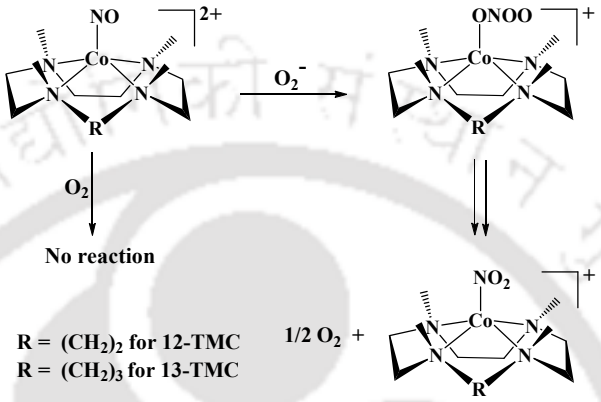

Scheme 1.9. Reaction of Co(II)-nitrosyl with superoxide ion.

The cobalt-nitrosyl complex of 14 memberd N-tetramethylated cylam ligand was reported to react with O_2 unlike the previous ones (Scheme 1.10).[26] The dioxygenation reaction was proposed to occur *via* the formation of a Co(II)–peroxynitrite intermediate, based on the observation of phenol ring nitration.

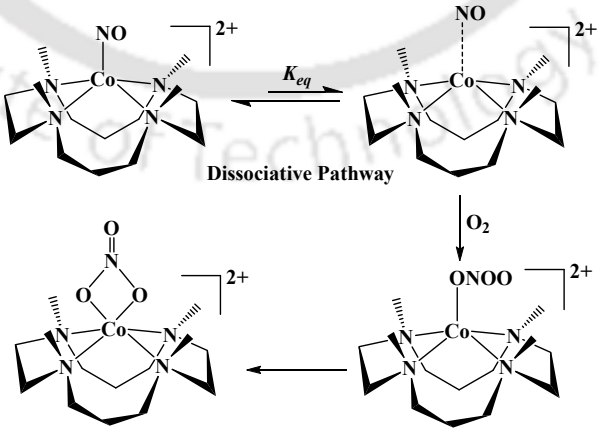

Scheme 1.10. Dioxygenation of Co(II)-nitrosyl *via* dissociative pathway.

Rate of the reaction was found to be independent of the O_2 concentration, indicating that the reaction proceeds *via* dissociation of NO ligand from the cobalt center to form a cage molecule, $\{(14\text{-TMC})Co\cdots NO\}^{2+}$, prior to the reaction with O_2.[26]

Metal nitrosyls (MNO) could serve as an alternative platform for HNO/NO^- delivery. Indeed, the heme enzyme responsible for NO synthesis (NO synthase) has been shown to release HNO *via* a Fe-bound N-hydroxy-L-arginine intermediate in the absence of its biopterin cofactor. In recent years several iron-nitrosyl complexes having $\{FeNO\}^8$ configuration have been studied which demonstrate nitroxyl-like reactivity.[27] But despite the formal assignment of the NO ligand as NO^- in most of the $\{CoNO\}^8$ systems, their chemical reactivity had not been explored in detail given their potential as HNO donors until Harrop *et al.* reported an example of proton-induced reactivity of NO^- from a $\{CoNO\}^8$ complex.[12] Reaction of $\{CoNO\}^8$ complex of {(*N*^{1}*E*, *N*^{2}*E*)-*N*^{1},*N*^{2}-*bis*((1H-pyrrol-2-yl)methylene)-4,5-dichloro-benzene-1,2-diamine} ligand with H^+ reported to generate the HNO donating intermediate towards HNO targets such as Fe(II)-heme, PPh_3 (Scheme 1.11). On the other hand the HNO donating intermediate ultimately leads to the formation of the Co-dinitrosyl complex in the absence of an HNO target.[12]

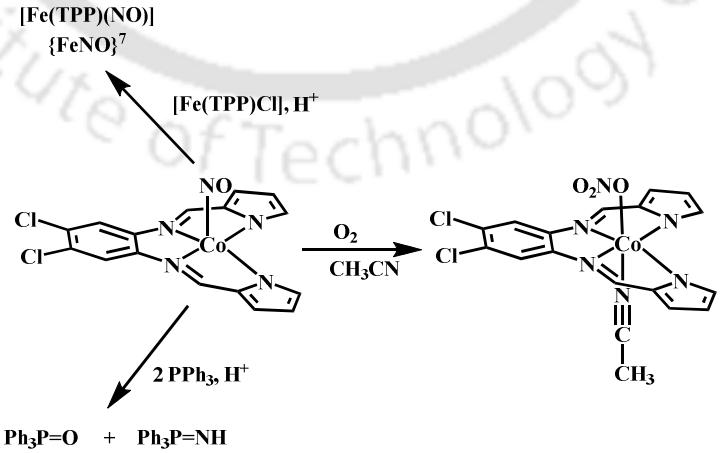

Scheme 1.11. Co(II)-nitrosyl complex as HNO donor.

The conversion of NO_2^- under hypoxic conditions to NO formation, the reaction which is catalyzed by bacterial nitrite reductases (NiR) enzyme is an important reaction involving metal bound NO_2^-.[6,28] Apart from NiR activity, metal-nitrite species also involved in the oxo-transfer reactions from coordinated nitro-groups in transition metal complexes to appropriate oxygen acceptors which can serve as important routes for oxidation of various substrates.[29-33] In those cases in which the nitrosyl complex thus formed is reoxidized by molecular oxygen, these processes may have a catalytic nature. This phenomenon is of special interest for metalloporphyrin nitro-complexes because of the biological significance of their reactions with various nitrogen-oxygen species (e.g., NO, NO_2, $OONO^-$ etc.).

1.3 Oxygen atom transfer (OAT) reactions of coordinated nitrite

Mascharak *et al*. reported the first example of a non-heme iron–nitro species that promotes stoichiometric and catalytic O-atom transfer to PPh_3 (Scheme 1.12).[29] $[(PaPy_3)Fe(NO_2)](ClO_4)$ [$PaPy_3$ = deprotonated *N*,*N*-bis-(2-pyridylmethyl)amine-*N*-ethyl-2-pyridine-2-carboxamide] was found to undergo reversible nitrite to nitrosyl conversion to give a $\{FeNO\}^7$ species.

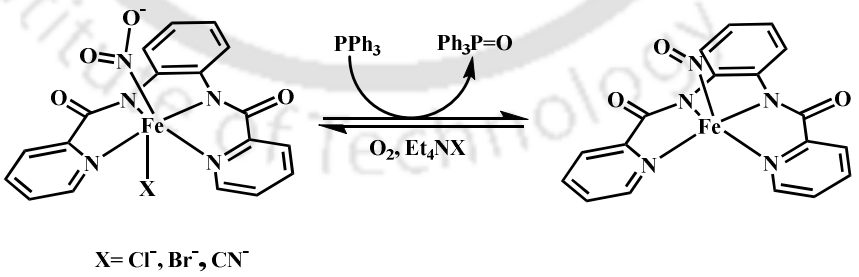

Scheme 1.12. Oxo transfer reactivity of Fe(III)-nitro complexes.

The reactivity of five-coordinate (nitro)cobaltporphyrins in the catalytic oxidation of alkenes, through oxo-transfer from the coordinated nitro ligand, was reported by Nitto and

co-workers.[30] The reduced cobalt(II) nitrosyl was found to be reoxidized to the cobalt(III) nitro in presence of molecular oxygen *via* peroxynitrite intermediate in solution, although direct observation of the intermediate was not possible (Scheme 1.13).

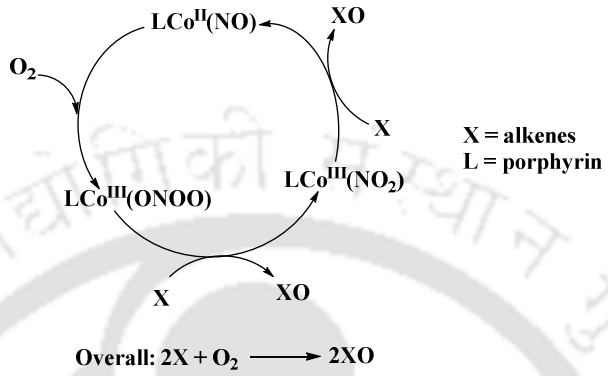

Scheme 1.13. Catalytic oxidation of alkenes *via* OAT reaction.

It was also observed that introduction of a pyridine ligand to the sixth coordination site of the cobalt center drastically reduce the oxidative capability of the nitro complex. These results were later supported by the works from Kurtikyan *et al.*[9,10]

Six-coordinate derivatives of the (nitro)cobalt porphyrins with nitrogen-bound[30] or oxygen-bound ligands trans to the nitro ligand were found to be not reactive with alkenes. This was attributed to unfavorable oxo-transfer thermodynamics.[31] However, derivatives with weakly bound sixth ligands are capable of alkene oxidation under appropriate conditions due to the five-coordinate nitro species that exists in equilibrium in solution.[31,32]

Tovrog and coworkers has synthesized a Co(III)-NO_2 complex of the Schiff base salophen, that undergoes catalytic O-atom transfer to Ph_3P in presence of excess pyridine with a catalytic turnover number (TN) of 8.7 (at 60 °C) in 16 h (Scheme 1.14).[33] The secondary O-atom transfer generates a five-coordinate $\{CoNO\}^8$ intermediate, [(salophen)Co(NO)], which is then reoxidized to the starting [(salophen)Co(NO_2)(py)] complex in the presence of dioxygen and pyridine.

$$Co(saloph)Py(NO_2) + PPh_3 \longrightarrow Co(saloph)Py(NO) + Ph_3P{=}O + Py$$

Scheme 1.14. Oxo transfer from non-porphyrin Co(III)-nitro complex.

Reactions of NO_2 with iron and manganese porphyrin models were described by Kurtikyan *et al*. (Scheme 1.15).[9,34] These reactions were shown to proceed through two distinct steps: (i) initially low NO_2 pressure leads to the formation of corresponding O-nitrito complex; (ii) additional increments of NO_2 result in the nitrato analogue with the release of NO. Studies were performed with the sublimed layers of metalloporphyrins in vacuum cryostats and FTIR spectroscopy using isotopic labeling.

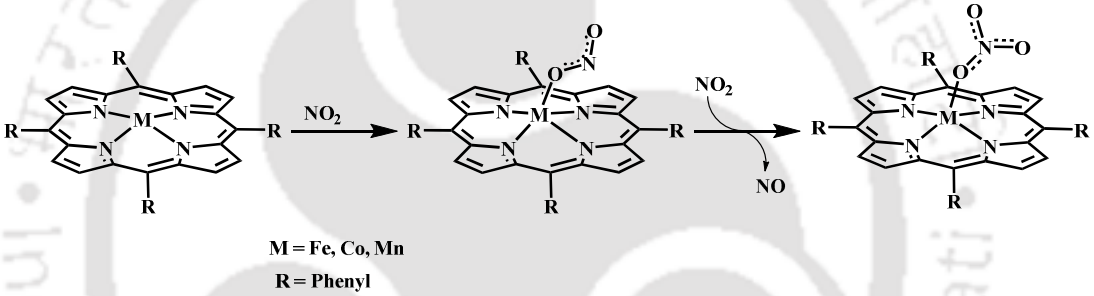

Scheme 1.15. NO_2 reactivity of metal-porphyrin complexes.

The reaction of NO_2 with copper(II) nitrite complexes have not yet been studied, though they are relevant for copper-containing nitrite reductases (CuNiR). These results instigate us also to study the NO_2 reactivity of a copper(II) nitrito complex along with the oxo transfer reactivity of several cobalt-nitro complexes.

1.4 Scope of the thesis

In this thesis, redox reactions of NOx assisted by transition metal complexes are presented. In chapter 2, oxo transfer reactivity of a Cu(II)-nitrito complex towards NO_2 is studied. Oxo transfer from free NO_2 to the nitrito complex leads to the formation of the corresponding Cu(II)-nitrate complex with concomitant release of NO.

Oxo transfer reactivity of cobalt(III)-nitro complexes with tetradentate and pentadentate ligands are discussed in chapter 3. Differences in reactivity for the complexes, where nitro complexes with tertradentate schif's base ligands are found to be active towards oxo transfer reactivity unlike the pentadentate ligand counterparts. These results are in good agreement with the previously reported cases for the nitro porphyrin cobalt complexes.

Since cobalt-nitrosyls having $\{CoNO\}^8$ configuration are known to be stable, chapter 4 has been originated from our interest to develop stable $\{CoNO\}^8$ complex and study its reactivity. Dioxygenation of the cobalt(II)-nitrosyl complex resulted in the generation of a superoxocobalt(III)nitrosyl intermediate via an associative pathway. This intermediate then decomposes to the corresponding nitrite complex. Chemical evidence suggests the involvement of putative peroxynitrite formation in the decomposition pathway.

The final chapter discusses the unusual synthesis of a $\{Fe(NO)_2\}^9$ DNIC *via* disproportionation of a $\{FeNO\}^7$ species.

1.5 References

(1) (a) Ignarro, L. J. *Nitric Oxide, Biology and Pathobiology* Ed. Academic Press, San Diego, CA, **2000**. (b) Richter-Addo, G. B.; Legzdins, P. *Metal Nitrosyls* Oxford University Press, New York, **1992**. (c) Feelisch, M.; Stamler, J. S. *Methods in Nitric Oxide Research* John Wiley and Sons, New York, **1996**.

(2) (a) Furchgott, R. F. *Angew. Chem. Int. Ed.* **1999**, *38*, 1870. (b) Ignarro, L. J.; Buga, G. M.; Wood, K. S.; Byrns, R. E.; Chaudhuri, G. *Proc. Natl. Acad. Sci. U.S.A.* **1987**, *84*, 9265. (c) Murrad, F. *Angew. Chem. Int. Ed.* **1999**, *38*, 1856. (d) Ignaro, L. J. *Angew. Chem. Int. Ed.* **1999**, *38*, 1882. (e) Palmer, R. M. J.; Ferrige, A. G.;

Moncada, S. *Nature* **1987**, *327*, 524. (f) Moncada, S.; Palmer, R. M. J.; Higgs, E. A. *Pharmacol. Rev.* **1991**, *43,* 109.

(3) (a) Bredt, D. S.; Snyder, S. H. *Annu. Rev. Biochem*. **1994**, *63*, 175. (b) Butler, A. R.; Williams, D. *Chem. Soc. Rev*. **1993**, 233. (c) Jia, L.; Bonaventura, C.; Bonaventura J.; Stamler, J. S. *Nature* **1996**, *380*, 221. (d) Hulse, C. L.; Averill, B. A.; Tiedje, J. M. *J. Am. Chem. Soc.* **1989**, *111*, 232.

(4) (a) Traylor, T. G.; Sharma, V. S. *Biochemistry.* **1992**, *31*, 2847. (b) Radi, R. *Chem. Res. Toxicol.* **1996**, *9*, 828.

(5) (a) Kim, S.; Deinum, G.; Gardner, M. T.; Marletta, M. A.; Babcock, G. T. *J. Am. Chem. Soc.* **1996**, *118*, 8769. (b) Burstyn, J. N.; Yu, A. E.; Dierks, E. A.; Hawkins, B. K.; Dawson, B. K. *Biochemistry* **1995**, *34*, 5896.

(6) (a) Tolman, W. B. *Adv. Chem. Ser.* **1995**, *246*, 195. (b) Ferguson, S. J. *Curr. Opin. Chem. Biol.* **1998**, *2*, 182. (c) Richardson, D. J.; Watmough, N. J. *Curr. Opin. Chem. Biol.* **1999**, *3*, 207. (d) Moura, I.; Moura, J. J. G. *Curr. Opin. Chem. Biol.* **2001**, *5*, 168.

(7) (a) Schopfer, M. P.; Mondal, B.; Lee, D.-H.; Sarjeant, A. A. N.; Karlin, K. D. *J. Am. Chem. Soc*. **2009**, *131*, 11304. (b) Maiti, D.; Lee, D.-H.; Sarjeant, A. A. N.; Pau, M. Y. M.; Solomon, E. I.; Gaoutchenova, K.; Sundermeyer, J.; Karlin, K. D. *J. Am. Chem. Soc*. **2008**, *130*, 6700. (c) Park, G. A.; Deepalatha, S.; Simona, C. P.; Lee, D.-H.; Mondal, B.; Sarjeant, A. A. N.; Rio, D. Del.; Pau, M. Y. M.; Solomon, E. I.; Karlin, K. D. *J. Biol. Inorg. Chem.* **2009**, *14*, 1301. (d) Kumar, V.; Kalita, A.; Mondal, B. *Dalton Trans*. **2013**, *42*, 16264.

(8) van der Vliet, A.; Eiserich, J. P.; Halliwell, B.; Cross, C. E. *J. Biol. Chem*. **1997**, *272*, 7617.

(9) (a) Kurtikyan, T. S.; Hayrapetyan, V. A.; Mehrabyan, M. M.; Ford, P. C. *Inorg. Chem.* **2014**, *53*, 11948. (b) Kurtikyan, T. S.; Ford, P. C. *Angew. Chem. Int. Ed.* **2006**, *45*, 492.

(10) Kurtikyan, T. S.; Hovhannisyan, A. A.; Gulyan, G. M.; Ford, P. C. *Inorg. Chem.* **2007**, *46*, 7024.

(11) (a) Brunner, H. *J. Organomet. Chem*. **1968**, *12*, 517. (b) Brunner, H.; Loskot, S. *Angew. Chem. Int. Ed*. **1971**, *10*, 515. (c) Weiner, W. P.; White, M. A.; Bergman, R. G. *J. Am. Chem. Soc*. **1981**, *103*, 3612. (d) Becker, N. P.; Bergman, R. G. *J. Am. Chem. Soc*. **1983**, *105*, 2985. (e) Becker, P. N.; Bergman, R. G. *Organometallics* **1983**, *2*, 787. (f) Weiner, W. P.; Hollander, F. J.; Bergman, R. G. *J. Am. Chem. Soc*. **1984**, *106*, 7462.

(12) Rhine, M. A.; Rodrigues, A. V.; Urbauer, R. L. B.; Urbauer, J. L.; Stemmler, T. L.; Harrop, T. C. *J. Am. Chem. Soc*. **2014**, *136*, 12560.

(13) (a) Cleeter, M. W. J.; Cooper, J. M.; Darley-Usmar, V. M.; Moncada, S.; Scapira, A. H. V. *FEBS Lett.* **1994**, *345*, 50. (b) Noguchi, T.; Hoshino, M.; Tsujimura, M.; Odaka, M.; Inoue, Y.; Endo, I. *Biochemistry* **1996**, *35,* 16777. (c) Odaka, M.; Fujii, K.; Hoshino, M.; Noguchi, T.; Tsujimura, M.; Nagashima, S.; Yohda, M.; Nagamune, T.; Inoue, Y.; Endo, I. *J. Am. Chem. Soc.* **1997**, *119,* 3785. (d) Brown, G. C. *Eur. J. Biochem.* **1995**, *232*, 188. (e) Ribiero, J. M. C.; Hazzard, J. M. H.; Nussenzveig, R. H.; Champagne, D. E.; Walker, F. A. *Science* **1993**, *260*, 539. (f) Ding, X. D.; Weichsel, A.; Balfour, C.; Shokhireva, T. Kh.; Pierik, A.; Averill, B. A.; Montfort, W. R.; Walker, F. A. *J. Am. Chem. Soc*. **1999**, *121*, 128.

(14) (a) Abu-Soud, H. M.; Ichimori, K.; Nakazawa, H.; Stuehr, D. J. *Biochemistry* **2001**, *40*, 6876. (b) Stuehr, D.; Pou, S.; Rosen, G. M. *J. Biol. Chem.* **2001**, *276*, 14533. (c) Ford, P. C. *Pure Appl. Chem.* **2004**, *76*, 335.

(15) Meininger, D. J.; Caranto, J. D.; Arman, H. D.; Tonzetich, Z. J. *Inorg. Chem.* **2013**, *52*, 12468.

(16) Pluthz, M. D.; Lippard, S. J. *Chem. Commun.* **2012**, *48*, 11981.

(17) Feig, A. L.; Bautista, M. T.; Lippard, S. J. *Inorg. Chem.* **1996**, *35*, 6892.

(18) (a) Tran, N. G.; Kalyvas, H.; Skodje, K. M.; Hayashi, T.; Moënne-Loccoz, P.; Callan, P. E.; Shearer, J.; Kirschenbaum, L. J.; Kim, E. *J. Am. Chem. Soc*. **2011**, *133*, 1184. (b) Skodje, K. M.; Williard, P. G.; Kim, E. *Dalton Trans.* **2012**, *41*, 7849.

(19) Speelman, A. L.; Zhang, B.; Silakov, A.; Skodje, K. M.; Alp, E. E.; Zhao, J.; Hu, M. Y.; Kim, E.; Krebs, C.; Lehnert, N. *Inorg. Chem*. **2016**, *55*, 5485.

(20) (a) Gwost, D. G.; Caulton, K. G. *Inorg. Chem.* **1973**, *12,* 2095. (b) Gwost, D. G.; Caulton, K. G. *Inorg. Synth*. **1976**, *16,* 16.

(21) Tomson, N. C.; Crimmin, M. R.; Petrenko, T.; Rosebrugh, L. E.; Sproules, S.; Boyd, W. C.; Bergman, R. G.; DeBeer, S.; Toste, F. D.; Wieghardt, K. *J. Am. Chem. Soc.* **2011**, *133,* 18785.

(22) (a) Franz, K. J.; Lippard, S. J. *Inorg. Chem.* **2000**, *39*, 3722. (b) Franz, K. J.; Doerrer, L. H.; Spingler, B.; Lippard, S. J. *Inorg. Chem.* **2001**, *40,* 3774. (c) Franz, K. J.; Singh, N.; Lippard, S. J. *Angew. Chem. Int. Ed.* **2000**, *39*, 2120. (d) Wright, A. M.; Wu, G.; Hayton, T. W. *J. Am. Chem. Soc.* **2012**, *134,* 9930. (e) Wright, A. M.; Zaman, H. T.; Wu, G.; Hayton, T. W. *Inorg. Chem.* **2014**, *53,* 3108.

(23) Tonzetich, Z. J.; Heroguel, F.; Do, L. H.; Lippard, S. J. *Inorg. Chem*. **2011**, *50,* 1570.

(24) Deka, H.; Ghosh, S.; Saha, S.; Gogoi, K.; Mondal, B. *Dalton Trans.* **2016**, *45,* 10979.

(25) Kumar, P.; Lee, Y. M.; Park, Y. J.; Siegler, M. A.; Karlin, K. D.; Nam, W. *J. Am. Chem. Soc.* **2015**, *137*, 4284.

(26) Kumar, P.; Lee, Y. M.; Hu, L.; Chen, J.; Park, Y. J.; Yao, J.; Chen, H.; Karlin, K. D.; Nam, W. *J. Am. Chem. Soc.* **2016**, *138*, 7753.

(27) (a) Harrop, T. C. *Adv. Inorg. Chem*. **2015**, *67*, 243. (b) Rhine, M. A.; Sanders, B. C.; Patra, A. K.; Harrop, T. C. *Inorg. Chem.* **2015**, *54*, 9351.

(28) (a) Ford, P. C. *Inorg. Chem*. **2010**, 49, 6226. (b) Feelisch, M.; Fernandez, B. O.; Bryan, N. S.; Garcia-Saura, M. F.; Bauer, S.; Whitlock, D. R.; Ford, P. C.; Janero, D. R.; Rodriguez, J.; Ashrafian, H. *J. Biol. Chem*. **2008**, *283*, 33927. (c) Shiva, S.; Sack, M. N.; Greer, J. J.; Duranski, M.; Ringwood, L. A.; Burwell, L.; Wang, X.; MacArthur, P. H.; Shoja, A.; Raghavachari, N.; Calvert, J. W.; Brookes, P. S.; Lefer, D. J.; Gladwin, M. T. *J. Exp. Med*. **2007**, *204*, 2089.

(29) (a) Afshar, R. K.; Eroy-Reveles, A. A.; Olmstead, M. M.; Mascharak, P. K. *Inorg. Chem*. **2006**, *45*, 10347. (b) Patra, A. K.; Afshar, R. K.; Rowland, J. M.; Olmstead, M. M.; Mascharak, P. K. *Angew. Chem. Int. Ed*. **2003**, *42*, 4517.

(30) Goodwin, J.; Bailey, R.; Pennington, W.; Rasberry, R.; Green, T.; Shasho, S.; Yongsavanh, M.; Echevarria, V.; Tiedeken, J.; Brown, C.; Fromm, G.; Lyerly, S.; Watson, N.; Long, A.; De Nitto, N. *Inorg. Chem*. **2001**, *40*, 4217.

(31) Goodwin, J. A.; Kurtikyan, T. S.; Zheng, B.; Parmley, D.; Howard, J.; Green, S.; Walsh, R.; Standard, J.; Mardyukov, A. N. *Inorg. Chem*. **2005**, *44*, 2215.

(32) Goodwin, J. A.; Coor, J. L.; Kavanagh, D. F.; Sabbagh, M.; Howard, J. W.; Adamec, J. R.; Parmley, D. J.; Tarsis, E. M.; Kurtikyan, T. S.; Hovhannisyan, A. A.; Desrochers, P. J.; Standard, J. M. *Inorg. Chem*. **2008**, *47*, 7852.

(33) (a) Tovrog, B. S.; Diamond, S. E.; Mares, F. *J. Am. Chem. Soc.* **1979**, *101*, 270. (b) Tovrog, B. S.; Mares, F.; Diamond, S. E. *J. Am. Chem. Soc.* **1980**, *102*, 6618. (c)

Tovrog, B. S.; Diamond, S. E.; Mares, F.; Szalkiewicz, A. *J. Am. Chem. Soc.* **1981**, *103*, 3522.

(34) (a) Kurtikyan, T. S.; Ford, P. C. *Coord. Chem. Rev*. **2008**, *252*, 1486. (b) Gulyan, G. M.; Kurtikyan, T. S.; Ford, P. C. *Inorg. Chem.* **2008**, *47*, 787. (c) Kurtikyan, T. S.; Hovhannisyan, A. A.; Hakobyan, M. E.; Patterson, J. C.; Iretskii, A.; Ford, P. C. *J. Am. Chem. Soc*. **2007**, *129*, 3576.

Chapter 2

Nitrogen Dioxide Reactivity of a Copper(II) Complex

Abstract

Reaction of Cu(II) complex $[Cu^{II}(L1H)(O_2CCH_3)_2]$ (**2.1**) [**L1H** = 2,4-di-*tert*-butyl-6-((isopropyl(pyridin-2-ylmethyl)amino)methyl)phenol] with equivalent amount of NO_2 leads to the reduction of Cu(II) to Cu(I) with concomitant nitration at the phenol ring of the ligand. This resulted in the in situ formation of intermediate Cu(I) complex of the nitrated ligand (L1′H). Additional equivalent of NO_2 coordinates to the Cu(I) complex to form corresponding O-nitrito Cu(II) complex $[Cu^{II}(L1')(\eta^1\text{-ONO})]$ (**2.2**). Subsequent addition of NO_2 led to the corresponding O-nitrato complex, $[Cu^{II}(L1')(\eta^1\text{-}ONO_2)]$ (**2.3**) with concomitant formation of NO. Complexes **2.2** and **2.3** were isolated and structurally characterized. The formation of NO in the reaction was established by spin-trapping experiment. Isotopic labelling experiment revealed that the oxo transfer takes place from NO_2 to the coordinated η^1-ONO group.

2.1 Introduction

The physiological chemistry of nitric oxide (NO) and other nitrogen oxides (NOx) are believed to be mediated by their interactions with metal centers, especially iron and copper of metalloproteins.[1] For instance, in the state of hypoxic ischemia, nitrite (NO_2^-) ion is believed to be reduced by heme proteins to generate NO.[2] On the other hand, nitrogen dioxide (NO_2) is known as the key intermediate for protein tyrosine nitration.[3] Hence, the reactivity of NO_2 with metal ions will be of interest with a goal of elucidating the redox transformations between various NOx complexes. In this context, reactions of NO_2 with iron porphyrin models were described by Kurtikyan *et al*. Fourier transform infrared (FT-IR) optical spectroscopy and isotope labelling experiments revealed that the reaction of small amounts of NO_2 with sublimed thin layers of the [Fe^{II}(Por)] complex [Por = *meso*-tetraphenylporphyrinato dianion, TPP, or *meso*-tetra-*p*-tolylporphyrinato dianion, TTP] resulted in the formation of the corresponding five-coordinated nitrito complexes [Fe(Por)(η^1-ONO)].[4] Further addition of NO_2 led to the nitrato complex [Fe(Por)(η^2-O_2NO)]. Another study from the same group demonstrated the reaction of NO_2 with amorphous layers of Mn(TPP) afforded the corresponding nitrate [Mn(TPP)(η^1-ONO_2)].[5] This reaction was shown to proceed through two distinct steps: (i) initially low NO_2 pressure leads to the formation of corresponding O-nitrito complex; (ii) additional increments of NO_2 result in the nitrato analogue with the release of NO. Studies were performed with the sublimed layers of metalloporphyrins in vacuum cryostats and FTIR spectroscopy using isotopic labeling. The reaction of NO_2 with copper(II) nitrite complexes have not yet been studied, though they are relevant for copper-containing nitrite reductases (CuNiR).[6] Here we describe the reaction of NO_2 with a copper(II) nitrite complex.

2.2 Results and discussion

The ligand 2,4-di-*tert*-butyl-6-((isopropyl(pyridin-2-ylmethyl)amino)methyl)phenol (**L1H**) was prepared by refluxing a mixture of *N*-isopropyl-2-picolylamine and 2,4-di-*tert*-butylphenol in the presence of formaldehyde in methanol. The formation of the ligand was confirmed by its spectral characterization and elemental analyses (Experimental Section). Mononuclear complex **2.1**, $[Cu^{II}(L1H)(O_2CCH_3)_2]$, was prepared by stirring a mixture of copper(II) acetate monohydrate with equivalent quantity of **L1H** in acetonitrile (Experimental Section). X-ray single crystal structure of **2.1** was determined. The ORTEP diagram is shown in figure 2.1. The crystallographic data and important bond lengths and angles are listed in tables 2.1, 2.2 and 2.3, respectively. The crystal structure reveals a distorted square pyramidal geometry around Cu(II) center in the mononuclear unit. Two acetate anions are coordinated to the metal center and balance the charge of the metal ion. The phenol moiety is coordinated to Cu(II) from an equatorial site, and $Cu–O_{phenol}$ distance is 1.960(2) Å, which is within the range of other reported analogous complexes.[7] The equatorial $Cu–O_{acetate}$ distance is 1.921(3) Å, whereas the apical one is 2.534(3) Å.

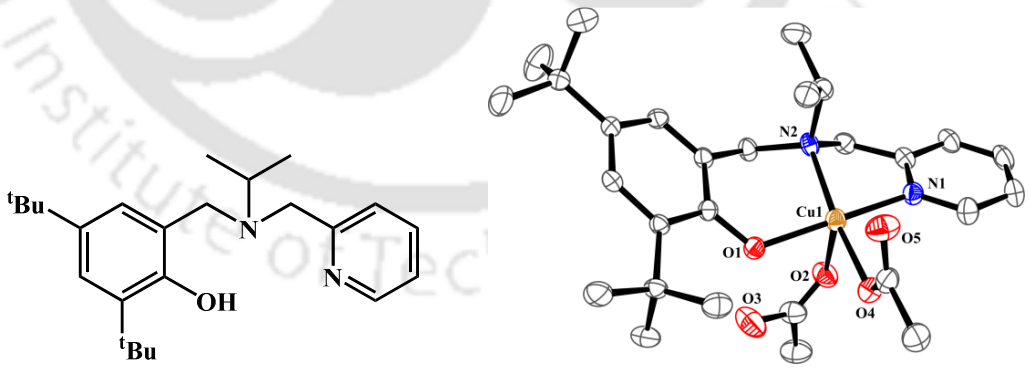

(a) **(b)**

Figure 2.1. (a) Ligand **L1H** used for present study and (b) ORTEP diagram of complex **2.1** (35% thermal ellipsoid plot; hydrogen atoms are not shown for clarity).

In methanol, **2.1** absorb at 470 nm ($\varepsilon/M^{-1}\ cm^{-1}$, 600) and 676 nm ($\varepsilon/M^{-1}\ cm^{-1}$, 400) along with strong intra ligand transitions (Figure 2.2). The 470 nm band is assigned as the charge

transfer, and the 676 nm band is attributed to the d–d transition. The crystalline complex **2.1** was dissolved in methanol, and electron paramagnetic resonance (EPR) spectra were recorded at room temperature as well as at 77 K (Appendix I). The $g_{\parallel}$, $g_{\perp}$, and A values are calculated as 2.369, 2.049, and 176 x 10^{-4} cm^{-1}, respectively.

Table 2.1. Crystallographic data for complexes **2.1**, **2.2** and **2.3**.

	2.1	**2.2**	**2.3**
Formulae	$C_{28}H_{42}CuN_2O_5$	$C_{20}H_{26}CuN_4O_5$	$C_{44}H_{58}Cu_2N_{10}O_{12}$
Mol. wt.	550.18	466.00	1046.08
Crystal system	Monoclinic	Orthorhombic	Triclinic
Space group	P2(1)/c	P 21 21 21	P-1
Temperature /K	296(2)	296(2)	296(2)
Wavelength /Å	0.71073	0.71073	0.71073
a /Å	10.116(2)	8.1018(6)	9.4692(7)
b /Å	15.428(3)	10.6660(7)	10.7391(7)
c /Å	18.573(4)	25.2840(16)	12.8212(11)
α/°	90.00	90.00	98.363(7)
β/°	94.603(6)	90.00	106.609(7)
γ/°	90.00	90.00	95.160(6)
V/ $Å^3$	2889.4(10)	2184.9(3)	1224.15(16)
Z	4	4	1
Density/Mgm^{-3}	1.265	1.417	1.419
Abs. Coeff. /mm^{-1}	0.793	1.038	0.938
Abs. correction	Multi-scan	Multi-scan	Multi-scan
F(000)	1172	972	546
Total no. of reflections	4986	2440	4310
Reflections, $I > 2\sigma(I)$	2360	2105	3508
Max. 2θ/°	25.00	25.25	25.00
Ranges (h, k, l)	$-11 \le h \le 11$ $-18 \le k \le 18$ $-19 \le l \le 21$	$-8 \le h \le 7$ $-10 \le k \le 10$ $-25 \le l \le 25$	$-11 \le h \le 11$ $-12 \le k \le 12$ $-15 \le l \le 11$
Complete to 2θ (%)	98.2	99.9	99.8
Refinement method	Full-matrix least-squares on F^2	Full-matrix least-squares on F^2	Full-matrix least-squares on F^2
Goof (F^2)	0.885	1.073	1.241
R indices [$I > 2\sigma(I)$]	0.0502	0.0362	0.0471
R indices (all data)	0.1097	0.0434	0.0602

Table 2.2. Selected bond length (Å) of complexes **2.1**, **2.2** and **2.3**.

	2.1	**2.2**	**2.3**
Cu1-N1	2.015(3)	2.000(4)	1.965(2)
Cu1-N2	2.026(3)	2.049(4)	2.015(2)
Cu1-O1	1.960(2)	1.839(3)	1.885(2)
Cu1-O2	2.534(3)	-	
Cu1-O4	1.921(3)	1.985(4)	2.015(2)
Cu1-O5	2.786(3)	2.732(4)	2.794(3)

C27-O2	1.193(7)	-	-
C27-O3	1.308(6)	-	-
N4-O4	-	1.250(7)	1.296(5)
N4-O5	-	1.202(7)	1.212(8)

Table 2.3. Selected bond angles (°) of complexes **2.1**, **2.2** and **2.3**.

	2.1	**2.2**	**2.3**
N1-Cu1-N2	81.4(1)	84.6(2)	84.50(9)
N1-Cu1-O1	170.0(1)	176.2(2)	171.61(9)
N1-Cu1-O2	86.2(1)	-	-
N1-Cu1-O4	93.8(1)	95.2(2)	94.91(2)
N2-Cu1-O1	94.6(1)	91.7(2)	92.81(9)
N2-Cu1-O2	93.3(1)	-	-
N2-Cu1-O4	173.1(1)	168.4(2)	179.09(5)
O1-Cu1-O2	84.9(1)	-	-
O1-Cu1-O4	90.9(1)	88.5(2)	87.82(2)
O2-N3-O3	-	122.3(5)	122.00(8)
O4-N4-O5	-	115.6(5)	118.75(5)

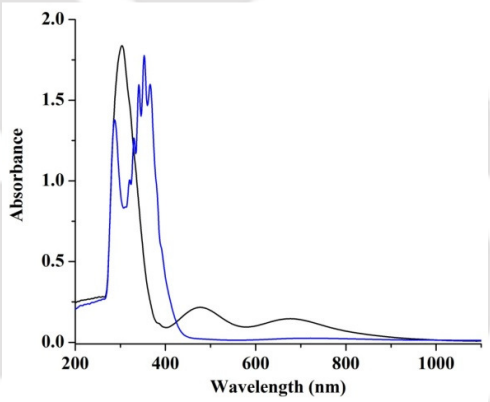

Figure 2.2. UV-visible spectra of complex **2.1** before (black) and after purging 1 equivalent of NO_2 (blue) in methanol at room temperature.

Addition of equivalent amount of NO_2 to the dry and degassed methanol solution of **2.1** resulted in the change of color from brown to light yellow. In the UV–visible spectral monitoring, both the 470 and 676 nm bands disappeared (Figure 2.2). EPR study revealed that the solution became EPR silent after addition of NO_2. These are attributed to the reduction of Cu(II) by NO_2 to Cu(I) (Scheme 2.1).[8]

In ^{1}H-NMR spectroscopy, the broad signals of paramagnetic complex **2.1** became well-resolved after addition of equivalent amount of NO_2 suggesting the formation of a

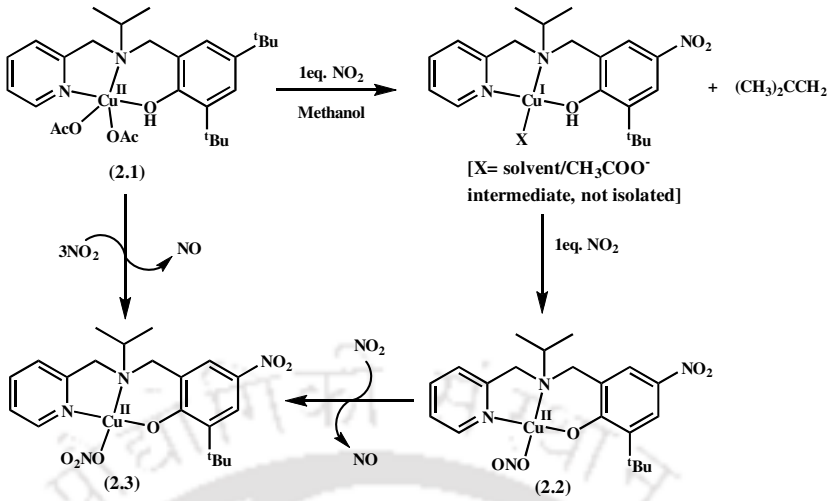

Scheme 2.1. Reaction of complex **2.1** with NO_2.

diamagnetic species (Figure 2.3). The positions of ^{1}H-NMR signals of the diamagnetic species are shifted from the positions for the free ligand. This is because of its coordination to the metal center. Earlier, it was reported that reduction of Cu(II) center of analogous complexes by NO_2 resulted in the formation of nitronium ion (NO_2^+), which in successive steps induced nitration of the phenol ring of ligand.

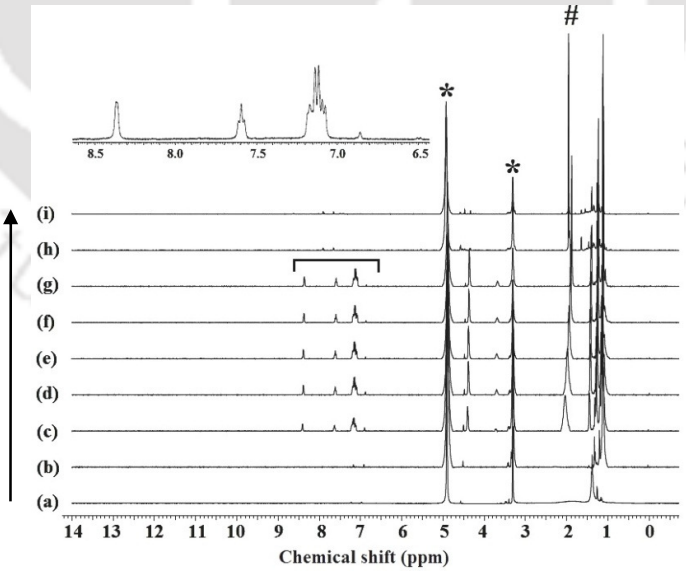

Figure 2.3. ^{1}H-NMR spectra of complex **2.1** before and after purging NO_2 in CD_3OD. (a) **2.1**. (b–i) **2.1** after the addition of 0.1, 0.2, 0.3, 0.5, 0.75, 1.0, 2.0 equivalent and excess NO_2, respectively. (inset) The aromatic region of (g) is expanded. The * marked signals are for solvent and # marked signal indicates the formation of $(CH_3)_3COD$.

The reaction is also associated with the simultaneous release of the tertiary butyl cation.[8] Gas chromatography–mass spectrometry (GC-MS) analysis of the head space gas from the reaction vessel confirmed the presence of isobutylene (Appendix I). This indicates the formation of tertiary butyl cation during the reaction. On the other hand, presence of traces of water affords tertiary butyl alcohol, as expected. In the ^{1}H-NMR studies, the reaction of **2.1** with NO_2 was found to associate with the formation of tertiary butyl signal in the aliphatic region (Figure 2.3). GC-MS of the reaction mixture also reveals the formation of tertiary butyl alcohol. Thus, it is assumed that reduction of the Cu(II) center resulted in the nitration of the phenol ring as observed earlier.[8] This was further confirmed by isolation and characterization of the modified ligand (Experimental Section).

To the reaction mixture, addition of one more equivalent of NO_2 resulted in the appearance of a new d–d band at 660 nm along with a charge transfer band at 386 nm. The shift of charge transfer band is attributed to nitration at the phenol ring leading to the formation of modified ligand **L1′H**.[5] The appearance of the d–d band is presumably because of the formation of the corresponding intermediate $[Cu^{I}–NO_2]$ complex, which can be considered as $[Cu^{II}–NO_2^{-}]$. In X-band EPR also, the four lines characteristic for Cu(II) center appeared. In ^{1}H-NMR, the signals became broadened (Figure 2.3). These all are in agreement with the $[Cu^{II}–NO_2^{-}]$ formulation of the intermediate **2.2**. The isolation of the intermediate and structural characterization, indeed, revealed the formulation as $[Cu^{II}–NO_2^{-}]$. The ORTEP diagram of **2.2** is shown in figure 2.4a. A η^{1}-O coordination mode of nitrite to the Cu(II) center is observed. It is worth mentioning that in type 2 center of CuNIR and in almost all of its models, the nitrite ion binds to Cu(II) in O,O mode.[9] The $Cu–O_{nitrito}$ distances are 1.985(4) and 2.732(4) Å. The $Cu–O_{nitrito}$ bonding distances in other reported examples are ~2 Å. Cu–O–N angle is 116.0(4)°. The N–O distances are 1.250(7) and 1.202(7) Å. Note that though in comparison to other known Cu(II) nitrito complexes

this binding mode is uncommon, in cases of nitrito complexes of metallo-porphyrins, this is mostly observed mode.[4,5] In FT-IR spectrum, the band at 1275 cm^{-1} is assigned to the symmetric N–O stretch, υ_s(N–O) of nitrite (Appendix I).[9]

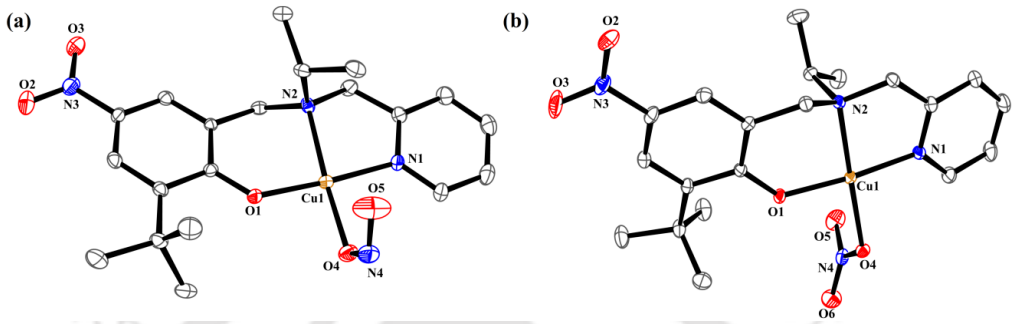

Figure 2.4. ORTEP diagrams of complexes (a) **2.2** and (b) **2.3** (35% thermal ellipsoid plot; hydrogen atoms are not shown for clarity).

Addition of NO_2 in the methanol solution of **2.2** leads to the shift of λ_{max} from 660 to 685 nm in UV-visible spectroscopy. In FT-IR studies, the nitrite stretching at 1275 cm^{-1} disappears with the appearance of a new intense stretching band at 1384 cm^{-1} (Appendix I). Isolation and structural characterization of the product revealed the formation of corresponding Cu(II) nitrate complex, **2.3**. The single-crystal X-ray structure of **2.3** is shown in figure 2.4b. In **2.3**, the nitrate ion is O-coordinated in a monodentate fashion.

In ESI-mass spectrum, the peak observed at *m/z* 900.088 corresponds to the mass of nitrato bridged dicopper unit $[\{Cu^{II}(L1')\}_2(NO_3)]^+$ (Appendix I). Expected and observed fragmentations in MS are found satisfactory. Thus, reaction of **2.2** with NO_2 in methanol results in the oxo transfer leading to the formation of corresponding nitrate complex, **2.3** and formation of NO is expected as side product. The release of NO was confirmed by GC-MS as well by spin trapping using iron(II)diethyldithiocarbamato complex.[10]

Note that addition of excess NO_2 in the methanol solution of **2.1** was found to result in the nitrato complex, **2.3** as the final product with simultaneous release of NO. In earlier

reports, Kurtikyan *et al.* has shown, using spectroscopic studies, that the reaction of Fe(II)(TPP) and Mn(II)(TPP) [TPP = *meso*-tetra-*p*-tolylporphyrinato dianion) with NO_2 leading to the formation of corresponding nitrato complex proceeds in two stages.[4,5] Low NO_2 pressure and short reaction time results in NO_2 coordination to the metal center and gives O-nitrito complex of Fe(III)(TPP) and Mn(III)(TPP), respectively. This was also reported earlier by Suslick and Watson.[11] Subsequently, presence of additional NO_2 leads to the formation of the corresponding η^1-ONO_2 complexes, presumably with the formation of NO.[4,5]

The conversion of **2.2** to **2.3**, *i.e.*, O-nitrito to O-nitrato analogue in the presence of NO_2, can be envisaged by two pathways as suggested earlier by Kurtikyan *et al*. in case of Fe(II)(TPP) or Mn(II)(TPP) complex.[4,5] The first mechanism would involve the attack of NO_2 to the coordinated O atom of nitrito moiety leading to the formation of O-nitrato analogue with concomitant displacement of NO from the originally coordinated nitrite (Scheme 2.2). Alternatively, oxygen atom transfers from free NO_2 to the nitrito N of Cu(II)–O–NO moiety (Scheme 2.2), which results in the O-nitrato analogue complex and NO. Though the possibility of the first pathway is very rare as the homolytic cleavage of O–N bond of O-nitrito Cu(II) complex is not known, to establish the mechanism, isotope labelling experiments were performed.

If the first pathway is operating, addition scrambled $^{16/18}O_2$ N will always result in **2.3** with single mass corresponding to [Cu(L1′)($^{16}O_2N^{18}O$)] with the formation of only $N^{16}O$ (Appendix I). On the other hand, if the second mechanism is operating, two equal intensity mass signals for [Cu(L1′)($^{16}O_2N^{18}O$)] and [Cu(L1′)($N^{16}O_3$)] are expected.

The mass spectrum of the reaction mixture, indeed, shows the presence of two equal intensity signals at *m*/*z* 902.0107 and 904.0239, respectively, for $[\{Cu^{II}(L1')\}_2(N^{16}O_3)]^+$

and $[\{Cu^{II}(L1')\}_2(^{18}ON^{16}O_2)]^+$ moiety (Appendix I). Thus, the second pathway is suggested as the most probable one (Scheme 2.2). On the other hand, when the reaction was performed with $^{15}NO_2$, the GC-MS analysis of the head space gas reveals the presence of ^{15}NO only (Appendix I). This is also in accord with the proposed mechanism (Scheme 2.2).

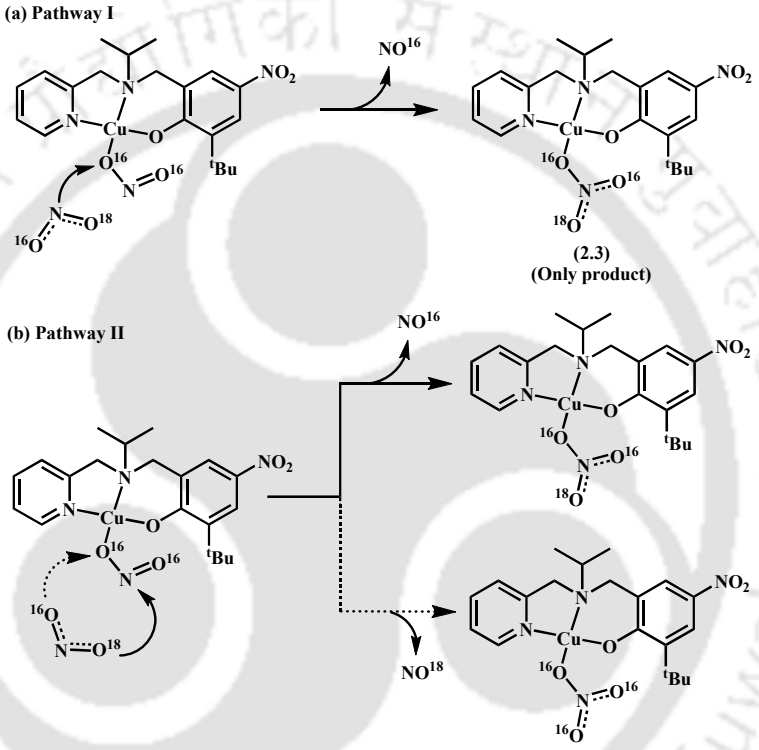

Scheme 2.2. Representative scheme for the probable mechanism.

The oxo transfer from NO_2 to Cu(II) nitrito complexes has not yet been observed, though found in Fe(II) and Mn(II) TPP complexes. However, only spectroscopic evidence was given for the intermediate steps. The reactivity of the present Cu(II) complex towards oxo transfer is perhaps due to the monodentate O-nitrito coordination of nitrite ion, which activates the nitrite for the reaction. This is in accord with the observations found in cases of other metal porphyrin complexes.

2.3 Experimental section

2.3.1 Materials and methods

All reagents and solvents of reagent grade were purchased from commercial sources and used as received except specified. $^{18}O_2$ was purchased from Icon Isotopes. Deoxygenation of the solvent and solutions was effected by repeated vacuum/purge cycles or bubbling with nitrogen or argon for 30 min. NO_2 was used from cylinder after purification using reported methods.[4,5] ^{18}ONO gas was prepared by the reaction of purified NO with $^{18}O_2$ in an airtight glass chamber fitted with a stoppered outlet at room temperature followed by removal of excess O_2 by passing through O_2 trap. Further purification was done following earlier reported methods of fractional distillation.[4,5] The isotopic enrichment of ^{18}O in $^{16/18}O_2N$ is 50% as measured by GC-MS. The dilution of NO_2 was effected with argon gas using Environics Series 4040 computerized gas dilution system. UV-visible spectra were recorded on a PerkinElmer Lambda 750 UV-vis spectrophotometer. FT-IR spectra of the solid samples were taken on a PerkinElmer spectrophotometer with samples prepared as KBr pellets. Solution electrical conductivity was measured using a Systronic 305 conductivity bridge. ^{1}H-NMR spectra were recorded in a 400 MHz Varian FT spectrometer. Chemical shifts (ppm) were referenced either with an internal standard (Me_4Si) or to the residual solvent peaks. The X-band EPR spectra were recorded on a JES-FA200 ESR spectrometer, at room temperature or at 77 K with microwave power of 0.998 mW, microwave frequency of 9.14 GHz, and modulation amplitude of 2. Elemental analyses were obtained from a PerkinElmer Series II Analyzer. The magnetic moment of complexes was measured on a Cambridge Magnetic Balance.

Single crystals were grown by slow diffusion followed by slow evaporation technique. The intensity data were collected using a Bruker SMART APEX-II CCD diffractometer,

equipped with a fine focus 1.75 kW sealed tube Mo Kα radiation (λ = 0.710 73 Å) at 293(3) K, with increasing ω (width of 0.3° per frame) at a scan speed of three seconds per frame. The SMART software was used for data acquisition.[12] Data integration and reduction were undertaken with SAINT and XPREP software.[13] Structures were solved by direct methods using SHELXS-97 and refined with full-matrix least-squares on F^2 using SHELXL-97.[14] Structural illustrations were drawn with ORTEP-3 for Windows.[15]

2.3.2 Synthesis of ligand L1H [L1H = 2,4-di-*tert*-butyl-6-((isopropyl(pyridin-2-ylmethyl)amino)methyl)phenol]

2-Picolylamine (1.08 g, 10 mmol) was dissolved in 20 mL of acetone and was stirred for 2 h to give Schiff's base, after which acetone was completely removed under vacuum. Then imine was dissolved in methanol (*ca.* 50 mL), and 2.1 equivalent of $NaBH_4$ was added slowly with continuous stirring. After completion of the reduction, the solvent was removed under vacuum, and to the crude mass 50 mL of water was added. The pH of the solution was maintained at ~7 pH by adding acetic acid. *N*-isopropyl-2-picolylamine was extracted from the solution by using dichloromethane (3 x 50 mL). Yield: 1.21 g (80%).

N-isopropyl-2-picolylamine (760 mg, 5 mmol), 2,4-di-*tert*-butylphenol (1.03 g, 5 mmol), and formalin (1.06 g of 37% solution, 13 mmol) were taken in methanol (*ca*. 10 mL), and the reaction mixture was refluxed for 24 h. Methanol was removed by using rotary evaporator, and after that 50 mL of water was added to the crude mixture; the organic part was extracted by dichloromethane. Purification using alumina column chromatography yielded pure ligand **L1H**. Yield: 1.19 g (65%). Elemental analysis for $C_{24}H_{36}N_2O$, calcd (%): C, 78.21; H, 9.85; N, 7.60; found (%): C, 78.28; H, 9.87; N, 7.73. FT-IR (KBr pellet) 2961, 1593, 1482, 1390, 1360, 1238, 1166, 1080 cm^{-1}: ^{1}H-NMR: (400 MHz, $CDCl_3$): δ_{ppm}: 8.51–8.50 (1H, d), 7.65–7.61 (1H, t), 7.42–7.40 (1H, d), 7.19 (1H, s), 7.15–7.12 (1H, t),

6.87 (1H, s), 3.80 (2H, s), 3.78 (2H, s), 3.15–3.06 (1H, m), 1.42 (9H, s), 1.27 (9H, s), 1.16–1.14 (6H, d). ^{13}C-NMR: (100 MHz, $CDCl_3$): δ_{ppm}: 159.1, 154.5, 149.1, 140.6, 136.8, 135.6, 124.0, 123.7, 122.9, 122.3, 121.5, 55.7, 53.8, 49.7, 35.1, 34.3, 31.9, 29.8, 17.3. Mass: Calcd: (368.283), Found: 369.295 (M+1).

2.3.3 Synthesis of complexes

(i) 2.1, [Cu(L1H)(O_2CCH_3)$_2$]

To a stirred solution of copper(II) acetate monohydrate $Cu(OAc)_2 \cdot H_2O$ (0.398 g, 2 mmol) in acetonitrile (*ca.* 20 mL) was added a solution of **L1H** (0.740 g, 2 mmol) in chloroform (*ca.* 20 mL). The reaction mixture was stirred for 2 h, and then the volume was reduced under vacuum to ~5 mL. A layer of benzene (10 mL) was made, and the mixture was kept in freezer over night to obtain **2.1** as green crystalline solid. Yield: 0.94 g (85%). Elemental analysis for $C_{28}H_{42}CuN_2O_5.CH_3CN$, calcd (%): C, 60.94; H, 7.67; N, 7.11; found (%): C, 60.99; H, 7.66; N, 7.19. UV–visible (methanol): λ_{max} 676 nm (ε/M^{-1} cm^{-1}, 400) and 470 nm (ε/M^{-1} cm^{-1}, 600). X-band EPR (in methanol at 77 K): $g_{\|}$, 2.369; $g_{\perp}$, 2.049. FT-IR (KBr pellet): 2948, 1707, 1687, 1610, 1587, 1474, 1385, 1288, 1174, 766 cm^{-1}. The complex **2.1** behaves as non-electrolyte in methanol solution [Λ_M (S cm^{-1}), 54]. The calculated magnetic moment is found to be 1.65 μ_B.

(ii) 2.2, [Cu(L1′)(η^1-ONO)]

Complex **2.1** (550 mg, 1.0 mmol) was dissolved in dry methanol (*ca*. 20 mL) in a Schlenk flask fitted with a rubber septum and degassed using argon gas. To this, 2 equivalent of NO_2/Ar (1:25 v/v) were added through a gastight syringe, and the mixture was stirred for 1/2 h. This volume of the solution was reduced under vacuum to ~5 mL, and a layer of diethyl ether (~10 mL) was made. The mixture was kept in freezer over night to afford **2.2**

as greenish solid. Yield: 0.350 g (~75%). Elemental analysis for $C_{20}H_{26}CuN_4O_5$, calcd (%): C, 51.55; H, 5.62; N, 12.02; found (%): C, 51.61; H, 5.61; N, 12.10. UV-visible (methanol): λ_{max} 660 nm (ε/M^{-1} cm^{-1}, 240), 386 nm (ε/M^{-1} cm^{-1}, 17890). X-band EPR (in methanol at 77 K): $g_{\parallel}$, 2.367; $g_{\perp}$, 2.058. FT-IR (KBr pellet): 2953, 1611, 1588, 1428, 1275, 1199, 1110, 770 cm^{-1}. The complex **2.2** behaves as non-electrolyte in methanol solution [Λ_M (S cm^{-1}), 40]. The calculated magnetic moment is found to be 1.68 μ_B.

(iii) 2.3, [Cu(L1′)(η^1-ONO_2)]

To a degassed solution of **2.1** (275 mg, 0.5 mmol) in dry methanol (*ca*. 10 mL), excess NO_2 gas was purged for 1 min. The resulting green colored solution was dried under vacuum to reduce its volume to ~5 mL. Diethyl ether (*ca*. 20 mL) was then added to give green precipitate of **2.3**. Product was further crystallized from acetonitrile solvent. Yield: 168 mg (70%). Elemental analysis for $C_{22}H_{29}CuN_5O_6.CH_3CN$, calcd (%): C, 51.10; H, 5.72; N, 14.89; found (%): C, 51.16; H, 5.74; N, 14.98. UV-visible (methanol): λ_{max} 685 nm (ε/M^{-1} cm^{-1}, 245), 370 nm (ε/M^{-1} cm^{-1}, 18840). X-band EPR (in methanol at 77 K): $g_{\parallel}$, 2.362; $g_{\perp}$, 2.060. FT-IR (KBr pellet): 2946, 1611, 1585, 1492, 1384, 1295, 1107, 776 cm^{-1}. The complex **2.3** behaves as non-electrolyte in methanol solution [Λ_M (S cm^{-1}), 47]. The calculated magnetic moment is found to be 1.60 μ_B. Alternatively, **2.3** can also be prepared by purging NO_2 into the methanol solution of **2.2**.

2.3.4 Isolation of modified ligand, L1′H [L1′H = 2-(*tert*-butyl)-6-((isopropyl(pyridin-2-ylmethyl)amino)methyl)-4-nitrophenol]

To 30 mL of methanol solution of **2.1** (550 mg), equivalent amount of freshly prepared NO_2/argon (1:25 v/v) was added through a gastight syringe. This resulting solution was allowed to stir for 10 min at room temperature. Then it was opened to air and continued

stirring for 1 h. The solvent was removed under vacuum using rotavapor, and then excess of aqueous Na_2S was added to give black precipitate. Solution was filtered and modified ligand **L1′H** was extracted with dichloromethane. Yield: 215 mg (60%). Elemental analyses for $C_{20}H_{27}N_3O_3$, calcd (%): C, 67.20; H, 7.61; N, 11.76; found (%): C, 67.29; H, 7.62; N, 11.87. FT-IR (in KBr): 2967, 1590, 1515, 1476, 1438, 1335, 1285, 1166, 1099, 902, 749 cm^{-1}. ^{1}H-NMR: (400 MHz, $CDCl_3$): δ_{ppm}: 8.56 (1H, s), 8.09 (1H, s), 7.83 (1H, s), 7.68–7.64 (1H, t), 7.32–7.30 (1H, d), 7.19 (1H, s), 3.88 (2H, s), 3.81 (2H, s), 3.13–3.10 (1H, m), 1.42 (9H, s), 1.18–1.16 (6H, d).). ^{13}C-NMR: (100 MHz, $CDCl_3$): δ_{ppm}: 164.0, 157.5, 149.4, 139.2, 137.5, 136.9, 123.5, 123.2, 122.6, 122.5, 54.8, 53.3, 49.9, 35.1, 29.1, 17.2. Mass: Calcd: (357.205), Found: 358.173 (M+1).

2.3.5 Spin-trapping experiment to establish the formation of NO

Complex **2.2** (300 mg) was dissolved in dry and degassed methanol (15 mL) in a Schlenk flask attached through a rubber tubing to another flask containing a solution of $[Fe^{II}(dtc)_2]$ (100 mg in 20 mL of acetonitrile). Equivalent amount of NO_2 gas (diluted using Ar gas; NO_2/Ar, 1:25 v/v) was purged in the solution of **2.2** using a gastight syringe. The mixture was stirred for 10 min. Ar gas was bubbled for 5 min through the reaction mixture to push the gas mixture into the flask containing $[Fe^{II}(dtc)_2]$. X-band EPR spectrum of this solution was then recorded to establish the presence of NO (Appendix I).

2.4 Conclusion

Thus, the reaction of Cu(II) complex $[Cu^{II}(L1H)(O_2CCH_3)_2]$ (**2.1**) with equivalent amount of NO_2 resulted in reduction of Cu(II) to Cu(I) with concomitant nitration at the phenol ring. The in situ generated intermediate Cu(I) complex of the nitrated ligand reacts with additional equivalent of NO_2 to afford corresponding O-nitrito Cu(II) complex, $[Cu^{II}(L1')(\eta^1\text{-ONO})]$ (**2.2**). It was not observed earlier. Subsequent addition of NO_2 led to

the corresponding O-nitrato complex $[Cu^{II}(L1')(\eta^1\text{-}ONO_2)]$ (**2.3**) with concomitant formation of NO. Complexes **2.2** and **2.3** were isolated and structurally characterized. Isotopic labeling experiment revealed that the oxo transfer takes place from NO_2 to the coordinated η^1-ONO group. The oxo transfer, though reported in cases of iron and manganese porphyrin complexes, was not found in literature in copper complexes.

2.5 References

(1) (a) Cosby, K.; Partovi, K. S.; Crawford, J. H.; Patel, R. P.; Reiter, C. D.; Martyr, S.; Yang, B. K.; Waclawiw, M. A.; Zalos, G.; Xu, X.; Huang, K. T.; Shields, H.; Kim-Shapiro, D. B.; Schechter, A. N.; Cannon, R. O.; Gladwin, M. T. *Nat. Med*. **2003**, *9*, 1498. (b) Feelisch, M.; Fernandez, B. O.; Bryan, N. S.; Garcia-Saura, M. F.; Bauer, S.; Whitlock, D. R.; Ford, P. C.; Janero, D. R.; Rodriguez, J.; Ashrafian, H. *J. Biol. Chem*. **2008**, *283*, 33927. (c) Luchsinger, B. P.; Rich, E. N.; Yan, Y.; Williams, E. M.; Stamler, J. S.; Singel, D. J. *J. Inorg. Biochem*. **2005**, *99*, 912.

(2) (a) Averill, B. A. *Chem. Rev*. **1996**, *96*, 2951. (b) Gladwin, M. T.; Grubina, R.; Doyle, M. P. *Acc. Chem. Res*. **2009**, *42*, 157. (c) Ford, P. C. *Inorg. Chem*. **2010**, *49*, 6226.

(3) van der Vliet, A.; Eiserich, J. P.; Halliwell, B.; Cross, C. E. *J. Biol. Chem*. **1997**, *272*, 7617.

(4) (a) Kurtikyan, T. S.; Hayrapetyan, V. A.; Mehrabyan, M. M.; Ford, P. C. *Inorg. Chem*. **2014**, *53*, 11948. (b) Kurtikyan, T. S.; Ford, P. C. *Angew. Chem. Int. Ed*. **2006**, *45*, 492.

(5) Kurtikyan, T. S.; Hovhannisyan, A. A.; Gulyan, G. M.; Ford, P. C. *Inorg. Chem*. **2007**, *46*, 7024.

(6) (a) Moura, I.; Moura, J. J. G. *Curr. Opin. Chem. Biol*. **2001**, *5*, 168. (b) Suzuki, S.; Kataoka, K.; Yamaguchi, K. *Acc. Chem. Res*. **2000**, *33*, 728.

(7) Thomas, F.; Gellon, G.; Gautier-Luneau, I.; Saint-Aman, E.; Pierre, J. L. *Angew. Chem. Int. Ed*. **2002**, *41*, 3047.

(8) Kumar, V.; Kalita, A.; Mondal, B. *Dalton Trans*. **2013**, *42*, 16264.

(9) Lehnert, N.; Cornelissen; Neese, F.; Ono, T.; Noguchi, Y.; Okamoto, K.-I.; Fujisawa, K. *Inorg. Chem*. **2007**, *46*, 3916.

(10) Melzer, M. M.; Mossin, S.; Dai, X.; Bartell, A. M.; Kapoor, P.; Meyer, K.; Warren, T. H. *Angew. Chem. Int. Ed*. **2010**, *49*, 904.

(11) Suslick, K. S.; Watson, R. A. *Inorg. Chem*. **1991**, *30*, 912.

(12) SMART, SAINT, and XPREP*;* Siemens Analytical X-ray Instruments Inc.: Madison, WI, **1995**.

(13) Sheldrick, G. M. SADABS*,* Software for Empirical Absorption Correction; University of Gottingen: Gottingen, Germany, **2003**.

(14) Sheldrick, G. M. SHELXS-97*;* University of Gottingen: Gottingen, Germany, **1997**.

(15) Farrugia, L. J. *J. Appl. Crystallogr*. **1997**, *30*, 565.

Chapter 3

Oxo Transfer Reaction in Cobalt(III)-nitro Complexes

Abstract

The oxo transfer reactivity in three Co(III)-nitro complex; **3.1**, **3.3** and **3.3** have been studied in degassed methanol solution with DMS. The complexes differ from each other from denticity and flexibility of the ligand frameworks. In case of **3.1** and **3.2** with tetradentate ligand, they give six coordinated nitro complexes with a weekly coordinated solvent molecule and were found to be active towards oxo transfer reaction stoichiometrically. On the other hand **3.3** with pentadentate ligand does not undergo the reaction in the given reaction condition.

3.1 Introduction

The development of metal catalysts that activate dioxygen and promote oxygen atom (O-atom) transfer has received increasing attention because of its biological significance and potential industrial applications.[1] In general, O-atom transfer reactions can be classified into two categories, namely, primary and secondary O-atom transfer. Primary O-atom transfer, which proceeds *via* metal-oxo intermediates (M^{n+}=O, where n = 4 or 5 and M = Mn, Fe, Ru or Re etc.), have been utilized to oxidize a variety of substrates, such as carbon monoxide, phosphines, and olefins.[2] In secondary O-atom transfer reactions, the oxygen atom transferred to the substrate is derived from a coordinated ligand.[1,3] An important set of such O-atom transfer reactions employs a coordinated nitro (NO_2) group. To date, various Fe(III)-NO_2 and Co(III)-NO_2 complexes, mostly derived from porphyrin and porphyrin-like ligands (heme-type catalysts), have been used to oxidize a variety of substrates that include nitric oxide, nitrite, carbon monoxide, dioxygen, dimethyl sulfide, alkenes, alcohols, phosphines and styrene *via* a nitro-nitrosyl redox couple.[4-6] The Fe(III)-NO_2 complexes have drawn special attention as biomimetic models of cytochrome P450 and nitrite reductase.[7] In contrast, the number of non-heme Fe(III)-NO_2 and non-porphyrin Co(III)-NO_2 catalysts that undergo stoichiometric, as well as catalytic, O-atom transfer remains quite limited.

This chapter demonstrates the difference of oxo transfer reactivity of cobalt(III)-nitro complexes with tetradentate and pentadentate salen type ligands. For the present study 2,4-di-*tert*-butylphenol derived three imine ligands [{**L2H$_2$** = 6,6'-((1E,1'E)-(((1R,2R)-cyclohexane-1,2-diyl)*bis*(azanylylidene))*bis*(methanylylidene))*bis*(2,4-di-*tert*-butyl-phenol)}; {**L3H$_2$** = 6,6'-((1E,1'E)-(propane-1,3-diyl)*bis*(azanylylidene)*bis*(methanyl-ylidene))*bis*(2,4-di-*tert*-butylphenol)} and {**L4H$_2$** = 6,6'-((1E,1'E)-((azanediylbis(ethane-

2,1-diyl))*bis*(azanylylidene))*bis*(methanylylidene))*bis*(2,4-di-*tert*-butylphenol)}] have been used (Figure 3.1).

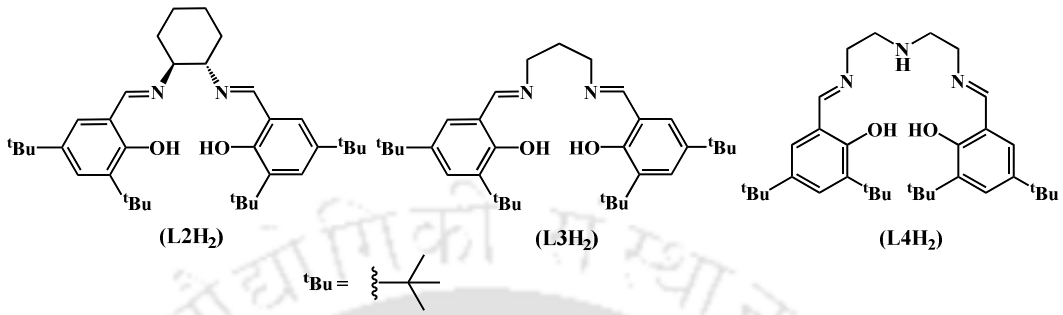

Figure 3.1. Ligands used for present study.

3.2 Results and discussion

The ligands were prepared by the general reaction of 3,5-di-*tert*-butylsalicylaldehyde with corresponding amine following an earlier reported procedure.[8] All the ligands were characterized by spectroscopic analyses as well as elemental analyses (Experimental Section).

Metallation was achieved by stirring the ligand with equivalent amount of cobalt(II) acetate tetrahydrate in methanol followed by the addition aqueous sodium nitrite solution (Experimental Section). The complexes were isolated as solid and characterized by spectral analyses (Experimental Section and Appendix II) and by their single crystal structure determination except for **3.2**. The ORTEP views of the complexes are given in figure 3.2. The crystal structure reveals that in **3.1**, the metal ion, Co(III) is in distorted octahedral geometry. Four N-atoms from ligand moiety occupy the square plane; one N-atom from nitro group and one solvent molecule occupies the axial positions. In **3.3**, Co(III) is also hexa-coordinated with five N-atoms from the ligand and one N-atom of nitro group to give a distorted octahedral geometry. The average Co-N distances were 1.889 and 1.919 Å,

respectively for **3.1** and **3.2**. The N-O distances of the coordinated NO_2^- were {1.244(8), 1.233(8)} and {1.256(6), 1.230(6)} Å, respectively. The Co-O_{phe} average bond distances were 1.891 and 1.899 Å, respectively. These values in the present cases are very much in agreement with the earlier reported cobalt(III)-nitro and cobalt(III)-phenolato complexes.[9] The crystallographic data, selected bond distances and angles are listed in tables 3.1, 3.2 and 3.3, respectively. However, even after several attempts X-ray quality single crystal of **3.2** was not obtained.

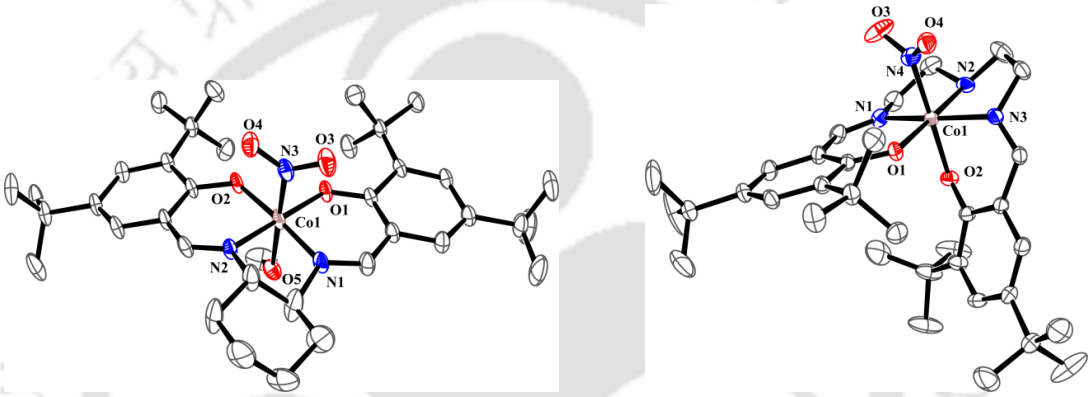

(a) **(b)**

Figure 3.2. ORTEP diagrams of complexes (a) **3.1** and (b) **3.3** (35% ellipsoid probability; H atoms and solvent atoms are not shown for clarity).

In the UV-visible spectroscopy, **3.1**, **3.2** and **3.3** in methanol solution show d-d transition at 690 nm (ε/M^{-1} cm^{-1}, 237), 650 nm (ε/M^{-1} cm^{-1}, 300) and 510 nm (ε/M^{-1} cm^{-1}, 110), respectively. All the three complexes are inactive in X-band EPR spectroscopy confirming the presence of Co(III) centre. ESI-mass spectrometry also confirms the formation of the corresponding complexes (Appendix II).

Oxo transfer reactivity

Addition of dimethyl sulfide (DMS) solution in methanol to dry and degassed methanol solution of complexes **3.1** and **3.2** at room temperature resulted in the formation of complexes **3.4** and **3.5**, respectively (Scheme 3.1).

Table 3.1. Crystallographic data of complexes **3.1**, **3.3**, **3.4** and **3.5**.

	3.1	**3.3**	**3.4**	**3.5**
Formulae	$C_{37}H_{55}CoN_3O_6$	$C_{34}H_{51}N_4CoO_5$	$C_{44}H_{68}CoN_3O_5$	$C_{68}H_{99}Co_2N_7O_6$
Mol. wt.	696.77	654.72	777.94	12228.40
Crystal system	Triclinic	Monoclinic	Monoclinic	Triclinic
Space group	P-1	P21/c	I2/c	P-1
Temperature /K	293(2)	293(2)	293(2)	293(2)
Wavelength /Å	0.71073	0.71073	0.71073	0.71073
a /Å	9.627(4)	177236(10)	33.5265(20)	14.3890(12)
b /Å	13.2214(11)	18.5021(7)	10.2466(6)	14.9164(11)
c /Å	16.8280(16)	12.1585(4)	28.366(2)	17.4843(14)
α/°	77.494(8)	90.00	90.00	77.639(6)
β/°	77.36(2)	102.530(5)	115.702(8)	70.221(7)
γ/°	88.740(18)	90.00	90.00	86.431(6)
V/ Å^3	2039.7(8)	3892.1(3)	8780.5(9)	3449.2(5)
Z	2	4	8	2
Density/Mgm^{-3}	1.134	1.117	1.177	1.183
Abs. Coeff. /mm^{-1}	0.463	0.480	0.435	0.533
Abs. correction	Multi-scan	Multi-scan	Multi-scan	Multi-scan
F(000)	746	1400	3360	1316
Total no. of reflections	7170	6848	7936	15582
Reflections, $I > 2\sigma(I)$	3603	4392	5247	9750
Max. 2θ/°	25.00	25.00	25.25	25.00
Ranges (h, k, l)	-10≤ h ≤11 -15≤ k ≤15 -19≤ l ≤ 19	-21≤ h ≤20 -21≤ k ≤22 -14≤ l ≤ 12	–40 ≤ h ≤ 40 –12 ≤ k ≤ 10 –21 ≤ l ≤ 34	–19 ≤ h ≤ 19 –16 ≤ k ≤ 18 –23 ≤ l ≤ 22
Complete to 2θ (%)	99.7	99.8	99.8	99.8
Refinement method	Full-matrix least-squares on F^2	Full-matrix least-squares on F^2	Full-matrix least-squares on F^2	Full-matrix least-squares on F^2
Goof (F^2)	1.055	0.979	1.182	0.806
R indices [$I > 2\sigma(I)$]	0.1063	0.0708	0.0730	0.0610
R indices (all data)	0.1738	0.1104	0.1116	0.1058

Table 3.2. List of selected bond lengths of complexes **3.1**, **3.3**, **3.4** and **3.5**.

	3.1	**3.3**	**3.4**	**3.5**
N3-O3	1.244(8)	-	1.085(6)	1.032(8)
N3-O4	1.233(8)	-	-	-
Co1-N1	1.877(7)	1.887(5)	1.893(3)	1.915(3)
Co1-N2	1.895(5)	1.943(4)	1.879(3)	1.920(3)
Co1-N3	1.896(7)	1.917(4)	1.809(5)	1.792(4)
Co1-O1	1.895(4)	1.895(3)	1.877(3)	1.904(2)
Co1-O2	1.887(5)	1.903(3)	1.869(3)	1.876(2)
N4-O3	-	1.256(6)	-	-
N4-O4	-	1.230(6)	-	-
Co1-N4	-	1.929(5)	-	-

Table 3.3. List of selected bond angles of complexes **3.1**, **3.3**, **3.4** and **3.5**.

	3.1	**3.3**	**3.4**	**3.5**
N1-Co1-O1	94.1(2)	95.07(16)	92.98(13)	90.96(10)
N1-Co1-O2	174.1(3)	87.91(17)	169.81(14)	147.55(12)
N2-Co1-O2	94.1(2)	90.79(16)	93.78(13)	92.59(11)
N2-Co1-O1	179.2(3)	177.96(16)	161.49(14)	176.26(12)
N1-Co1-N2	85.2(3	85.75(19)	85.03(14)	90.15(12)
N3-Co1-O5	179.5(3)	-	-	-
O1-Co1-O2	86.6(2)	91.11(15)	84.94(12)	84.57(10)
N1-Co1-N3	-	166.02(17)	95.59(19)	102.92(19)
Co1-N3-O3	118.7(6)	-	125.8(5)	130.6(9)
Co1-N3-O4	120.3(6)	-	-	-
O3-N3-O4	121.0(8)	-	-	-
O3-N4-O4	-	119.0(5)	-	-
Co1-N4-O3	-	120.8(4)	-	-
Co1-N4-O4	-	120.0(4)	-	-

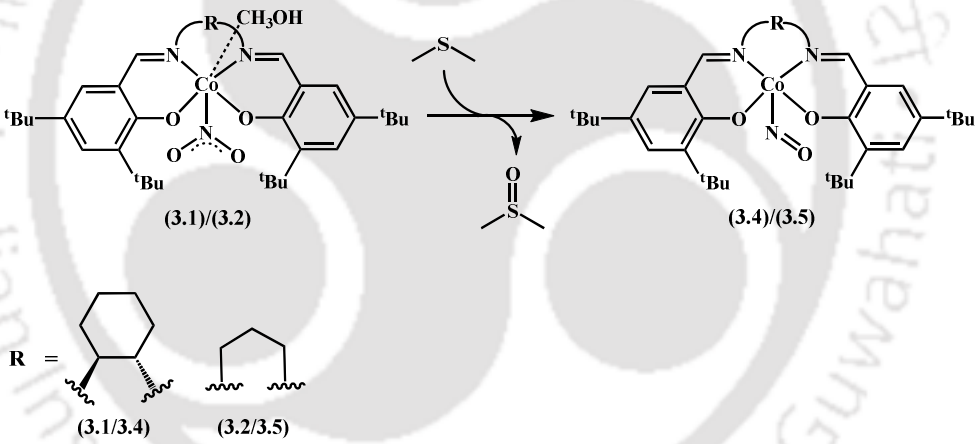

Scheme 3.1. Reaction of complexes **3.1** and **3.2** with DMS in methanol.

The color of the solutions changed to reddish brown from light red in course of the reaction. In UV-visible spectroscopy, the absorption bands at 690 and 650 nm for **3.1** and **3.2**, respectively diminished upon addition of DMS (Figure 3.3). In FT-IR spectroscopy, N-O stretching of coordinated NO_2^- groups which appear at 1358 and 1361 cm^{-1}, respectively, for **3.1** and **3.2**, were found to diminish after addition of DMS and new stretching frequencies appeared at 1650 and 1659 cm^{-1} (Figure 3.4).

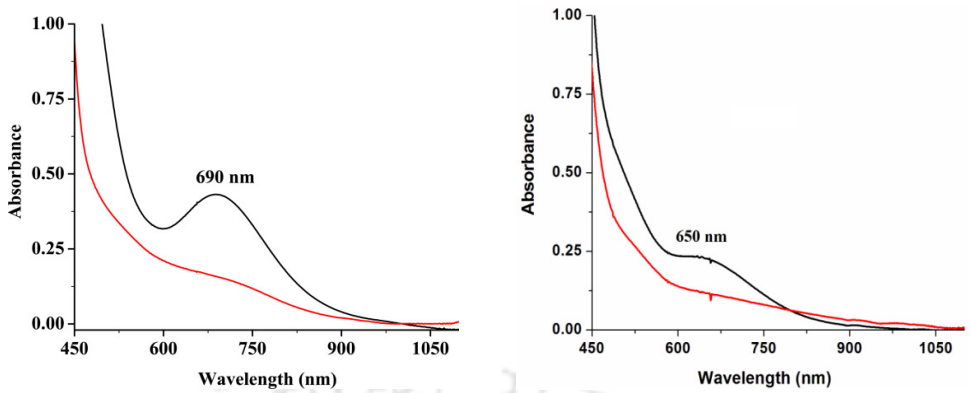

(a) **(b)**

Figure 3.3. UV-visible spectra of complexes (a) **3.1** (black) and after addition of DMS (red); (b) **3.2** (black) and after addition of DMS (red).

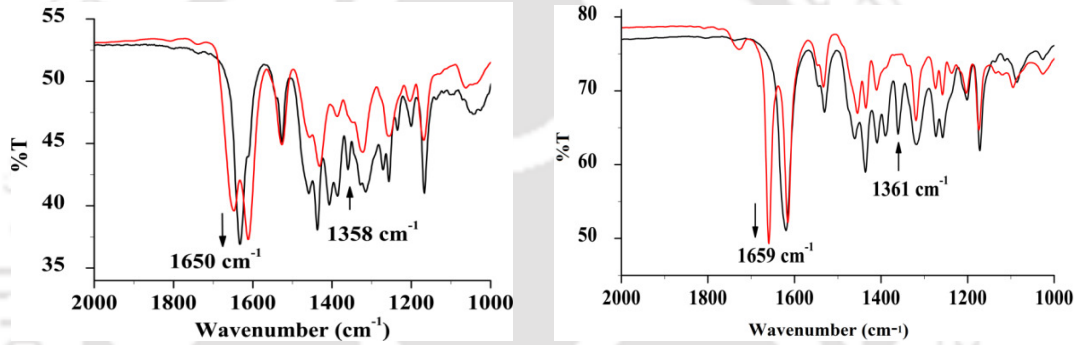

(a) **(b)**

Figure 3.4. FT-IR spectra of complexes (a) **3.1** (black) and after addition of DMS (red); (b) **3.2** (black) and after addition of DMS (red).

These frequencies are assignable to the coordinated nitrosyl group. These low energy stretching band for metal-nitrosyl is consistent with $[Co^{III}(NO^{-})]$ or $\{CoNO\}^{8}$ formulation.[10] In the case of recently reported $[Co^{III}(NO^{-})]$ complexes bearing 12- and 13-membered N-tetramethylated cyclam (TMC) ligands, $[(12\text{-TMC})Co^{III}(NO)]^{2+}$ (12-TMC = 1,4,7,10-tetramethyl-1,4,7,10-tetraazacyclododecane) and $[(13\text{-TMC})Co^{III}(NO)]^{2+}$ (13-TMC = 1,4,7,10-tetramethyl-1,4,7,10-tetraazacyclotridecane), these frequencies were observed at 1712 and 1716 cm^{-1}, respectively.[11] In X-band EPR studies, both **3.4** and **3.5** were found to be inactive supporting the formation of $\{CoNO\}^{8}$ species.[10,11] ESI-mass of **3.4** and **3.5** exhibit ion peak at m/z 603.29 and 563.36 respectively (Appendix II).

Both the complexes **3.4** and **3.5** were characterized by single crystal X-ray structure determination. ORTEP diagrams are shown in figure 3.5. Single crystal structures of both **3.4** and **3.5** reveal the presence of $\{CoNO\}^8$ moieties where cobalt is coordinated by four N-atoms from the ligand to occupy the square plane and one axial NO group which gives a distorted square pyramidal geometry. The Co-N_{NO} distances were 1.809(5) and 1.792(4) Å, respectively for **3.4** and **3.5**. The N-O distances of the coordinated NO were 1.085(6) and 1.032(8) Å, respectively. This distance is within the range of bent nitrosyls. In cases of $[(12\text{-TMC})Co(NO)]^{2+}$ and $[(13\text{-TMC})Co(NO)]^{2+}$, the N-O bond lengths were 1.155 and 1.159 Å respectively.[11] The Co-N-O angles are 125.8° and 130.6°, respectively in **3.4** and **3.5** suggesting a large bending of the metal nitrosyl unit. For $[(12\text{-TMC})Co(NO)]^{2+}$ and $[(13\text{-TMC})Co(NO)]^{2+}$, the Co-N-O angles were reported as 128.50° and 124.4°, respectively. The values in the present cases are very much in agreement with the earlier reported $[Co^{III}(NO^{-})]$ complexes. The bending nature is also consistent with the NO^{-} description.[10,11]

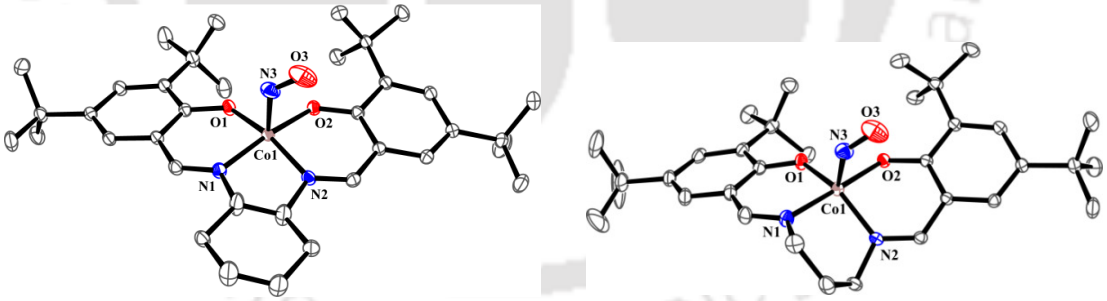

(a) **(b)**

Figure 3.5. ORTEP diagrams of complexes (a) **3.4** and (b) **3.5** (35% ellipsoid probability; H atoms and solvent atoms are not shown for clarity).

The conversion of nitro groups of **3.1** and **3.2** to corresponding nitrosyl moieties is presumably proceeds *via* an oxo transfer mechanism. The reaction is initiated by the addition of DMS and thus it is expected to result in the formation of dimethyl sulfoxide (DMSO). GC-mass analysis of the headspace gas of the reaction mixtures shows the

presence of unreacted DMS, while analysis of the solution part suggests the presence of DMSO (Appendix II). Again, addition of equivalent amount of DMS only results in formation of DMSO, but when the reaction was performed with two or more equivalents of DMS, presence of excess DMS was observed. This also confirms that the reaction was stoichiometric in nature and was not found to be catalytic even when reaction was performed in presence of O_2. This can be attributed to the un-reactive nature of the **3.4** and **3.5** towards O_2 in the given reaction conditions. However, complex **3.3** was found to be inert toward oxo transfer reactivity in similar reaction condition. No spectral change was observed after addition of DMS.

Thus, while moving from complexes **3.1**, **3.2** to **3.3**, the oxo transfer reactivity of the complexes changes. The ligand framework including denticity has a considerable effect on dictating oxo transfer reactivity of a complex.

3.3 Experimental section

3.3.1 Materials and methods

All reagents and solvents of reagent grade were purchased from commercial sources and used as received. All the reactions were performed under inert conditions unless specified. Deoxygenation of the solvent and solutions was effected by repeated vacuum/purge cycles or bubbling with argon for 30 min. UV-visible spectra were recorded on an Agilent Technologies Cary 8454 UV-visible spectrophotometer. FT-IR spectra of the samples were taken on a Perkin Elmer spectrophotometer with samples prepared either as KBr pellets or in dichloromethane solution in KBr cell. ^{1}H-NMR spectra were recorded in a 600 MHz Varian FT spectrometer. Chemical shifts (ppm) were referenced either with an internal standard (Me_4Si) or to the residual solvent peaks. The X-band Electron Paramagnetic Resonance (EPR) spectra were recorded on a JES-FA200 ESR spectrometer, at room

temperature with microwave power, 0.998 mW; microwave frequency, 9.14 GHz and modulation amplitude, 2. Elemental analyses were obtained from a Perkin Elmer Series II Analyzer.

Single crystals were grown by slow evaporation of solvents from the corresponding complex solutions. The intensity data were collected using a Bruker SMART APEX-II CCD diffractometer, equipped with a fine focus 1.75 kW sealed tube MoK_α radiation (λ = 0.71073 Å) at 293(3) K, with increasing ω (width of 0.3° per frame) at a scan speed of 3 s/frame. The SMART software was used for data acquisition. Data integration and reduction were undertaken with SAINT and XPREP software.[12] Multi-scan empirical absorption corrections were applied to the data using the program SADABS.[13] Structures were solved by direct methods using SHELXS-2014 and refined with full-matrix least squares on F^2 using SHELXL-2014/7.[14] Structural illustrations have been drawn with ORTEP-3 for Windows.[15]

3.3.2 Synthesis of ligands

(i) $L2H_2$ [$L2H_2$ = 6,6'-((1E,1'E)-(((1R,2R)-cyclohexane-1,2-diyl)*bis*(azanylylidene))-*bis*(methanylylidene))*bis*(2,4-di-*tert*-butylphenol)]

The imine ligand, **$L2H_2$** was prepared following an earlier reported procedure.[16] *trans*-1,2-Cyclohexanediamine (1.14 g, 10 mmol) was treated the presence of 2 equivalent of 2,4-di-*tert*-butylsalicylaldehyde (4.68 g, 20 mmol) in 20 mL ethanol solution at room temperature. The reaction mixture was allowed to stir for 4 h. A yellow colored solid was precipitated out. It was filtered off and washed with cold ethanol. After washing the solid was dried in air and kept in desiccators for overnight. Yield: 4.81 g (88%). Elemental analyses for $C_{36}H_{54}N_2O_2$, Calcd (%): C, 79.07; H, 9.95; N, 5.12. Found (%): C, 78.95; H,

9.98; N, 5.24. FT-IR (in KBr): 3430, 2959, 2867, 1630, 1468, 1438, 1270, 1173, 878, 772, 644 cm^{-1}. ^{1}H-NMR (400 MHz, $CDCl_3$): δ_{ppm}, 8.30 (1H, s), 7.30-7.29 (1H, d), 6.99-6.98 (1H, d), 3.35-3.28 (1H, m), 2.02-1.93 (2H, m), 1.80-1.69 (2H, m), 1.41 (9H, s), 1.23 (9H, s). ^{13}C-NMR (100 MHz, $CDCl_3$): δ_{ppm}, 166.0, 158.2, 140.1, 136.5, 126.9, 126.2, 118.0, 72.6, 35.1, 34.2, 33.5, 31.6, 29.6, 24.6.

(ii) $L3H_2$ [$L3H_2$ = 6,6'-((1E,1'E)-(propane-1,3-diyl)*bis*(azanylylidene)*bis*-(methanylylidene))*bis*(2,4-di-*tert*-butylphenol)]

The reported imine ligand **$L3H_2$** was also prepared following the same procedure as for **$L2H_2$**. To the solution of 1,3-diaminopropylamine (0.6 g, 10 mmol) in 10 mL ethanol, 20 mL ethanol solution of 2,4-di-*tert*-butylsalicylaldehyde (4.68 g, 20 mmol) was added drop wise at room temperature. The reaction mixture was allowed to stir for 4 h till yellow colored precipitate formed. It was filtered off and washed with cold ethanol. After washing the solid was dried in air and kept in desiccators for overnight. Yield: 4.1 g (83%). Elemental analyses for $C_{33}H_{50}N_2O_2$, Calcd. (%): C, 78.21; H, 9.95; N, 5.53. Found (%): C, 78.05; H, 9.98; N, 5.65. FT-IR (in KBr): 3436, 2958, 2867, 1632, 1466, 1441, 1275, 1254, 1173, 1032, 829, 774 cm^{-1}. ^{1}H-NMR (400 MHz, $CDCl_3$): δ_{ppm}, 8.37 (1H, s), 7.37-7.36 (1H, d), 7.07-7.06 (1H, d), 3.70-3.67 (2H, t), 2.14-2.07 (1H, m), 1.43 (9H, s), 1.28 (9H, s). ^{13}C-NMR (100 MHz, $CDCl_3$): δ_{ppm}, 167.7, 158.3, 140.2, 136.8, 127.1, 126.0, 118.0, 57.0, 35.3, 34.4, 31.9, 31.7, 29.6.

(iii) $L4H_2$ [$L4H_2$ = 6,6'-((1E,1'E)-((azanediyl)*bis*(ethane-2,1-diyl))*bis*-(azanylylidene))*bis*(methanylylidene))*bis*(2,4-di-*tert*-butylphenol)]

The reported imine ligand **$L4H_2$** was also prepared following the same procedure as for **$L2H_2$**. *N*-(2-aminoethyl)ethane-1,2-diamine (1.03 g, 10 mmol) was taken in a round

bottom flask in 50 mL of ethanol. To this, 2.96 g (20 mmol) of 2,4-di-*tert*-butylsalicylaldehyde was added drop wise. The reaction mixture was stirred for 2 hour to give yellow precipitate of ligand **L4H$_2$**. Yield: 2.75 g (75%). Elemental analyses for $C_{34}H_{53}N_3O_2$, Calcd (%): C, 76.22; H, 9.97; N, 7.84; Found (%): C, 76.08; H, 9.95; N, 7.95. FT-IR (in KBr): 3438, 2957, 2867, 1631, 1472, 1441, 1360, 1272, 1248, 1175, 880, 773 cm^{-1}. ^{1}H-NMR (400 MHz, $CDCl_3$) δ_{ppm}: 8.41 (1H, s), 7.41-7.40 (1H, d), 7.11-7.10 (1H, d), 3.74-3.72 (2H, t), 3.03-3.01 (2H, t), 1.46 (9H, s), 1.32 (9H, s). ^{13}C-NMR (100 MHz, $CDCl_3$) δ_{ppm}: 167.3, 158.2, 140.2, 136.8, 127.1, 126.1, 118.0, 59.8, 50.1, 35.2, 34.3, 31.7, 29.6.

3.3.3 Synthesis of complexes

(i) 3.1, [(L2)Co(NO$_2$)(CH$_3$OH)]

Cobalt(II) acetate tetrahydrate (1.25 g, 5 mmol) was taken in a 50 mL round bottom flask, dissolved in 10 mL of methanol. To this, equivalent amount of ligand **L2H$_2$** (2.73 g, 5 mmol) in hot methanol (25 mL) was added followed by the addition of 2 mL of an aqueous solution of sodium nitrite (10 mmol) and stirred for 24 h in aerobic condition. Resulting brown colored solution was dried under vacuum, and residue was washed with distilled water. Finally it was kept in desiccators for overnight and was then recrystallized from slow evaporation of methanol/chloroform solution. Yield: 2.11 g (70%). Elemental analyses for $C_{36}H_{52}N_3O_4Co$, Calcd (%): C, 66.55; H, 8.07; N, 6.47. Found (%): C, 66.47; H, 8.20; N, 6.59. FT-IR (in KBr): 3436, 2950, 2864, 1632, 1526, 1436, 1407, 1358, 1314, 1166, 782 cm^{-1}. UV-visible (methanol): 690 nm (ε/M^{-1}cm^{-1}, 237). Mass (m/z): calcd: 649.33 for [Co(L2)(NO$_2$)], found: 650.31 (M+1).

(ii) 3.2, [(L3)Co(NO$_2$)(CH$_3$OH)]

Complex **3.2** was prepared with ligand **L3H$_2$** following the same procedure as for **3.1** (2.46 g, 5 mmol). Even after several attempts X-ray quality crystals were not grown. Yield: 1.77g (72%). Elemental analyses for $C_{33}H_{48}N_3O_4Co$, Calcd (%): C, 65.01; H, 7.94; N, 6.89. Found (%): C, 64.95; H, 7.98; N, 6.92. FT-IR (in KBr): 2953, 2867, 1620, 1513, 1436, 1408, 1361, 1318, 1171, 778 cm^{-1}. UV-visible (CH_3OH): 650 nm (ε/M^{-1}cm^{-1}, 300). Mass (m/z): calcd: 609.30 for [Co(L3)(NO_2)], found: 610.36 (M+1).

(iii) 3.3, [(L4)Co(NO_2)]

Complex **3.3** was prepared with ligand **L4H$_2$** following the same procedure as for **3.1** (2.46 g, 5 mmol). X-ray quality crystals were grown by slow diffusion of dichloromethane solution. Yield: 1.77g (72%). Elemental analyses for $C_{34}H_{51}N_4O_4Co$, Calcd (%): C, 63.93; H, 8.05; N, 8.77. Found (%): C, 63.88; H, 8.17; N, 8.71. FT-IR (in KBr): 2955, 2868, 1636, 1530, 1437, 1362, 1314, 1169, 780 cm^{-1}. UV-visible (methanol): 510 nm (ε/M^{-1} cm^{-1}, 110). Mass (m/z): calcd: 638.32 for [Co(L4)(NO_2)], found: 639.34 (M+1).

(iv) 3.4, [(L2)Co(NO)]

To a degassed solution of **3.1** (89 mg, 0.2 mmol) in methanol (*ca*. 5 mL), excess of DMS (1 mmol) was added. The solution was then allowed to stir for 2 h at room temperature. To this resulting light reddish brown solution, degassed diethyl ether (*ca.* 20 mL) was added and kept in freeze for overnight. Dark brown solid of **3.4** was obtained and washed with cold and degassed methanol. Yield: (77%). X-ray quality crystals were obtained when saturated THF solution was kept at room temperature for several days. Elemental analyses for $C_{36}H_{52}N_3O_3Co$, Calcd (%): C, 68.23; H, 8.27; N, 6.63. Found (%): C, 68.05; H, 8.44; N, 6.77. FT-IR (KBr pellet): 2952, 2863, 1650, 1611, 1525, 1432, 1322, 1255, 1167, 783 cm^{-1}. Mass (m/z): calcd: 603.33 for [Co(L2)]$^+$, found: 603.29.

(v) 3.5, [(L3)Co(NO)]

Complex **3.5** was prepared from **3.2** following the same procedure as for **3.4**. Yield: (68%). X-ray quality crystals were grown from slow diffusion of acetonitrile solution into diethyl ether at room temperature. Elemental analyses for $C_{33}H_{48}N_3O_3Co$, Calcd (%): C, 66.76; H, 8.15; N, 7.08. Found (%): C, 66.68; H, 8.23; N, 7.10. FT-IR (KBr pellet): 2954, 2868, 1659, 1615, 1532, 1454, 1409, 1319, 1172, 784 cm^{-1}. Mass (m/z): calcd: 563.31 for $[Co(L3)]^+$, found: 563.36.

3.3.4 Detection of DMSO by GC-mass

Dilute methanol solution of complexes **3.1** or **3.2** was taken in a 10 mL round bottom flask. To this, two equivalent of DMS solution in methanol was added and was allowed to stir for 2 h. Analysis of the headspace gas of the reaction mixture by GC-mass suggests the presence of unreacted DMS. The resulting solution was then dried under vaccum and residue was washed with hexane to collect the organic part for GC-mass analysis. Formation of DMSO was observed. When the same reaction was carried out with equivalent amount of DMS, presence of excess DMS was not observed in GC-mass.

3.4 Conclusion

The oxo transfer reactivity of three Co(III)-nitro complex; **3.1**, **3.3** and **3.3** have been studied in degassed methanol solution with DMS. The complexes differ from each other from denticity and flexibility of the ligand frameworks. In case of **3.1** and **3.2** with tetradentate ligand, they give six coordinated nitro complexes with a weekly coordinated solvent molecule and were found to be active towards oxo transfer reaction stoichiometrically. On the other hand complex **3.3** with pentadentate ligand does not undergo the reaction in the given reaction condition.

3.5 References

(1) (a) Holm, R. H. *Chem. Rev*. **1987**, *87*, 1401. (b) Meunier, B. *Metal-Oxo and Metal-Peroxo Species in Catalytic Oxidations*; *Structure and Bonding*, Vol. 97, Springer, Berlin, **2000**. (c) Meunier, B. *Biomimetic Oxidations Catalyzed by Transition Metal Complexes* Imperial College Press, London, **2000**.

(2) (a) Miller, C. G.; Gordon-Wylie, S. W.; Horwitz, C. P.; Strazisar, S. A.; Periano, D. K.; Clark, G. R.; Weintraub, S. T.; Collins, T. J. *J. Am. Chem. Soc.* **1998**, *120*, 11540. (b) Chen, M. J.; Fremgen, D. E.; Rathke, J. W. *J. Porphyrins Phthalocyanines* **1998**, *2*, 473. (c) Bhattacharya, S.; Chakraborty, I.; Dirghangi, B. K.; Chakravorty, A. *Inorg. Chem.* **2001**, *40*, 286.

(3) a) Foote, C. S.; Valentine, J. S.; Greenberg, A.; Liebman, J. F. *Active Oxygen in Chemistry* Vol. 2, Chapman & Hall, London, **1995**. (b) Barton, D. H. R.; Martell, A. E.; Sawyer, D. T. *The Activation of Dioxygen and Homogeneous Catalytic Oxidation* Plenum, New York, **1993**.

(4) (a) Kurtikyan, T. S.; Hayrapetyan, V. A.; Mehrabyan, M. M.; Ford, P. C. *Inorg. Chem.* **2014**, *53*, 11948. (b) Kurtikyan, T. S.; Ford, P. C. *Angew. Chem. Int. Ed.* **2006**, *45*, 492. (c) Kurtikyan, T. S.; Hovhannisyan, A. A.; Gulyan, G. M.; Ford, P. C. *Inorg. Chem.* **2007**, *46*, 7024.

(5) Feltham, R. D.; Kreige, J. C. *J. Am. Chem. Soc*. **1979**, *101*, 5064.

(6) (a) Patra, A. K.; Afshar, R. K.; Rowland, J. M.; Olmstead, M. M.; Mascharak, P. K. *Angew. Chem. Int. ed.* **2003**, *115*, 4655. (b) Afshar, R. K.; Eroy-Reveles, A. A.; Olmstead, M. M.; Mascharak, P. K. *Inorg. Chem*. **2006**, *45*, 10347.

(7) (a) Finnegan, M. G.; Lappin, A. G.; Scheidt, R. W. *Inorg. Chem.* **1990**, *29*, 181. (b) Nasri, H.; Wang, Y.; Huynh, B. H.; Scheidt, R. W. *J. Am. Chem. Soc.* **1991**, *113*, 717. (c) Munro, O. Q.; Scheidt, R. W. *Inorg. Chem.* **1998**, *37*, 2308.

(8) (a) Chiang, L.; Herasymchuk, K.; Thomas, F.; Storr, T. *Inorg. Chem.* **2015***, 54,* 5970. (b) Rotthaus, O.; Thomas, F.; Jarjayes, O.; Philouze, C.; Saint-Aman, E.; Pierre, J.-L. *Chem. Eur. J*. **2006**, *12*, 6953.

(9) (a) Guzeia, I. A.; Arderne, C. *Acta Cryst.* **2015**. *C71*, 695. (b) Cohen, C. T.; Thomas, C. M.; Peretti, K. L.; Lobkovsky, E. B.; Coates, G. W. *Dalton Trans*. **2006**, 237. (c) Cyriac, A.; Jeon, J. Y.; Varghese, J. K.; Park, J. H.; Choi, S. Y.; Chung, Y. K.; Lee, B. Y. *Dalton Trans*. **2012**, *41*, 1444.

(10) (a) Enemark, J. H.; Feltham, R. D. *Coord. Chem. Rev.* **1974**, *5*, 686. (b) Richter-Addo, G. B.; Legzdins, P. *Metal Nitrosyls*, Oxford University Press: New York, **1992**. (c) McCleverty, J. A. *Chem. Rev.* **2004**, *104*, 403. (d) Berto, T. C.; Speelman, A. L.; Zheng, S.; Lehnert, N. *Coord. Chem. Rev.* **2013**, *257*, 244.

(11) Kumar, P.; Lee, Y. M.; Park, Y. J.; Siegler, M. A.; Karlin, K. D.; Nam, W. *J. Am. Chem. Soc.* **2015**, *137*, 4284.

(12) *SMART*, *SAINT and XPREP*, Siemens Analytical X-ray Instruments Inc., Madison, Wisconsin, USA, **1995**.

(13) Sheldrick, G. M. *SADABS*: *software for Empirical Absorption Correction*, University of Gottingen, Institut fur Anorganische Chemieder Universitat, Tammanstrasse 4, D-3400 Gottingen, Germany, **1999**.

(14) Sheldrick, G. M. *SHELXS-2014*, University of Gottingen, Germany.

(15) Farrugia, L. J. *J. Appl. Crystallogr.* **1997**, *30*, 565.

(16) a) Chiang, L.; Herasymchuk, K.; Thomas, F.; Storr, T. *Inorg. Chem.* **2015**, *54*, 5970. (b) Rotthaus, O.; Thomas, F.; Jarjayes, O.; Philouze, C.; Saint-Aman, E.; Pierre, J.-L. *Chem. Eur. J*. **2006**, *12*, 6953.

Chapter 4

Dioxygenation Reaction of a Cobalt-nitrosyl: Putative Formation of a Cobalt–peroxynitrite *via* a $\{Co^{III}(NO)(O_2^-)\}$ Intermediate

Abstract

A cobalt-nitrosyl complex, [(L5)Co(NO)(OAc)], **4.1** {**L5H** = 1,3-bis(2′-pyridylimino)isoindol} was prepared and characterized. Structural characterization revealed that the cobalt center is having a distorted square pyramidal geometry with the NO group coordinated from the apical position in a bent fashion. The addition of dioxygen (O_2) to the dichloromethane solution of complex **4.1** resulted in the formation of nitro complex, [(L5)Co(NO_2)(OAc)], **4.2**. It was characterized structurally. Kinetic studies suggested the involvement of an associative mechanism. FT-IR spectroscopic studies suggested the formation of the intermediate **4.1a** [(L5)Co^{III}(NO)(O_2^-)(OAc)] in the reaction. The intermediate **4.1a** decomposed to complex **4.2** *via* a presumed peroxynitrite intermediate which was implicated by its characteristic phenol ring nitration reaction.

4.1 Introduction

Nitric oxide (NO) is an important regulatory molecule in mammalian biology. It is known to play the key roles in diverse biological processes such as neurotransmission, immune response etc.[1-4] It has been found that the submicromolar concentrations of NO are sufficient for its functions but an overproduction of it has a detrimental effect due to the formation of peroxynitrite anion (PN, $ONOO^-$) and other secondary reactive nitrogen species which induce oxidative damage to DNA, lipids, proteins etc.[5,6] Nitric oxide deoxygenases (NOD) are known to control the level of NO in biological systems. In NODs, the reaction of the Fe(III)-superoxide species with NO results in the biologically benign nitrate (NO_3^-) ion.[7] This reaction is believed to proceed through the formation of a metal-peroxynitrite intermediate.[7,8] It is believed that $ONOO^-$ intermediate forms in the diffusion controlled reaction between NO and superoxide anion or H_2O_2 and nitrite (NO_2^-) in the presence of the peroxidase enzymes.[9]

The biological relevance of NO inspires a wide range of studies of its coordination and interaction with transition metal centers and subsequently, their dioxygenation reaction. An extensive study has been done in this direction with the Fe-proteins and their models.[7,10] Recently, the examples involving other transition metal ions in the generation and reactivity of $ONOO^-$ are reported.[11] Recently, Karlin's group reported the example of a peroxynitrite complex from the reaction of a mixed-valent nitrosyl complex of Cu(I)Cu(II), $[Cu^{I,II}_2(UN\text{-}O^-)(NO)]^{2+}$ with O_2. It has been shown that the reaction resulted in the corresponding superoxide and nitrosyl adduct, $[Cu^{II}_2(UN\text{-}O^-)(NO)(O_2^-)]^{2+}$ in the first step and it was subsequently converted to the corresponding peroxynitrite complex.[12] A Cu-peroxynitrite intermediate was also

proposed recently in the reaction of a Cu(I)-nitrosyl complex with O_2 to result in the corresponding NO_2^-.[13] Recently, it has been shown that the reaction Cu(II)-nitrosyl complexes with H_2O_2 results in the copper-nitrato complexes *via* a presumed Cu-peroxynitrite intermediate.[14] The reaction of non-heme Cr(IV)-peroxo and Cr(III)-superoxo complexes with NO were reported to result in the presumed Cr(III)-peroxynitrite intermediate.[15] A Co-nitrosyl complex was reported to react with O_2 to result in the corresponding nitrite (NO_2^-) product by Clarkson and Basolo.[16] The Co(III)-nitrosyl complexes of 12 and 13 membered N-tetramethylated cyclam ligands, $[(12\text{-TMC})Co^{III}(NO)]^{2+}$ and $[(13\text{-TMC})Co^{III}(NO)]^{2+}$ [12-TMC = 1,4,7,10-tetramethyl-1,4,7,10-tetraazacyclododecane] were reported to react with the superoxide ion resulting in the Co(II)-nitrite where the involvement of Co(III)-peroxynitrite intermediate was presumed.[17] Very recently it has been demonstrated that a nitrosyl complex of Co-porphyrinate reacts with H_2O_2 to result in Co(III)-nitrite.[18] The chemical evidence suggested the involvement of a peroxynitrite intermediate in the reaction. Thus, the reaction of metal-nitrosyl complexes with O_2, O_2^- or O_2^{2-} is of potential interest from the NOD point of view. On the other hand, a pyrrole/imine ligand derived cobalt nitrosyl complex having $\{CoNO\}^8$ configuration has been shown to serve as potential HNO donor.[19]

The Co-nitrosyl complexes having $\{CoNO\}^8$ configuration has attracted attention since they can serve as the good replacement of $\{FeNO\}^8$ complexes which are inherently reactive.[19] On the other hand, cobalamins (Cbls) are known to react with NO to form nitrosocobalamins (NOCbls) in diffusion controlled rate and are believed to scavenge NO efficiently *in vivo*.[20] In addition, the Co-containing systems are found more promising with respect to the observation of peroxynitrite complexes.[11] In the present work, a cobalt(II) complex of a tridentate N-donor ligand, 1,3-bis(2′-pyridylimino)isoindol (**L5H**) (Figure

4.1) has been used for the preparation of nitrosyl complex followed by its study with dioxygen. The spectral characterization and kinetics studies suggest that in the present study the reaction of the $\{CoNO\}^8$ complex with O_2 led to the formation of an unusual

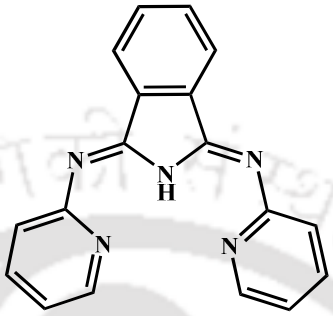

Figure 4.1. Ligand **L5H** used for the present study.

superoxide species, $[(L5)Co(NO)(O_2^-)]^+$ which then resulted in the corresponding nitro product in subsequent step. Chemical evidence suggests the involvement of a putative peroxynitrite intermediate in the process of decomposition of the $[(L5)Co(NO)(O_2^-)]^+$ to the nitro complex.

4.2 Results and discussion

The ligand **L5H**, 1,3-bis(2′-pyridylimino)isoindol was prepared using earlier reported procedure by Siegl and coworkers.[21] It was characterized using FT-IR, ^{1}H-NMR spectroscopy and ESI-mass spectrometry and microanalysis (Experimental Section). These data matched well with the earlier reported one. The bubbling of NO gas to the degassed methanol solution of the ligand followed by the addition of an equivalent amount of cobalt acetate tetrahydrate resulted in the precipitation of the Co(II)-nitrosyl complex, [(L5)Co(NO)(OAc)] (**4.1**) (Scheme 4.1 and Experimental Section). It was isolated as solid and characterized by spectroscopic analyses as well as by single crystal X-ray structure

determination. The ORTEP diagram of complex **4.1** is shown in figure 4.2a. The crystallographic data and metric parameters are listed in the tables 4.1, 4.2 and 4.3.

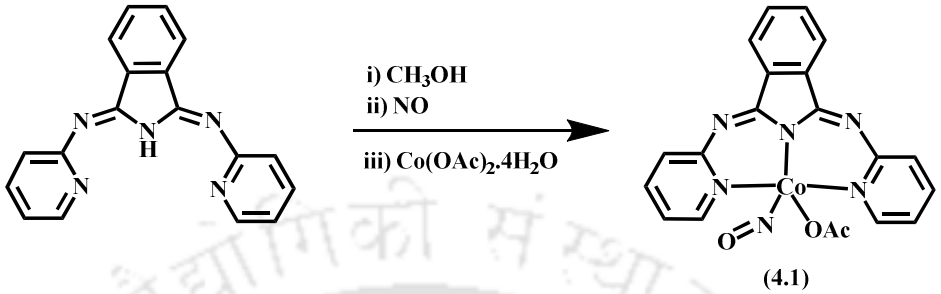

Scheme 4.1. Synthesis of complex **4.1**.

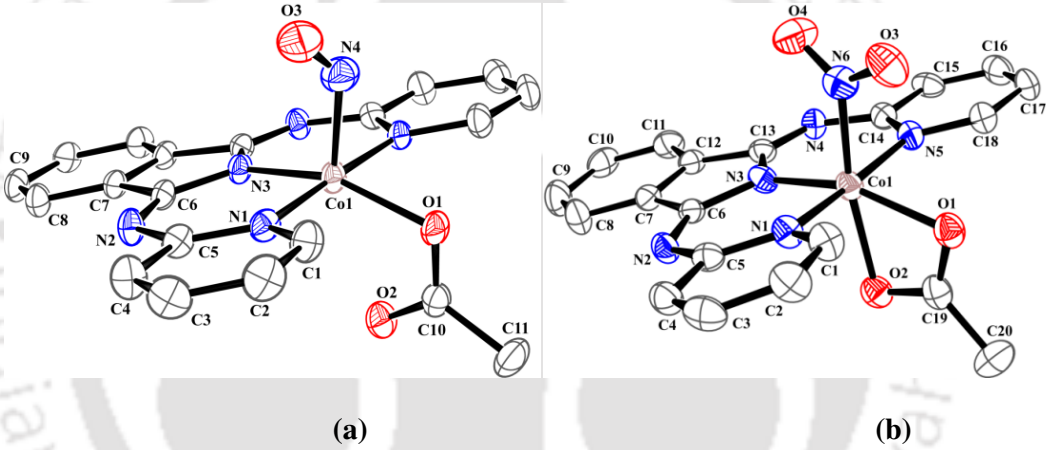

Figure 4.2. ORTEP diagram of complexes (a) **4.1** and (b) **4.2** (35% ellipsoid probability; H atoms and solvent molecule are not shown for clarity).

The crystal structure revealed that the cobalt center is in distorted square pyramidal geometry. The O-atom from monodentate acetate group and the three N-atoms from the **L5** moiety formed the square plane and the NO group is coordinated from the apical position. The Co-N_{NO} distance is 1.828(8) Å. The N-O distance and the Co-N-O angle were 1.014(8) Å and 132.7(7)°, respectively. Though the Co-N_{NO} distance is within the range of other reported values in analogous complexes, the N-O distance is relatively shorter.[17,22] The bent geometry of the cobalt-nitrosyl, **4.1** is consistent with the $\{CoNO\}^8$ configuration as per the Enemerk-Feltham notation.[23]

It is to be noted that in cases of recently structurally characterized Co-nitrosyl complexes of 12 and 13 membered N-tetramethylated cyclam ligands, $[(12\text{-TMC})Co(NO)]^{2+}$ and $[(13\text{-TMC})Co(NO)]^{2+}$, the Co-N-O angles are 128.5 and 124.4°; whereas, the N-O distances are 1.155 and 1.159 Å, respectively.[17b]

Table 4.1. Crystallographic data of complexes **4.1** and **4.2**.

	4.1	**4.2**
Formulae	$C_{21}H_{15}N_6CoO_4$	$C_{20}H_{15}N_6CoO_5$
Mol. wt.	474.32	478.31
Crystal system	Monoclinic	Monoclinic
Space group	I2/m	P21/n
Temperature /K	293(2)	293(2)
Wavelength /Å	0.71073	0.71073
a /Å	8.5221(9)	8.7548(8)
b /Å	16.0737(15)	11.7772(11)
c /Å	15.6997(17)	18.9485(17)
α/°	90.00	90.00
β/°	105.719(13)	93.988(7)
γ/°	90.00	90.00
V/ $Å^3$	2070.2(4)	1949.0(3)
Z	4	4
Density/Mgm^{-3}	1.522	1.630
Abs. Coeff. /mm^{-1}	0.871	0.930
Abs. correction	Multi-scan	Multi-scan
F(000)	968	976.0
Total no. of reflections	1895	3417
Reflections, $I > 2\sigma(I)$	1347	2432
Max. 2θ/°	24.999	24.997
Ranges (h, k, l)	$-10 \le h \le 9$ $-11 \le k \le 19$ $-18 \le l \le 18$	$-9 \le h \le 10$ $-10 \le k \le 14$ $-20 \le l \le 22$
Complete to 2θ (%)	99.7	99.8
Refinement method	Full-matrix least-squares on F^2	Full-matrix least-squares on F^2
Goof (F^2)	0.847	1.009
R indices [$I > 2\sigma(I)$]	0.0557	0.0775
R indices (all data)	0.0820	0.1068

In case of Co(II)-nitrosyl complex of N^1-(2,4,6-trimethylbenzyl)-N^2-(2-((2,4,6-trimethylbenzyl)amino)ethyl-1,2-diamine ligand having $\{CoNO\}^8$ description, the Co-N_{NO} distance was reported to be 1.765(10) Å; whereas, the N-O distance and

Co-N-O angles were 1.103(9)Å and 124.6(10)°.[24] The short Co-N_{NO} distance is an indication of greater extent of metal-nitrosyl back bonding. In this case of 5-coordinated square pyramidal Co(II)-nitrosyl, the NO stretching frequency appeared at 1659 cm^{-1}.[24]

Table 4.2. List of selected bond lengths (Å) of complexes **4.1** and **4.2**.

	4.1	**4.2**
N4-O3	1.014(8)	-
Co1-N1	1.970(4)	1.964(4)
Co1-N3	1.879(5)	1.858(5)
Co1-N4	1.828(8)	-
Co1-O1	1.941(4)	1.989(4)
N2-C6	1.301(6)	1.295(6)
N6-O3	-	1.208(7)
N6-O4	-	1.204(7)
Co1-N5	-	1.978(5)
Co1-N6	-	1.890(6)
Co1-O2	-	2.016(4)

Table 4.3. List of selected bond angles (°) of complexes **4.1** and **4.2**.

	4.1	**4.2**
N1-Co1-N1	177.7(2)	-
N1-Co1-N3	91.11(10)	91.50(19)
Co1-N4-O3	132.7(7)	-
N3-Co1-O1	158.3(2)	159.6(2)
O1-Co1-O2	56.75(18)	64.99(17)
N1-Co1-N5	-	173.73(19)
Co1-N6-O3	-	115.8(5)
Co1-N6-O4	-	121.5(5)
O3-N6-O4	-	122.6(6)

In FT-IR spectrum of **4.1**, the NO stretching frequency appeared at 1673 cm^{-1}. However, in case of $[(12\text{-TMC})Co(NO)]^{2+}$ and $[(13\text{-TMC})Co(NO)]^{2+}$, the nitrosyl stretching frequency appeared at 1712 and 1716 cm^{-1} in acetonitrile solution.[17b] The complex **4.1** was silent in the X-band EPR spectroscopy which is consistent with its $\{CoNO\}^8$ description (Appendix III). The ESI-mass spectrum of **4.1** was populated by the molecular ion peak at m/z 387.28 which is assignable to the $[(L5)Co(NO)]^+$

unit (calculated m/z, 387.04) (Appendix III). The observed isotopic distribution pattern was found to match well with the simulated one.

Dioxygen reactivity of 4.1

In the UV-visible spectroscopy, dichloromethane solution of **4.1** absorbs at 467 nm ($\varepsilon/M^{-1}cm^{-1}$, 6230), 348 nm ($\varepsilon/M^{-1}cm^{-1}$, 12400) (Figure 4.3). The addition of O_2 gas to the degassed dichloromethane solution of **4.1** at -20 °C resulted in the appearance of bands at 477 nm and 450 nm, respectively (Figure 4.3a). The intensity of these bands were found to increase gradually with time and reached to the maximum within 30 minutes of O_2 addition. The compound corresponding to this final spectrum was isolated as solid and characterized as **4.2** [(L5)Co(NO_2)(OAc)] (Experimental Section).

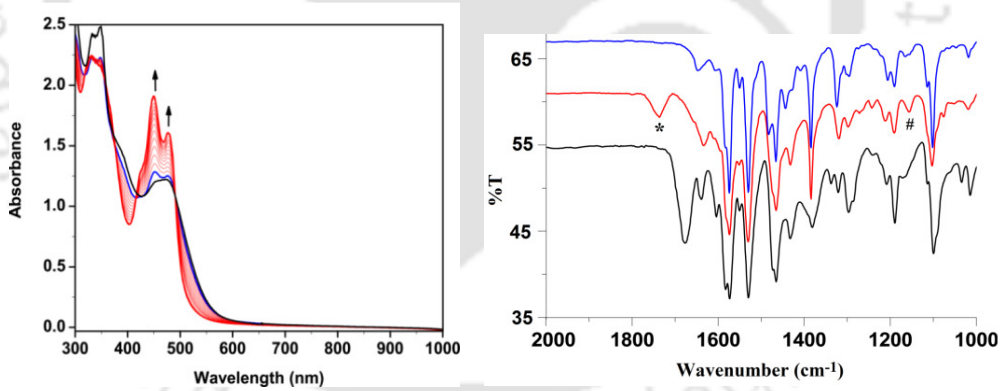

Figure 4.3. (a) UV-visible spectra of complex **4.1** (black) and after addition of O_2 (blue; immediately after addition and red lines) in CH_2Cl_2 at -20 °C. (b) FT-IR spectra of **4.1** (black); immediately after addition of O_2 (red; $^{*}\upsilon_{NO}$ shifted to 1740 cm^{-1} and $^{\#}\upsilon_{O\text{-}O}$ appeared at 1155 cm^{-1}) and after 1/2 h of addition of O_2 (blue) in CH_2Cl_2.

The kinetic studies revealed that the reaction of **4.1** with O_2 depends on the concentration of the added O_2 (Figure 4.4) suggesting the involvement of an associative mechanism.[17a] It is to be noted that the Co-nitrosyl complex of 14

membered N-tetramethylated cyclam ligands, $[(14\text{-TMC})Co(NO)]^{2+}$ reacted with O_2 to result in $[(14\text{-TMC})Co(NO_3)]^{+}$ in a dissociative pathway where the dissociation of NO group from the nitrosyl complex was proposed in the rate determining step to form a cage intermediate, $\{(14\text{-TMC})Co \ldots NO\}^{2+}$, prior to the reaction with O_2.[17a] Thus, the overall rate of the reaction was independent of concentration of O_2.

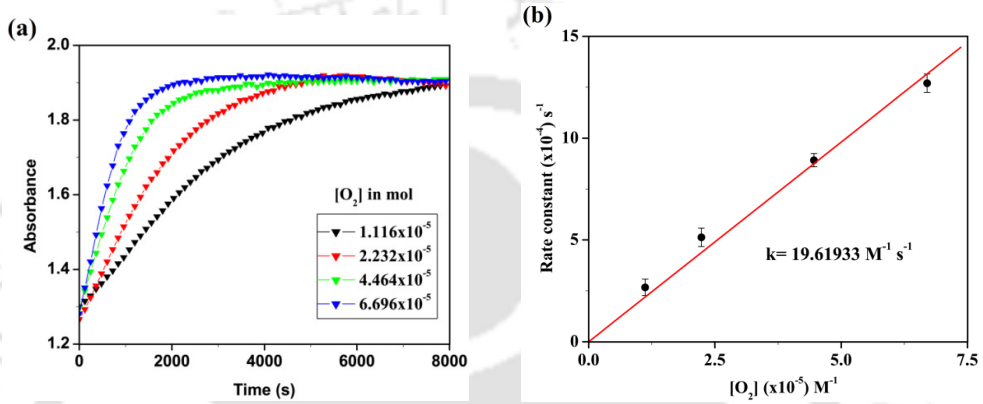

Figure 4.4. (a) Time *versus* absorbance plot at 450 nm for the reaction of complex **4.1** with different O_2 concentrations in CH_2Cl_2 at 298 K. (b) $[O_2]$ concentration *versus* rate constant plot for the reaction of complex **4.1** with O_2.

In FT-IR spectrum, the addition of O_2 gas to the degassed dichloromethane solution of **4.1** resulted in the disappearance of the NO stretching frequency at 1673 cm^{-1}, while new band appeared at 1740 cm^{-1} (Figure 4.3b). This band was assigned to the NO stretching of the resulting intermediate, **4.1a** (Scheme 4.2).

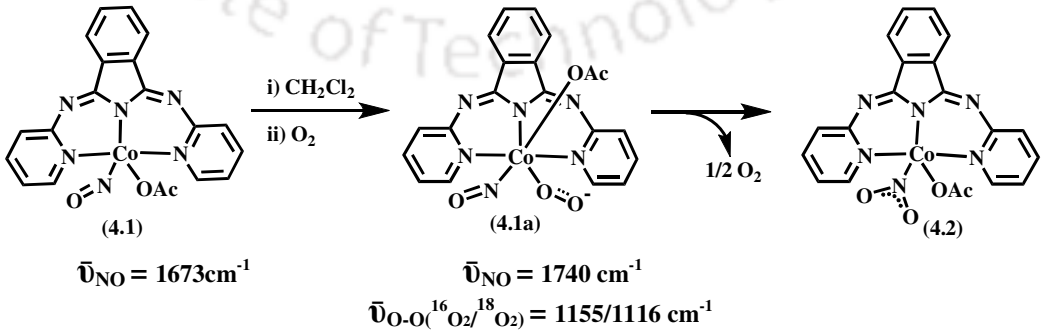

Scheme 4.2. Reaction of complex **4.1** with O_2 in CH_2Cl_2.

Recently, Karlin and coworkers reported that addition of O_2 gas to the dichloromethane solution of $[Cu^{I,II}_2(UN\text{-}O^-)(\mu\text{-}NO)]^{2+}$ resulted in the formation of $[Cu^{II}_2(UN\text{-}O^-)(NO)(O_2^-)]^{2+}$ where the NO stretching appeared at 1853 cm^{-1}.[12] On the other hand, Theopold *et al.* reported that the reaction of a *tris*(3-tert-butyl-5-methylpyrazole)borate ligand derived cobalt(III) superoxo complex with NO at -78 °C resulted in the appearance of a new stretching band at 1849 cm^{-1} and it was assigned to corresponding unstable nitrosyl intermediate.[25] It was reported earlier that in case of cobalt(II)-nitrosyl complexes, the NO stretching frequency shifts *ca.* 100-150 cm^{-1} upon oxidation of the cobalt(II) center to cobalt(III).[26] Thus, the addition of O_2 to the solution of **4.1** resulted in an intermediate where $[Co^{III}\text{-}NO]$ is suggestive. On the other hand, in addition to the 1740 cm^{-1} band, a new stretching frequency at 1155 cm^{-1} was observed in the FT-IR spectrum (Figure 4.5a). This frequency was sensitive to the $^{18}O_2$ and found to shift to 1116 cm^{-1} (Figure 4.5).

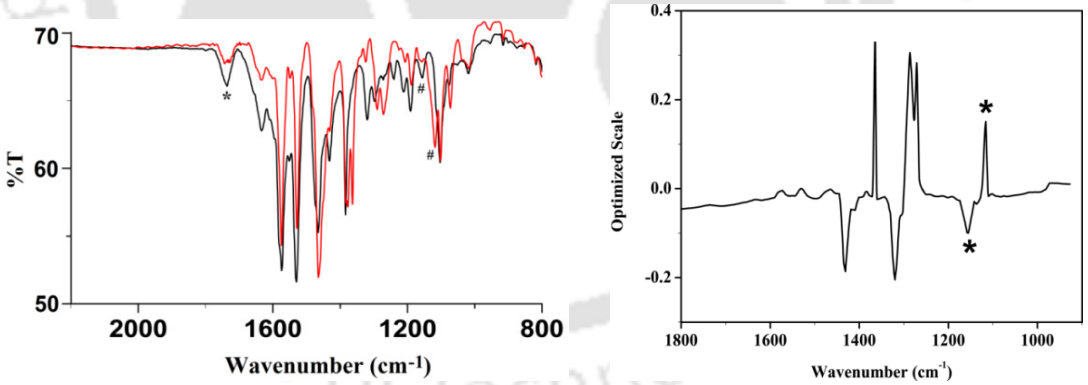

(a) **(b)**

Figure 4.5. (a) FT-IR spectra of complex **4.1** immediately after addition of $^{16}O_2$ (black; $^{*}\upsilon_{NO}$ at 1740 cm^{-1} and $^{\#}\upsilon_{O\text{-}O}$ at 1155 cm^{-1}) and upon labelling with $^{18}O_2$ (red; $^{\#}\upsilon_{O\text{-}O}$ shifted to 1116 cm^{-1}) in CH_2Cl_2 at -20 °C. (b) Subtracted FT-IR spectrum of the reaction mixture obtained from the reaction of complex **4.1** with $^{16}O_2$ and $^{18}O_2$, respectively, in CH_2Cl_2 (*stretching frequencies for coordinated O-O group). The other isotope sensitive peaks are due to the presence of the decomposition product, **4.2**.

It is to be noted that O_2 is known to bind with Co(II) and other transition metal ions in their reduced state to result in electron transfer reactions leading to the formation of corresponding Co(III)-superoxide complex.[27] The observed stretching frequency at 1155 cm^{-1} is also suggestive to the formation of a metal-bound superoxide.[27] Hence the formulation of the intermediate **4.1a** as $[(L5)Co^{III}(NO)(O_2^-)]^+$ is logical (Scheme 4.2). Both the 1740 and 1155 cm^{-1} bands disappeared with time and the appearance of two stretching frequencies at 1322 and 1297 cm^{-1} assignable to the nitro group in **4.2** were observed (Appendix III).[18,28] The labelling experiment with $^{18}O_2$ resulted in the shift of these characteristic frequencies to 1290 and 1271 cm^{-1}, respectively suggesting the incorporation of ^{18}O-atom into the **4.2** (Appendix III). It was further confirmed by isolation of **4.2** followed by structural characterization. It is to be noted that the O_2 addition to the solution of **4.1** led to the formation of the superoxo species **4.1a** which is thermally unstable and decomposes to the corresponding nitro complex **4.2** quite fast. The spectrum, we could manage to record with our existing facility, thus contains the stretching of the nitro product as impurity. It should be noted that in UV-visible spectroscopic monitoring, the formation of the two new bands at 450 and 477 nm were observed which correspond to the decomposition product, **4.2**. The reaction proceeds through clean isosbestic points indicating the involvement of only one new species. No indication of formation of any intermediate was observed in the reaction even at -40 °C. This is perhaps because of the very fast reaction at the concentration of *ca*. 0.2 mM which was used for UV-visible study. The complex **4.2** was isolated as solid and characterized by spectroscopic as well as by single crystal X-ray structure determination. The ORTEP diagram of **4.2** is shown in figure 4.2b.

The diamagnetic nature of **4.2** is in agreement with the presence of trivalent Co center in it. In the ESI-mass spectrum of **4.2**, the $[(L5)Co(NO_2)]^+$ was observed at m/z 403.06 (calculated 403.03). When the reaction was carried out with $^{18}O_2$, the molecular ion peak of **4.2** appeared at m/z 405.10 (Appendix III) suggesting the incorporation of one O-atom from the added O_2.

The decomposition of the intermediate **4.1a** to **4.2** presumably proceeds *via* the formation of a putative peroxynitrite intermediate, though no indication was observed in UV-visible studies. We sought chemical evidence to establish the formation of peroxynitrite intermediate. In this regard the nitration of the phenol ring has been reported extensively as evidence in favour of the formation of peroxynitrite intermediate.[11b,e,f,16] When the oxygenation reaction of **4.1** was carried out in presence of 2,4-di-*tert*-butylphenol (DTBP), the formation of corresponding nitrophenol with an yield of *ca.* 50% (Experimental Section) was observed (Scheme 4.3). Though, it is expected that the peroxynitrite intermediate will afford quantitative conversion of the phenol to nitrophenol, the parallel decomposition of the intermediate to **4.2** at the reaction temperature resulted in the formation of nitrophenol with a less yield.

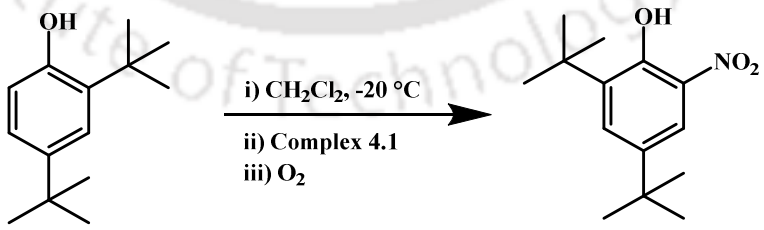

Scheme 4.3. Reaction of complex **4.1** with O_2 in presence of DTBP.

However, when DTBP was added in the reaction mixture after the addition of O_2 in the solution of **4.1** at -20 °C, the isolation of the products using chromatographic

purification revealed the exclusive formation of **4.2** with unreacted DTBP (*ca.* 94%). Thus, it is implicated that the reaction of **4.1** with O_2 resulted in the formation of a peroxynitrite species *via* **4.1a**. It should be noted that only **4.1** or **4.2** did not result phenol ring nitration at the experimental condition.

The decomposition of the presumed peroxynitrite intermediate to **4.2** could be envisaged either through the release of ½O_2 or *via* the mechanism proposed by Basalo where a peroxynitrite intermediate interacts with one unit of nitrosyl complex in fast step to result in –N-O-O-N- linkage which decomposed to two units of corresponding nitro complex.[16] Although, there is no direct evidence to confirm which mechanism is operating in the present case, considering the yield of isolated nitrophenol (*ca.* 50%), the first pathway seems more logical.

4.3 Experimental section

4.3.1 Materials and methods

All reagents and solvents of reagent grade were purchased from commercial sources and used as received except specified. All the reactions were performed under inert conditions unless specified. $^{18}O_2$ was purchased from Icon Isotopes. Deoxygenation of the solvent and solutions was effected by repeated vacuum/purge cycles or bubbling with argon for 30 min. UV-visible spectra were recorded on an Agilent Technologies Cary 8454 UV-visible spectrophotometer. FT-IR spectra of the samples were taken on a Perkin Elmer spectrophotometer with samples prepared either as KBr pellets or in dichloromethane solution in KBr cell. ^{1}H-NMR spectra were recorded in a 600 MHz Varian FT spectrometer. Chemical shifts (ppm) were referenced either with an internal standard (Me_4Si) or to the residual solvent peaks. The X-band Electron Paramagnetic Resonance

(EPR) spectra were recorded on a JES-FA200 ESR spectrometer, at room temperature with microwave power, 0.998 mW; microwave frequency, 9.14 GHz and modulation amplitude, 2. Elemental analyses were obtained from a Perkin Elmer Series II Analyzer.

Kinetic study: The rates of the reactions of **4.1** with different O_2 concentration were followed by monitoring the UV-visible spectral change of the solution using Agilent Technologies Cary 8454 UV-visible spectrophotometer installed with Chemstation kinetics software. The instrument was equipped with a Unisoku cryostat USP- 203 B having thermostated cell holder. For the kinetic study, the temperature was regulated at 25 °C. O_2 gas was diluted with Ar using Environics Series 4040 computerized gas dilution system and then the calculated amount was added to the reaction mixture through a gas tight Hamilton syringe.

Single crystals were grown by slow evaporation of methanol and CH_2Cl_2 solution of **4.1** and **4.2**, respectively. The intensity data were collected using a Bruker SMART APEX-II CCD diffractometer, equipped with a fine focus 1.75 kW sealed tube MoK_α radiation (λ = 0.71073 Å) at 293(3) K, with increasing ω (width of 0.3° per frame) at a scan speed of 3 s/frame. The SMART software was used for data acquisition. Data integration and reduction were undertaken with SAINT and XPREP software.[29] Multi-scan empirical absorption corrections were applied to the data using the program SADABS.[30] Structures were solved by direct methods using SHELXS-2014 and refined with full-matrix least squares on F^2 using SHELXL-2014/7.[31] Structural illustrations have been drawn with ORTEP-3 for Windows.[32]

4.3.2 Syntheses of ligand L5H [L5H= 1,3-bis(2′-pyridylimino)isoindol]

Ligand **L5H** was synthesized following an earlier reported procedure with a minor

modification.[21] A mixture of 1,2-dicyanobenzene (2.56 g, 20 mmol), 2-aminopyridine (3.95 g, 42 mmol) and $CaCl_2$ (0.22 g, 2 mmol) in 30 mL 1-butanol was refluxed for 48 h. Upon cooling to room temperature, the product began to precipitate. The precipitate was collected by filtration, washed with water and recrystallized as pale yellow needles from ethanol/water. Yield: 4.42 g (*ca.* 74%). Elemental analyses for $C_{18}H_{13}N_5$: Calcd. (%): C, 72.23; H, 4.38; N, 23.40; found (%): C, 72.29; H, 4.36; N, 23.51. FT-IR (KBr pellet): 3061, 1631, 1582, 1457, 1429, 1305, 1259, 1220, 1098, 1034, 793 cm^{-1}. ^{1}H-NMR: (600 MHz, $CDCl_3$): δ_{ppm}: 8.62-8.61 (1H, d), 8.09-8.07 (1H, dd), 7.78-7.75 (1H, t), 7.66-7.64 (1H, dd), 7.47-7.45 (1H, d), 7.13-7.11 (1H, t). ^{13}C-NMR: (150 MHz, $CDCl_3$): δ_{ppm}: 160.7, 154.0, 148.0, 138.3, 136.0, 131.9, 123.4, 122.8, 120.4. Mass (m/z): calcd: 299.12, found: 300.03 (M+1).

4.3.3 Synthesis of complexes

(i) 4.1, [(L5)Co(NO)(OAc)]

To an over saturated solution of **L5H** (150 mg, 0.5 mmol) in 10 mL methanol, NO gas was bubbled for 2 min followed by the addition of $Co(OAc)_2{\cdot}4H_2O$ (125 mg, 0.5 mmol) in methanol (*ca.* 10 mL). The reaction mixture was stirred for 5 min which resulted in dark brown precipitate. The excess of NO gas was removed by bubbling with Ar. Then the precipitate was filtered using a Schlenk frit fitted in the Schlenk line. Finally precipitate was washed under Ar with degassed methanol to get the pure **4.1**. X-ray quality crystal of **4.1** was obtained when the reaction mixture was allowed to stand for 1-2 days. Yield: 123 mg (55%). Elemental analyses for $C_{20}H_{15}CoN_6O_3$: Calcd. (%): C, 53.82; H, 3.39; N, 18.83; found (%): C, 53.73; H, 3.42; N, 18.90. UV-visible (dichloromethane): λ_{max} 467 nm (ε/M^{-1} cm^{-1}, 6230), 348 nm (ε/M^{-1} cm^{-1}, 12400). FT-IR (KBr pellet): 2962, 1673 (ν_{NO}),

1637, 1581, 1529, 1465, 1261, 1098, 1017, 801 cm^{-1}. Mass (m/z): calcd: 387.04 for $[Co(L5)(NO)]^+$, found: 387.28.

(ii) 4.2, [(L5)Co(NO_2)(OAc)]

To a degassed solution of **4.1** (89 mg, 0.2 mmol) in dichloromethane (*ca*. 20 mL), excess of O_2 gas was bubbled for 1 min. The solution was then allowed to stir for 2 h at room temperature. The resulting light red solution was dried under vacuum and light brown solid of **4.2** was obtained. It was crystallized by slow evaporation of a dichloromethane solution. Yield: 85 mg (92%). Elemental analyses for $C_{20}H_{15}CoN_6O_4$: Calcd. (%): C, 51.96; H, 3.27; N, 18.18; found (%): C, 51.91; H, 3.29; N, 18.27. UV-visible (CH_2Cl_2): λ_{max} 477 nm (ε/M^{-1} cm^{-1}, 8200), 450 nm (ε/M^{-1} cm^{-1}, 9830) and 329 nm (ε/M^{-1} cm^{-1}, 11200). FT-IR (KBr pellet): 2934, 1646, 1582, 1531, 1464, 1378, 1320, 1296, 1099, 1017, 953, 775 cm^{-1}. Mass (m/z): calcd: 403.03 for $[Co(L5)(NO_2)]^+$, found: 403.06.

4.3.4 Reaction of 4.1 with O_2 in presence of 2,4-di-*tert*-butylphenol : Isolation of 2,4-di-*tert*-butyl-6-nitrophenol

To a degassed solution of **4.1** (89 mg, 0.2 mmol) in 20 mL of dichloromethane was added 2,4-di-*tert*-butylphenol (206 mg, 1 mmol); stirred for 5 min and the solution was cooled at -20 °C. O_2 gas was then bubbled through the solution for 1 min and the resulting mixture was stirred for 3 h at -20 °C. The reaction mixture was then warmed to room temperature and dried under reduce pressure. The solid mass was then subjected to column chromatography using silica gel column and hexane as eluent to obtain 2,4-di-*tert*-butyl-6-nitrophenol. Yield: 21 mg (*ca.* 42%). Elemental analyses for $C_{14}H_{21}NO_3$, Calcd. (%): C, 66.91; H, 8.42; N, 5.57, found (%): C, 66.86; H, 8.43; N, 5.66. ^{1}H-NMR (600 MHz, $CDCl_3$): δ_{ppm}, 7.39 (s, 1H), 7.12 (s, 1H), 5.22 (s, 1H), 1.45 (s, 9H), 1.32 (s, 9H). ^{13}C-NMR

(150 MHz, $CDCl_3$): δ_{ppm}, 150.0, 143.2, 136.4, 125.5, 125.0, 122.5, 35.4, 34.7, 31.9, 29.9. Mass (m/z): calcd: 251.15, found: 250.47 (M-1).

4.4 Conclusion

A cobalt-nitrosyl complex, [(L5)Co(NO)(OAc)], **4.1** having $\{CoNO\}^8$ description was prepared. Structural characterization revealed that NO is bonded to the cobalt center in a bent fashion with a relatively shorter N-O distance. The addition of dioxygen to the dichloromethane solution of **4.1** resulted in the formation of corresponding nitro complex, [(L5)Co(NO_2)(OAc)], **4.2**. Spectroscopic studies suggested the involvement of the intermediate **4.1a**, [(L5)Co^{III}(NO)(O_2^-)(OAc)]. The complex **4.1a** decomposed to complex **4.2** *via* a presumed peroxynitrite intermediate which was implicated by its characteristic phenol ring nitration reaction.

4.5 References

(1) Goyal, R. K.; Hirano, I. *N. Engl. J. Med.* **1996**, *334*, 1106.

(2) Stark, M. E.; Szurszewski, J. H. *Gastroenterology* **1992**, *103*, 1928.

(3) Jaffrey, S. R.; Snyder, S. H. *Annu. Rev. Cell Dev. Biol.* **1995**, *11*, 417.

(4) Bogdan, C. *Nature Immunology* **2001**, *2*, 907.

(5) (a) Moreno, V. R.; Beddell, C.; Moncada, S. **1993**, 215, 801. (b) Ignarro, L. J. *Annu. Rev. Pharmacol. Toxicol.* **1990**, *30*, 535. (c) Radi, R. *Proc. Natl. Acad. Sci. U.S.A.* **2004**, *101*, 4003.

(6) (a) Liaudet, L.; Soriano, F. G.; Szabo, C. *Crit. Care Med.* **2000**, *28,* 169. (b) Pacher, P.; Beckman, J. S.; Liaudet, L. *Physiol. Rev*. **2007**, *87*, 315. (c) Beckman J. S.; Koppenol, W. H. *Am. J. Physiol*. **1996**, *271*, 1424.

(7) (a) Pfeiffer, S.; Gorren, A. C. F.; Schmidt, K.; Werner, E. R.; Hansert, B.; Bohle, D. S.; Mayer, B. *J. Biol. Chem.* **1997**, *272*, 3465. (b) Coddington, J. W.; Hurst, J.

K.; Lymar, S. V. *J. Am. Chem. Soc.* **1999**, *121*, 2438. (c) Koppenol, W. H.; Bounds, P. L.; Nauser, T.; Kissner, R.; Rüegger, H. *Dalton Trans.* **2012**, *41*, 13779. (d) Lymar, S. V.; Khairutdinov, R. F.; Hurst, J. K. *Inorg. Chem.* **2003**, *42*, 5259. (e) Goldstein, S.; Lind, J.; Merényi, G. *Chem. Rev*. **2005**, *105*, 2457. (f) Molina, C.; Kissner, R.; Koppenol, W. H. *Dalton Trans*. **2013**, *42*, 9898.

(8) (a) Schopfer, M. P.; Wang, J.; Karlin, K. D. *Inorg. Chem.* **2010**, *49*, 6267. (b) Ouellet, H.; Ouellet, Y.; Richard, C.; Labarre, M.; Wittenberg, B.; Wittenberg, J.; Guertin, M. *Proc. Natl. Acad. Sci. U. S. A.* **2002**, *99*, 5902. (c) Gardner, P. R.; Gardner, A. M.; Martin, L. A.; Salzman, A. L. *Proc. Natl. Acad. Sci. U. S. A*. **1998**, *95*, 10378. (d) Ford, P. C.; Lorkovic, I. M. *Chem. Rev*. **2002**, *102*, 993. (e) Gardner, P. R.; Gardner, A. M.; Brashear, W. T.; Suzuki, T.; Hvitved, A. N.; Setchell, K. D. R.; Olson, J. S. *J. Inorg. Biochem*. **2006**, *100*, 542.

(9) (a) Qiao, L; Lu, Y.; Liu, B.; Girault, H. H. *J. Am. Chem. Soc*. **2011**, *133*, 19823. (b) Vilet, A.; Eiserich, J. P.; Halliwell, B.; Cross, C. E. *J. Biol. Chem.* **1997**, *272*, 7617.

(10) (a) Kurtikyan, T. S.; Ford, P. C. *Chem. Commun*. **2010**, *46*, 8570. (b) Yokoyama, A.; Han, J. E.; Karlin, K. D.; Nam, W. *Chem. Commun*. **2014**, *50*, 1742. (c) Skodje, K. M.; Williard, P. G.; Kim, E. *Dalton Trans.* **2012**, *41*, 7849.

(11) (a) Roncaroli, F.; Videla, M.; Slep, L. D.; Olabe, J. A. *Coord. Chem. Rev.* **2007**, *251*, 1903. (b) Maiti, D.; Lee, D.-H.; Sarjeant, A. A. N.; Pau, M. Y. M.; Solomon, E. I.; Gaoutchenova, K.; Sundermeyer, J.; Karlin, K. D. *J. Am. Chem. Soc.* **2008**, *130*, 6700. (c) Goodwin, J. A.; Coor, J. L.; Kavanagh, D. F.; Sabbagh, M.; Howard, J. W.; Adamec, J. R.; Parmley, D. J.; Tarsis, E. M.; Kurtikyan, T. S.; Hovhannisyan, A. A.; Desrochers, P. J.; Standard, J. M. *Inorg. Chem.* **2008**, *47*, 7852. (d) Kurtikyan, T. S.; Eksuzyan, S. R.; Goodwin, J. A.; Hovhannisyan, G. S.

Inorg. Chem. **2013**, *52*, 12046. (e) Herold, S.; Koppenol, W. H. *Coord. Chem. Rev*. **2005**, *249*, 499. (f) Subedi, H.; Brasch, N. E. *Inorg. Chem*. **2013**, *52*, 11608.

(12) Cao, R.; Elrod, L. T.; Lehane, R. L.; Kim, E.; Karlin, K. D. *J. Am. Chem. Soc.* **2016**, *138*, 16148.

(13) Park, G. Y.; Deepalatha, S.; Puiu, S. C.; Lee, D.-H.; Mondal, B.; Sarjeant, A. A. N.; del Rio, D.; Pau, M. Y. M.; Solomon, E. I.; Karlin, K. D. *J. Biol. Inorg. Chem*. **2009**, *14*, 1301.

(14) (a) Kalita, A.; Kumar, P.; Mondal, B. *Chem. Commun.* **2012**, *48*, 4636. (b) Kalita, A.; Deka, R. C.; Mondal, B. *Inorg. Chem.* **2013***, 52,* 10897.

(15) (a) Yokoyama, A.; Han, J. E.; Cho, J.; Kubo, M.; Ogura, T.; Siegler, M. A.; Karlin, K. D.; Nam, W. *J. Am. Chem. Soc.* **2012**, *134*, 15269. (b) Yokoyama, A.; Cho, K.-B.; Karlin, K. D.; Nam, W. *J. Am. Chem. Soc.* **2013**, *135*, 14900.

(16) (a) Clarkson, S. G.; Basolo, F. *J. Chem. Soc. Chem. Commun.* **1972**, 670. (b) Clarkson, S. G.; Basolo, F. *Inorg. Chem.* **1973**, *12*, 1528.

(17) (a) Kumar, P.; Lee, Y.-M.; Hu, L.; Chen, J.; Park, J. Y.; Yao, J; Chen, H.; Karlin, K. D.; Nam, W. *J. Am. Chem. Soc.* **2016**, *138*, 7753. (b) Kumar, P.; Lee, Y.-M.; Park, Y. J.; Siegler, M. A.; Karlin, K. D.; Nam, W. *J. Am. Chem. Soc.* **2015**, *137*, 4284.

(18) Saha, S.; Gogoi, K.; Mondal, B.; Ghosh, S.; Deka, H.; Mondal, B. *Inorg. Chem.* **2017**, *56,* 7781.

(19) Rhine, M. A.; Rodrigues, A. V.; Urbauer, R. J. B.; Urbauer, J. L.; Stemmler, T. L.; Harrop, T. C. *J. Am. Chem. Soc*. **2014**, *136*, 12560.

(20) Wolak, M.; Zahl, A.; Schneppensieper, T.; Stochel, G.; van Eldik, R. *J. Am. Chem. Soc*. **2001**, *123*, 9780.

(21) (a) Siegl, W. O. *J. Org. Chem.* **1977**, *42*, 1872. (b) Siegl, W. O.; Ferris, F. C.; Mucci, P. A. *J. Org. Chem.* **1977**, *42*, 3442. (c) Siegl, W. O. *J. Heterocyclic Chem.* **1981**, *18*, 1613. (d) Hanson, K.; Roskop, L.; Djurovich, P. I.; Zahariev, F.; Gordon, M. S.; Thompson, M. E. *J. Am. Chem. Soc.* **2010**, *132*, 16247.

(22) (a) Kozhukh, J.; Lippard, S. J. *J. Am. Chem. Soc*. **2012**, *134*, 11120. (b) Franz, K. J.; Doerrer, L. H.; Springler, B.; Lippard, S. J. *Inorg. Chem*. **2001**, *40*, 3774. (c) Scott, M. J.; Lippard, S. J. *J. Am. Chem. Soc*. **1997**, *119*, 3411. (d) Villacorta, G. M.; Lippard, S. J. *Pure Appl. Chem*. **1986**, *58*, 1474. (e) Jaynes, B. S.; Doerrer, L. H.; Liu, S.; Lippard, S. J. *Inorg. Chem*. **1995**, *34*, 5735.

(23) Enemark, J. H.; Feltham, R. D. *Coord. Chem. Rev.* **1974**, *13*, 339.

(24) Deka, H.; Ghosh, S.; Saha, S.; Gogoi, K.; Mondal, B. *Dalton Trans.* **2016**, *45*, 10979.

(25) Thyagarajan, S.; Incarvito, C. D.; Rheingold, A. L.; Theopold, K. H. *Inorg. Chim. Acta* **2003**, *345*, 333.

(26) (a) Richter-Addo, G. B.; Hodge, S. J.; Yi, G. B.; Khan, M. A.; Ma, T.; Van Caemelbecke, E.; Guo, N.; Kadish, K. M. *Inorg. Chem*. **1996**, *35*, 6530. (b) Kini, A. D.; Washington, J.; Kubiak , C. P.; Morimoto, B. H. *Inorg. Chem*. **1996**, 35, 6904.

(27) (a) Wang, C.-C.; Chang, H.-C.; Lai, Y.-C.; Fang, H.; Li, C.-C.; Hsu, H.-K.; Li, Z.-Y.; Lin, T.-S.; Kuo, T.-S.; Neese, F.; Ye, S.; Chiang, Y.-W.; Tsai, M.-Li.; Liaw, W.-F.; Lee, W.-Z. *J. Am. Chem. Soc.* **2016**, *138*, 14186. (b) Fielding, A. J.; Lipscomb, J. D.; Que, L. Jr. *J. Am. Chem. Soc.* **2012**, *134*, 796. (c) Huber, A.; Muller, L.; Elias, H.; Klement, R.; Volko, M. *Eur. J. Inorg. Chem*. **2005**, *8*, 1459. (d) Fritch, J. R.; Christoph, G. G.; Schaefer, W. P. *Inorg. Chem*. **1973**, *12*, 2170. (e) Schaefer, W. P.; Marsh, R. E. *J. Am. Chem. Soc.* **1966**, *88*, 178. (f) Gall, R. S.;

Rogers, J. F.; Schaefer, W. P.; Christoph, G. G. *J. Am. Chem. Soc.* **1976**, *98*, 5135. (g) Floriani, C.; Calderazzo, F. *J. Chem. Soc. A* **1969**, 946. (h) Collman, J. P.; Gagne, R. R.; Kouba, J.; Ljusberg-Wahren, H. *J. Am. Chem. Soc.* **1974**, *96*, 6800. (i) Nguyen, A. I.; Hadt, R. G.; Solomon, E. I.; Tilley, T. D. *Chem. Sci.* **2014**, *5*, 2874. (j) Corcos, A. R.; Villanueva, O.; Walroth, R. C.; Sharma, S. K.; Bacsa, J.; Lancaster, K. M.; MacBeth, C. E.; Berry, J. F. *J. Am. Chem. Soc*. **2016**, *138*, 1796.

(28) (a) Goodwin, J.; Kurtikyan, T.; Standard, J.; Walsh, R.; Zheng, B.; Parmley, D.; Howard, J.; Green, S.; Mardyukov, A.; Przybyla, D. E. *Inorg. Chem*. **2005**, *44*, 2215. (b) Wyllie, G. R. A.; Scheidt, W. R. *Chem. Rev.* **2002**, *102*, 1067.

(29) *SMART*, *SAINT and XPREP*, Siemens Analytical X-ray Instruments Inc., Madison, Wisconsin, USA, **1995**.

(30) Sheldrick, G. M. *SADABS*: *software for Empirical Absorption Correction*, University of Gottingen, Institut fur Anorganische Chemieder Universitat, Tammanstrasse 4, D-3400 Gottingen, Germany, **1999**.

(31) Sheldrick, G. M. *SHELXS-2014*, University of Gottingen, Germany.

(32) Farrugia, L. J. *J. Appl. Crystallogr.* **1997**, *30*, 565.

Chapter 5

Disproportion of a $[FeNO]^7$ Species into $[Fe(NO)_2]^9$ and Ferric Complex

Abstract

A dinitrosyl iron(I) complex, $[Fe(L5)(NO)_2]$, **5.1**, of the tridentate N-donor ligand, **L5H** {**L5H** = 1,3-bis(2′-pyridylimino)isoindol} has been synthesized from the ferrous precursor. The complex **5.1** was characterized by various spectroscopic techniques as well as by single crystal X-ray structure determination. The reaction was found to proceed *via* a pathway involving the disproportionation of the corresponding $\{FeNO\}^7$ intermediate, [Fe(L5)(NO)(Cl)], **5.2**. Complex **5.2** was isolated and structurally characterized.

5.1 Introduction

Nitric oxide (NO) plays important roles in mammalian biology and it has been identified as the signaling agent in immune response, cardiovascular and nervous system.[1-3] Only a submircomolar concentration is of NO is required for its functions. It is known to behave as a cytotoxic effector and pathogenic mediator when produced at high concentrations.[3,4] Most of the physiological roles of NO are believed to be mediated by the formation of nitrosyl complexes of metallo-proteins, mostly iron or copper.[5] A few cellular dinitrosyl iron complexes (DNICs) have been considered to be biological NO storage and carrier molecules. Natural DNICs are formed by reaction between NO and cellular non-heme iron species such as iron-sulfur clusters and labile iron pools (LIP).[6] Although, the chemical functionality of DNICs were largely unknown, protein bound DNICs have been observed during the activation of several regulatory proteins. Glutathione-bound DNICs have been reported to bind to glutathione transferases (GSTs). It has been suggested that their redox properties may be intimately tied to many of these physiological processes. In addition, the formation of the DNIC from the ferrous component is not very clear. Previously DNICs formed from iron complexes with ligand TMEDA [TMEDA = N,N,N´,N´-tetramethylethylenediamine] and its reactivity with molecular oxygen was reported by Kim *et al*.[7] N-bound DNIC [Fe(TMEDA)$(NO)_2$], which is described as a $\{Fe(NO)_2\}^{10}$ species in Enemark-Feltham notation reacts with molecular oxygen to give nitrate as end product formed *via* peroxynitrite intermediate. Lehnert *et al*. reported the same for iron-DMP [DMP = 2,9-dimethyl-1,10-phenanthroline] based complexes. They have synthesized the $\{Fe(NO)_2\}^9$ DNIC [Fe(DMP)$(NO)_2$](OTf), from a ferrous precursor *via* an unusual pathway which involves disproportionation of a $\{Fe(NO)\}^7$ complex to yield the $\{Fe(NO)_2\}^9$ and a ferric species, which is subsequently reduced by NO and re-enters the reaction cycle.[8]

In the present study we report the synthesis and structural characterization of a $\{Fe(NO)_2\}^9$ DNIC, $[Fe(L5)(NO)_2]$, **5.1** {L5= deprotonated 1,3-bis(2′-pyridylimino)isoindol} from Fe(II) precursor. The complex **5.1** was formed in a pathway involving the disproportionation of an intermediate $\{FeNO\}^7$ complex, [Fe(L5)(NO)(Cl)], **5.2**. The intermediate **5.2** was isolated and structurally characterized.

5.2 Results and discussion

Complex **5.1** was prepared by stirring the ligand **L5H** with equivalent amount of anhydrous $FeCl_2$ in dry and degassed methanol under excess NO gas (Scheme 5.1 and Experimental Section). The complex **5.1** was precipitated and isolated as brown solid. It was characterized by spectral analyses (Experimental Section and Appendix IV) and single crystal X-ray structure determination.

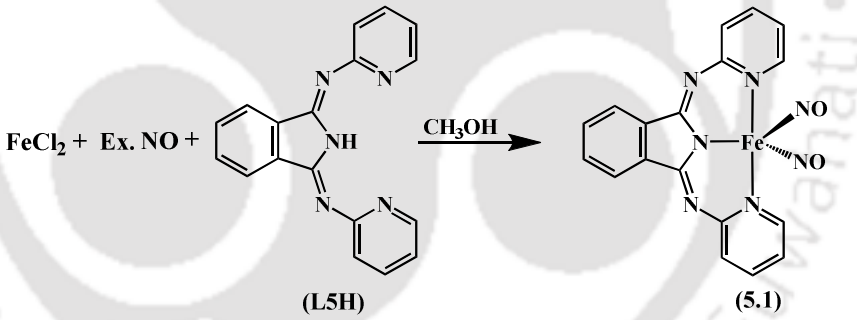

Scheme 5.1. Synthesis of complex **5.1**.

The ORTEP diagram of **5.1** is shown is shown in figure 5.1a. The crystallographic data, selected bond lengths and angles are listed in tables 5.1, 5.2 and 5.3, respectively. Single crystal structure of **5.1** revealed the presence of Fe(I)-dinitrosyl, $\{Fe(NO)_2\}^9$ moiety where Fe(I) is coordinated by three N-atoms from the ligand and two NO groups in a trigonal-bipyramidal geometry. The Fe-N_{indole} distance is 2.013 (5) Å which is considerably shorter than the Fe-N_{py} distances {2.159(5) and 2.162(5) Å}. The Fe-N_{NO} distances were 1.712(7) and 1.696(6) Å, respectively.

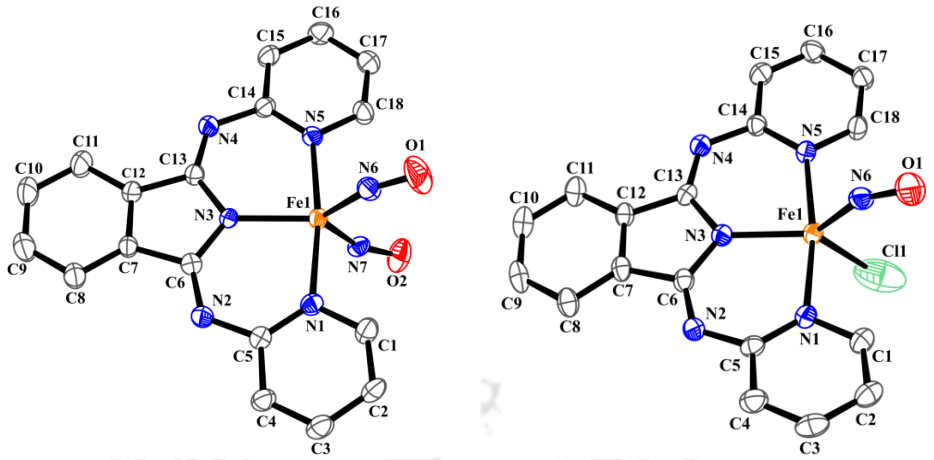

Figure 5.1. ORTEP diagrams of complexes (a) **5.1** and (b) **5.2** (35% thermal ellipsoid plot; H-atoms are not shown for clarity).

The Fe-N_{NO} distances are also significantly shorter than the Fe-N_{L5H} distances. This is perhaps because of the π-backbonding from the metal center to the NO.[9] The Fe-N-O angles were found to be 154.9(6)° and 155.8(6)°, respectively. The N-O distances of the coordinated NO were 1.15(1) and 1.146(9) Å (Tables 5.2 and 5.3). These distances are within the range of previously reported coordinated nitrosyls. For [(Ar-nacnac)$Fe(NO)_2$] DNIC having $\{Fe(NO)_2\}^9$ configuration the Fe-N-O angles were reported at 162.7(2)° and 170.1(2)°; and the N-O distances were at 1.177(2) and 1.174(2) Å.[10] Liaw and co-workers have reported a anionic $\{Fe(NO)_2\}^9$ DNIC, [PPN][$(S(CH_2)_3S)Fe(NO)_2$] where the Fe-N-O angles were found to be 172.8(2)° and 167.4(3)°; whereas the N-O distances were reported at 1.181(3) and 1.174(3) Å.[11]

It was found to be X-band EPR and the isotropic nature of the signal suggests the existence of the unpaired electron (S = 1/2) on one of the NO group.[12] This is also in agreement with the monovalency of the iron centre and formally $\{Fe(NO)_2\}^9$ description (Appendix IV). In the UV-visible spectroscopy, complex **5.1** in acetonitrile solution does not show any significant absorption band in the visible range.

Table 5.1. Crystallographic data of complexes **5.1** and **5.2**.

	5.1	**5.2**
Formulae	C_{18} H_{12} N_7 Fe O_2	C_{18} H_{12} N_6 Fe O Cl
Mol. wt.	414.20	419.64
Crystal system	Monoclinic	Monoclinic
Space group	P21/n	P21/c
Temperature /K	293(2)	293(2)
Wavelength /Å	0.71073	0.71073
a /Å	7.0184(7)	8.2423(14)
b /Å	22.6879(18)	19.015(10)
c /Å	21.9395(16)	12.7463(18)
α/°	90.00	90.00
β/°	93.666(8)	119.771(10)
γ/°	90.00	90.00
V/ Å^3	3486.4(5)	1734.0(10)
Z	8	4
Density/Mgm^{-3}	1.578	1.607
Abs. Coeff. /mm^{-1}	0.896	1.046
Abs. correction	Multi-scan	Multi-scan
F(000)	1688	852
Total no. of reflections	6127	3040
Reflections, $I > 2\sigma(I)$	4038	2148
Max. 2θ/°	24.998	24.999
Ranges (h, k, l)	-8≤ h ≤8 -26≤ k ≤25 -26≤ l ≤ 19	-8≤ h ≤9 -22≤ k ≤14 -14≤ l ≤ 15
Complete to 2θ (%)	99.9	99.6
Refinement method	Full-matrix least-squares on F^2	Full-matrix least-squares on F^2
Goof (F^2)	1.137	0.958
R indices [$I > 2\sigma(I)$]	0.0807	0.0646
R indices (all data)	0.1174	0.0913

Table 5.2. List of selected bond lengths of complexes **5.1** and **5.2**.

	5.1	**5.2**
N6-O1	1.142(7)	1.149(5)
N7-O2	1.145(7)	-
Fe1-N6	1.719(6)	1.726(4)
Fe1-N7	1.701(6)	-
Fe1-N1	2.159(6)	2.148(4)
Fe1-N3	2.013(5)	2.014(4)
Fe1-N5	2.162(5)	2.177(4)
C6-N2	1.296(8)	1.295(6)
C13-N4	1.296(8)	1.291(6)
Fe1-Cl1	-	2.241(4)

Table 5.3. List of selected bond angles of complexes **5.1** and **5.2**.

	5.1	**5.2**
Fe1-N6-O1	152.3(6)	153.8(5)
Fe1-N7-O2	154.9(6)	-
N1-Fe1-N5	171.6(2)	85.38(16)
N1-Fe1-N3	86.1(2)	86.40(16)
N3-Fe1-N5	86.1(2)	91.91(17)
N6-Fe1-N7	105.5(3)	-
N6-Fe1-Cl1	-	101.38(18)

In the FT-IR spectrum of **5.1** in KBr pellet, the NO stretching frequencies appeared at 1722 and 1665 cm^{-1} (Appendix IV). It is to be noted that in case of $[Fe(dmp)(NO)_2]$ (OTf), the NO stretching were observed at 1840 and 1746 cm^{-1} in KBr pellet.[8] For the [Fe(ar-nacnac)$(NO)_2$] DNIC reported by Lippard and co-workers these stretching were observed at 1755, 1705 cm^{-1}.[13] In case of five-coordinated DNIC these were reported at 1770, 1715 cm^{-1} for $[(TMEDA)Fe(NO)_2I]$.[14]

The cationic $\{Fe(NO)_2\}^9$ DNICs are generally not prepared from the ferrous precursor; although $\{Fe(NO)_2\}^9$ DNICs with anionic tetrathiolate ligands are reported to form from the ferrous precursor.[15] In case of tetrathiolate ferrous complexes, it has been found that the ligand substitution by the NO group leads to the formation of an $\{FeNO\}^7$ intermediate complex. This intermediate upon binding with one more equivalent of NO resulted in the anionic $\{Fe(NO)_2\}^9$ DNICs. Since the ferrous complexes with the neutral N-donor ligands cannot reductively eliminate ligands, the direct formation of $\{Fe(NO)_2\}^9$ DNICs from these precursors are relatively unknown. In these cases, an external reductant is required to provide the additional election needed for the reduction of iron center to result in $\{Fe(NO)_2\}^9$. For instance, reductive nitrosylation of $\{FeNO\}^7$ or $\{Fe(NO)_2\}^8$ by NO may lead to the formation of $\{Fe(NO)_2\}^9$ DNICs. In fact, the formation of a DNIC in the ferric uptake protein (FuR) was proposed to proceed through the reductive nitrosylation

pathway.[16] In this case NO was proposed as the reductant based on stoichiometric requirement of NO for the formation of $\{Fe(NO)_2\}^9$ from the Fe(II) state. In principle, the reduction of $\{FeNO\}^7$ by NO is less likely from the redox potential point of view.[17] On the other hand, $\{Fe(NO)_2\}^8$ are rare; so the intermediate formation of it is an unlikely event.[18] Disproportionation pathway was also proposed as an alternative for the formation of DNICs from the ferrous precursors. For instance, the reaction of NO with ferrous complex of 6-Me_3-TPA [*tris*{(6-methyl)-pyridylmethyl}amine)] with a deprotonated catecholate co-ligand resulted in the formation of $Fe(NO)_2\}^9$ DNIC and ferric catecholate complex. The disproportionation of a metastable $\{FeNO\}^7$ intermediate was proposed in this reaction (Eq. 5.1).[19]

$$\mathbf{2[Fe(6\text{-}Me_3TPA)(CatH)(NO)]^+ \longrightarrow [Fe(6\text{-}Me_3TPA)(NO)_2]^+ + [Fe(6\text{-}Me_3TPA)(Cat)]^+ + CatH_2}$$

…….. Eq. 5.1

[Fe(Ar-nacnac)(NO)(Br)] was also reported to disproportionate to an $\{Fe(NO)_2\}^9$ DNIC and corresponding ferric complex.[13] Recently, Lehnert and coworkers reported the synthesis of a $\{Fe(NO)_2\}^9$ DNIC, [Fe(dmp)$(NO)_2$](Otf) (dmp= 2,9-dimethyl-1,10-phenanthroline) from a ferrous precursor. The reaction was proposed to follow the disproportionation of a $\{FeNO\}^7$ complex to result $\{Fe(NO)_2\}^9$ DNIC and ferric complex. The ferric complex was found to undergo reduction in presence of excess NO gas in subsequent step and re-enters in to the reaction cycle. Albeit, the $\{FeNO\}^7$ complex was not isolated as solid as it was prone to release NO even at solid state.[8]

In the present case, the reaction was found to proceed through the formation of a green intermediate, **5.2**, which gradually decomposed to the brown mixture. Isolation and characterization of the complexes from the brown mixture revealed the equimolar presence of **5.1** and a ferric complex, **5.3** (Experimental Section). The intermediate green complex

5.2 was isolated as solid and characterized by spectroscopic analyses as well as by structure determination (Experimental Section). The ORTEP diagram is shown in figure 5.1b. The crystallographic data, selected bond lengths and angles are listed in tables 5.1, 5.2 and 5.3, respectively. The single crystal structure of **5.2** revealed the presence of a monomeric $\{FeNO\}^7$ system with Fe(II) center. The three N-atoms from the ligand, one NO group and a Cl atom are coordinated to the Fe(II) center in a distorted trigonal bipyramidal geometry. The Fe-N_{indole} distance is 2.014(4) Å and other Fe-N_{L5H} distances are also comparable to the same of **5.1**. The Fe-N_{NO} distance, 1.726 Å and the Fe-N-O angle is also comparable to those of **5.1**. These are within the range of reported values for $\{FeNO\}^7$ complexes.[17,20]

In UV-visible spectroscopy, **5.2** in acetonitrile solution absorbs at 630 nm (ε/M^{-1} cm^{-1}, 160) in the visible range. But the absorption band was found to be unstable and the intensity decreased rapidly (Figure 5.2a). In FT-IR spectrum, a strong stretching frequency was observed at 1795 cm^{-1} (Figure 5.2b). It was attributed to the NO stretching of $\{FeNO\}^7$ complex.

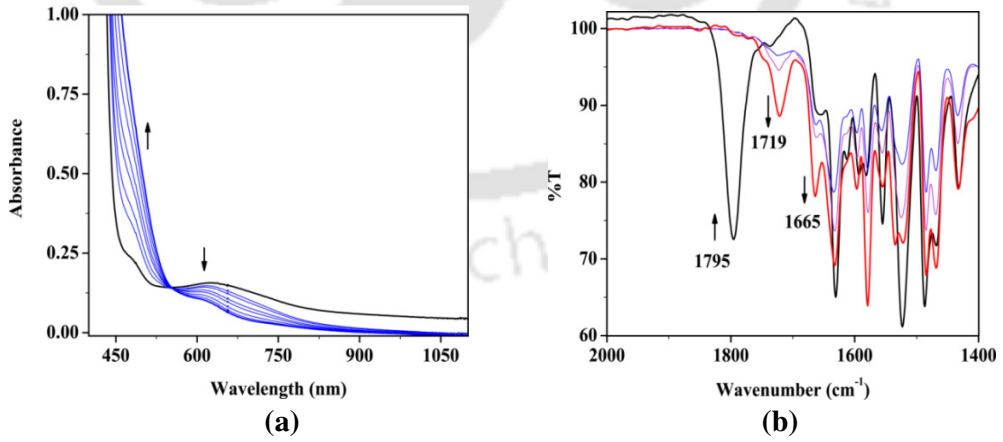

Figure 5.2. (a) Changes in UV-visible spectra of complex **5.2** after in acetonitrile (black- immediately after making the solution and blue- changes with time) (b) FT-IR spectra of complex **5.2** (black) and after addition of acetonitrile in KBr pellet.

The complex **5.2** was found to be unstable in solution at room temperature. FT-IR monitoring of the solution of **5.2** revealed the gradual decrease of the intensity of the 1795 cm^{-1} band with a simultaneous appearance of two new stretching frequencies at 1722 and 1665 cm^{-1}, respectively (Figure 5.2b). These two bands are assignable to the NO stretching frequencies of **5.1**. It is attributed to the disproportionation of **5.2** to **5.1**. The concomitant formation of a high-spin Fe(III) complex is expected in this disproportionation mechanism. When the reaction was monitored by EPR spectroscopic studies, the frozen CH_3CN solution of **5.2** displayed signal (g, 5.03 and 1.99) corresponding to the monomeric high-spin $\{FeNO\}^7$ complex.[17-20] When the spectrum was recorded at room temperature, the intensity of the signal of monomeric $\{FeNO\}^7$ was diminished with gradual increase of the intensity of the **5.1** along with a signal (g, 14.36, 6.68 and 5.13) assignable to the high-spin Fe(III) complex, **5.3** (Figure 5.3 and Scheme 5.2).

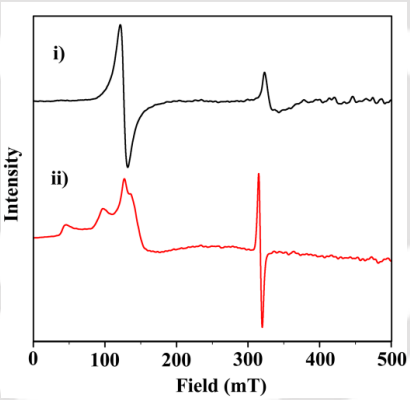

Figure 5.3. X-band EPR spectra of (i) in situ generated complex **5.2** in $CH_3CN/CHCl_3$ at 77 K and (ii) after disproportion at room temperature.

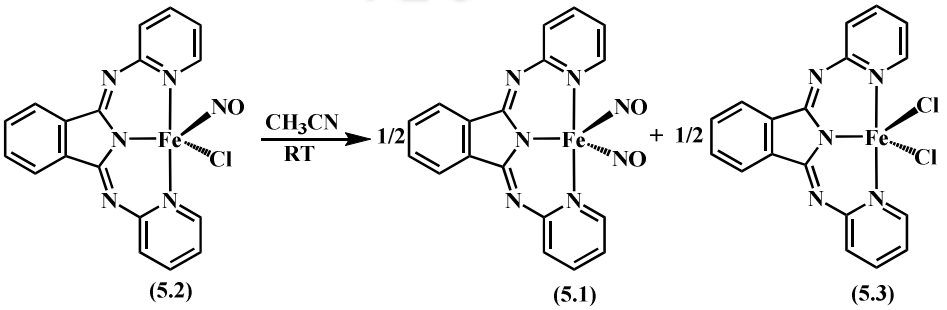

Scheme 5.2. Disproportionation of **5.2** into **5.1** and **5.3** in CH_3CN at room temperature (RT).

Isolation and characterization of **5.3** confirmed this assignment (Experimental Section). Thus, complex **5.2** in solution undergoes disproportionation rapidly to the DNIC **5.1** and a Fe(III) complex, **5.3**. It should be noted here that in case of $\{Fe(dmp)(NO)_2\}^+$ complex, though the intermediate formation of the $\{FeNO\}^7$ was observed in EPR studies, the Fe(III) species was not observed.[8]

5.3 Experimental section

5.3.1 Materials and methods

All reagents and solvents of reagent grade were purchased from commercial sources and used as received except specified. All the reactions were performed under inert conditions unless specified. Deoxygenation of the solvent and solutions was effected by repeated vacuum/purge cycles or bubbling with argon for 30 minutes. UV-visible spectra were recorded on an Agilent Technologies Cary 8454 UV-visible spectrophotometer. FT-IR spectra of the samples were taken on a Perkin Elmer spectrophotometer with samples prepared as KBr pellets. ^{1}H-NMR spectra were recorded in a 600 MHz Varian FT spectrometer. Chemical shifts (ppm) were referenced either with an internal standard (Me_4Si) or to the residual solvent peaks. The X-band Electron Paramagnetic Resonance (EPR) spectra were recorded on a JES-FA200 ESR spectrometer, at room temperature with microwave power, 0.998 mW; microwave frequency, 9.14 GHz and modulation amplitude, 2. Elemental analyses were obtained from a Perkin Elmer Series II Analyzer.

Single crystals were grown by slow evaporation of CH_3OH and $CHCl_3$ solution of **5.1** and **5.2**, respectively. The intensity data were collected using a Bruker SMART APEX-II CCD diffractometer, equipped with a fine focus 1.75 kW sealed tube MoK_α radiation (λ = 0.71073 Å) at 293(3) K, with increasing ω(width of 0.3° per frame) at a scan speed of 3 s/frame. The SMART software was used for data acquisition. Data integration and

reduction were undertaken with SAINT and XPREP software.[21] Multi-scan empirical absorption corrections were applied to the data using the program SADABS.[22] Structures were solved by direct methods using SHELXS-2014 and refined with full-matrix least squares on F^2 using SHELXL-2014/7.[23] Structural illustrations have been drawn with ORTEP-3 for Windows.[24]

5.3.2 Synthesis of complexes

(i) 5.1, [(L5)Fe(NO)$_2$]

Excess of NO was purged to a 50 mL round bottom flask containing anhydrous $FeCl_2$ (63 mg, 0.5 mmol). A solution of **L5H** (150 mg, 0.5 mmol) in 20 mL CH_3OH was added to this mixture and was allowed to stir. The yellow color solution then turned into brown and after stirring for another 30 min, the excess of NO was removed by purging Ar. Volume of the solution was reduced to *ca.* 5 mL by flashing Ar into it for 30 min. Diethyl ether was then added to make a layer on it and after keeping the solution for overnight it gives dark brown precipitate of **5.1**. Yield: 75 mg (36%). X-ray quality crystals were obtained by slow diffusion of diethyl ether in to methanol solution. FT-IR (KBr pellet): 3393, 2970, 1719, 1665, 1632, 1581, 1520, 1486, 1469, 1438, 1376, 1081, 1054, 772, 709 cm^{-1}. X-band EPR: (isolated, CH_3CN/DMF at 77 K; g_{avg}, 2.01), (in situ, $CHCl_3$/CH_3CN at 77 K; g_{avg}, 2.05). ESI-mass (m/z): calcd: 384.04 for [(L5)Fe(NO)], found: 384.99 (M+1).

(ii) 5.2, [(L5)Fe(NO)Cl]

Excess of NO was purged to a 50 mL round bottom flask containing anhydrous $FeCl_2$ (126 mg, 1 mmol). A solution of **L5H** (299 mg, 1 mmol) in 10 mL $CHCl_3$ was added to this mixture and was allowed to stir. The yellow color solution then turned into brown and within 10 min it started to give light green color precipitate of **5.2**. Excess of solvent was removed with a syringe and the resulting compound was dried by flashing Ar into it for 30

min. Product was found to be stable for several days in solid state. Yield: 360 mg (86%). Single crystals of X-ray quality was obtained when reaction mixture was kept at -40 °C for several days before getting precipitated. UV-visible (CH_3CN): λ_{max} 480 nm (ε/M^{-1} cm^{-1}, 235) and 630 nm (ε/M^{-1} cm^{-1}, 160). FT-IR (in KBr): 3290, 3078, 1795, 1630, 1555, 1523, 1487, 1467, 1430, 1206, 1055, 777, 710 cm^{-1}. X-band EPR ($CHCl_3$ at 77 K; g_1, 5.03; g_2, 1.99). ESI-mass (m/z): calcd: 389.01 for [(L5)FeCl], found: 389.80 (M+1).

(iii) 5.3, [(L5)$FeCl_2$]

Complex **5.3** was prepared following an earlier reported procedure.[25] Ligand **L5H** (299 mg, 1 mmol) was added to a refluxing methanol (*ca.* 10 mL) solution of $FeCl_2$ (126 mg, 1 mmol) under O_2. After 1 h of stirring it gave brown precipitate which was collected by filtration and dried under vacuum. Yield: 275 mg (65%). UV-visible (CH_3CN): λ_{max} 608 nm (ε/M^{-1} cm^{-1}, 104). FT-IR (in KBr): 3424, 2921, 1637, 1578, 1535, 1477, 1466, 1430, 1270, 1182, 1055, 780, 705 cm^{-1}. ESI-mass (m/z): calcd: 423.98 for [(L5)$FeCl_2$], found: 424.96 (M+1). X-band EPR: (isolated, CH_3CN/DMF at 77 K; g_1, 14.21; g_2, 6.67; g_3, 5.22), (in situ, $CHCl_3$/CH_3CN at 77 K; g_1, 14.36; g_2, 6.68; g_3, 5.13).

5.3.3 Disproportionation of complex 5.2 to complexes 5.1 and 5.3

Complex **5.2** (100 mg) was taken in a 25 mL round bottom flask and to this 10 mL of acetonitrile was added. Stirring of the reaction mixture was continued and reaction was monitored with FT-IR and UV-visible spectroscopy in various time intervals. After 2 h of stirring it gives brown color precipitate of **5.3** and the solution part contained **5.1**. Yield: **5.1**, 37.5 mg (38%); **5.3**, 41.5 mg (41%).

5.4 Conclusion

In conclusion the present study demonstrates the formation of $\{Fe(NO)_2\}^9$ DNIC, **5.1**,

from the reaction of ferrous precursor and NO gas. The complex was structurally characterized. Detail study identified the involvement of a $\{FeNO\}^7$ intermediate, **5.2** in the reaction. Complex **5.2** was isolated and structurally characterized. It has been found that **5.2** undergoes disproportionation reaction to afford **5.1** and a Fe(III) complex, **5.3**. The synthesis of $\{Fe(NO)_2\}^9$ DNICs from the ferrous precursors are also reported for N,O-ligand systems, though the mechanism were not known. Lehnert and coworkers report suggests the formation of the intermediate $\{FeNO\}^7$ complex in solution.[8] The present study shown the formation of a $\{Fe(NO)_2\}^9$ DNIC from a ferrous precursor through the $\{FeNO\}^7$ intermediate complex.

5.5 References

(1) Stamler, J. S.; Singel, D. J.; Loscalzo, J. *Science* **1992**, *258*, 1898.

(2) (a) Lin, Y. L.; Huang K. T. *Nitric Oxide* **2009**, *21*, 44. (b) Murad, F. *Angew. Chem. Int. Ed.* **1999**, *38*, 1856.

(3) Sulok, C. D.; Bauer, J. L.; Speelman, A. L.; Weber, B.; Lenhert, N. *Inorg. Chim. Acta.* **2012**, *380*, 148.

(4) a) Ostrowski, A. D.; Ford, P. C. *Dalton Trans.* **2009**, 10660. (b) Ignaro, L. J. *Angew. Chem. Int. Ed.* **1999**, *38*, 1882.

(5) (a) Ignaro, L. J. *Nitric Oxide: Biology and Pathology* Academic Press; San Diego, **2000**. (b) Martin, C. T.; Morse, R. H.; Kanne, R. M.; Gray, H. B.; Malmstroom, B. G.; Chan, S. I. *Biochemistry* **1981**, *20*, 5147.

(6) Skodje, M. K.; Kwon, M. Y.; Chung, S. W.; Kim, E. *Chem. Sci.* **2014**, *5*, 2374.

(7) Tran, N. G.; Kalyvas, H.; Skodje, K. M.; Hayashi, T.; Loccoz, P. M.; Callan, P. E.; Shearer, J.; Kirschenbaum, L. J.; Kim, E. *J. Am. Chem. Soc.* **2011**, *133*, 1184.

(8) Speelman, A. L.; Zhang, B.; Silakov, A.; Skodje, K. M.; Alp, E. E.; Zhao, J.; Hu, M. Y.; Kim, E.; Krebs, C.; Lehnert, N. *Inorg. Chem.* **2016**, *55*, 5485.

(9) Ye, S.; Neese, F. *J. Am. Chem. Soc*. **2010**, *132*, 3646.

(10) Tonzetich, Z. J.; Do, L. H.; Lippard, S. J. *J. Am. Chem. Soc.* **2009**, *131*, 7964.

(11) Hung, M.-C.; Tsai, M.-C.; Lee, G.-H.; Liaw, W.-F. *Inorg. Chem*. **2006**, *45*, 6041.

(12) (a) Hickok, J. R.; Sahni, S.; Shen, H.; Arvind, A.; Antoniou, C.; Fung, L. W. M.; Thomas, D. D. *Free Radical Biol. Med*. **2011**, *51*, 1558. (b) Tran, C. T.; Skodje, K. M.; Kim, E. *Prog. Inorg. Chem*. **2014**, *59*, 339. (c) Enemark, J. H.; Feltham, R. D. *Coord. Chem. Rev*. **1974**, *13*, 339.

(13) Tonzetich, Z. J.; Héroguel, F.; Do, L. H.; Lippard, S. J. *Inorg. Chem*. **2011**, *50*, 1570.

(14) Chen, C.-H.; Ho, Y.-C.; Lee, G.-H. *J. Organomet. Chem.* **2009**, *694*, 3395.

(15) (a) Harrop, T. C.; Song, D.; Lippard, S. J. *J. Am. Chem. Soc*. **2006**, *128*, 3528. (b) Harrop, T. C.; Song, D.; Lippard, S. J. J. *Inorg. Biochem*. **2007**, *101*, 1730. (c) Lu, T.-T.; Chiou, S.-J.; Chen, C.-Y.; Liaw, W.-F. *Inorg. Chem*. **2006**, *45*, 8799.

(16) D'Autréaux, B.; Horner, O.; Oddou, J.-L.; Jeandey, C.; Gambarelli, S.; Berthomieu, C.; Latour, J.-M.; Michaud-Soret, I. *J. Am. Chem. Soc*. **2004**, *126*, 6005.

(17) Berto, T. C.; Hoffman, M. B.; Murata, Y.; Landenberger, K. B.; Alp, E. E.; Zhao, J.; Lehnert, N. *J. Am. Chem. Soc*. **2011**, *133*, 16714.

(18) (a) Lorković, I.; Ford, P. C. *J. Am. Chem. Soc*. **2000**, *122*, 6516. (b) Roncaroli, F.; van Eldik, R.; Olabe, J. A. *Inorg. Chem*. **2005**, *44*, 2781. (c) Wang, J.; Schopfer, M. P.; Sarjeant, A. A. N.; Karlin, K. D. *J. Am. Chem. Soc*. **2009**, *131*, 450.

(19) Jo, D.-H.; Chiou, Y.-M.; Que, L. *Inorg. Chem*. **2001**, *40*, 3181.

(20) Ray, M.; Golombek, A. P.; Hendrich, M. P.; Yap, G. P. A.; Liable-Sands, L. M.; Rheingold L, A.; Borovik, A. S. *Inorg. Chem*. **1999**, *38*, 3110.

(21) *SMART*, *SAINT and XPREP*, Siemens Analytical X-ray Instruments Inc., Madison, Wisconsin, USA, **1995**.

(22) Sheldrick, G. M. *SADABS*: *software for Empirical Absorption Correction*, University of Gottingen, Institut fur Anorganische Chemieder Universitat, Tammanstrasse 4, D-3400 Gottingen, Germany, **1999**.

(23) Sheldrick, G. M. *SHELXS-2014*, University of Gottingen, Germany.

(24) Farrugia, L. J. *J. Appl. Crystallogr.* **1997**, *30*, 565.

(25) Balogh-Hergovich, E.; Speier, G.; Tapodi, B.; Reglier, M.; Giorgi, M. *Z. Kristallogr. NCS* **1999**, *214*, 579.

Appendix I

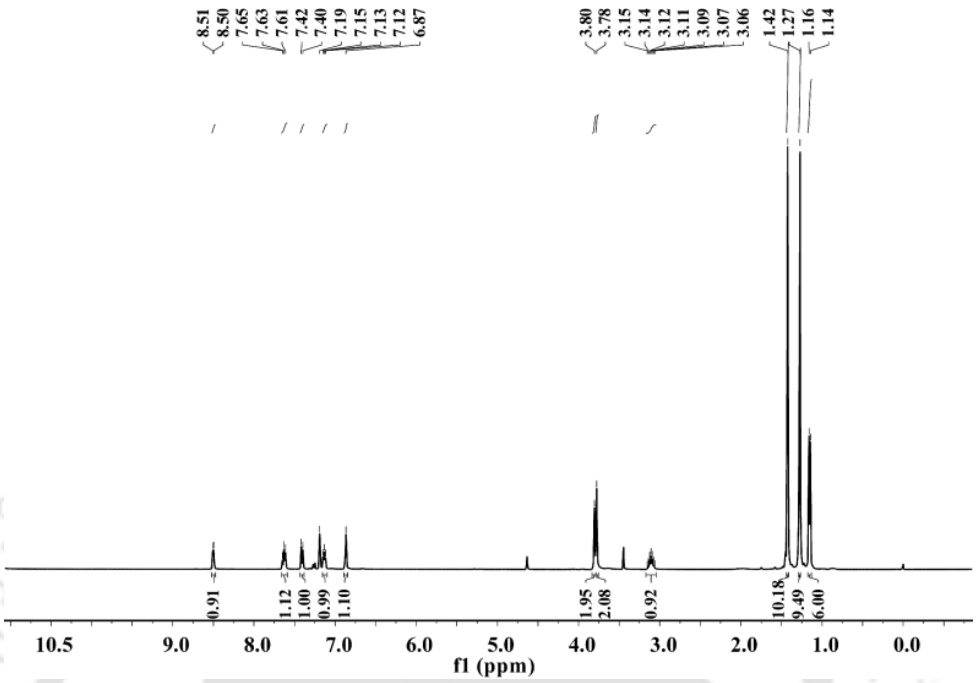

Figure A1.1. ^{1}H-NMR spectrum of ligand **L1H** in $CDCl_3$.

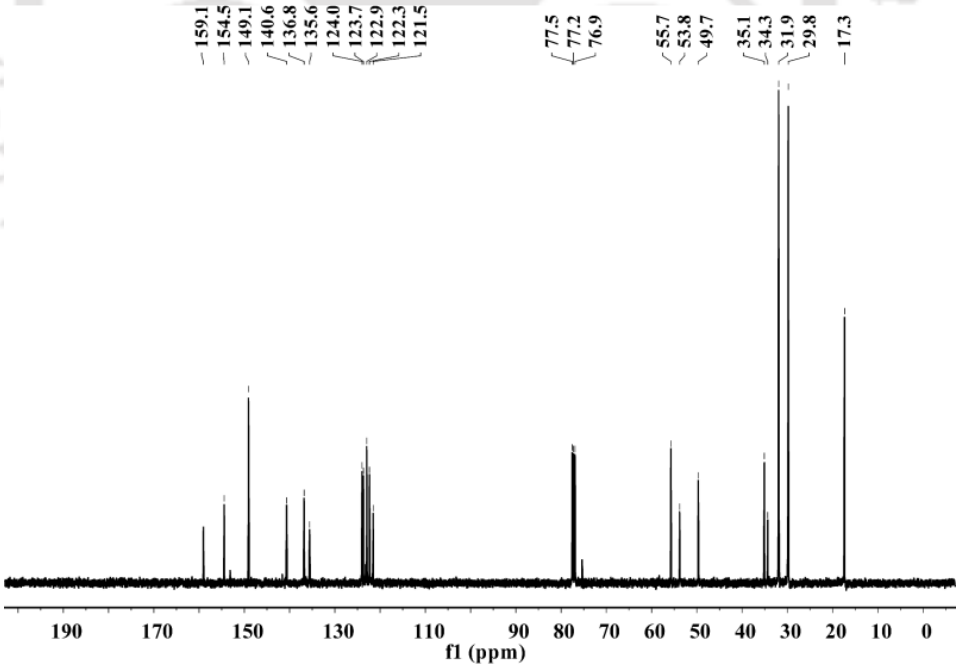

Figure A1.2. ^{13}C-NMR spectrum of ligand **L1H** in $CDCl_3$.

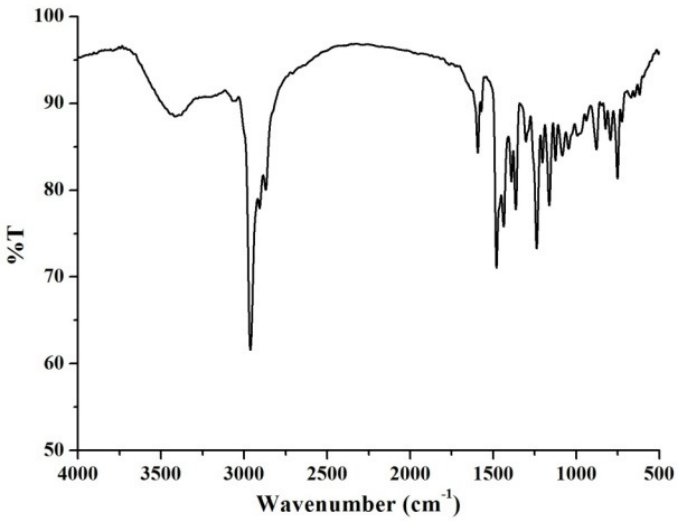

Figure A1.3. FT-IR spectrum of ligand **L1H** in KBr pellet.

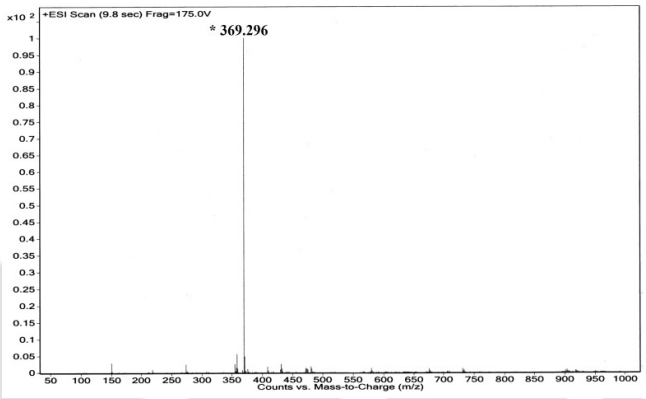

Figure A1.4. ESI-mass spectrum of ligand **L1H** in methanol.

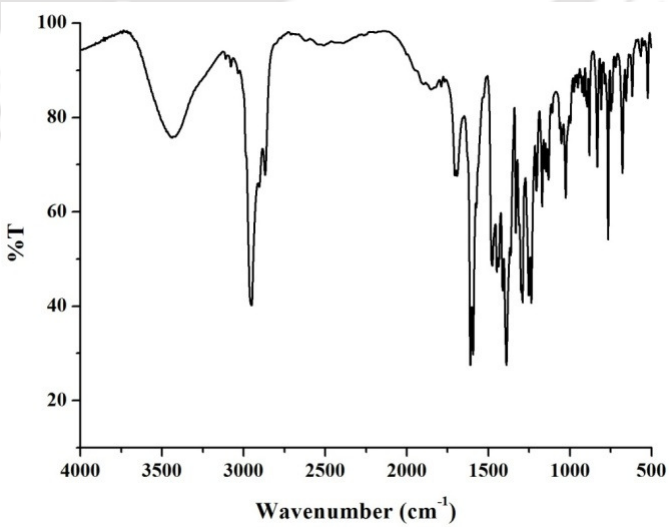

Figure A1.5. FT-IR spectrum of complex **2.1** in KBr pellet.

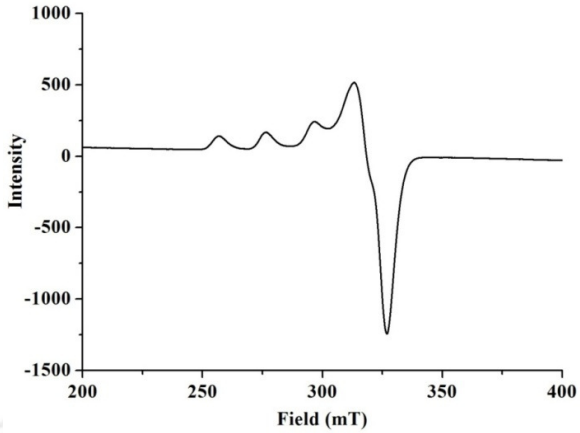

Figure A1.6. X-band EPR spectrum of complex **2.1** in methanol at 77 K.

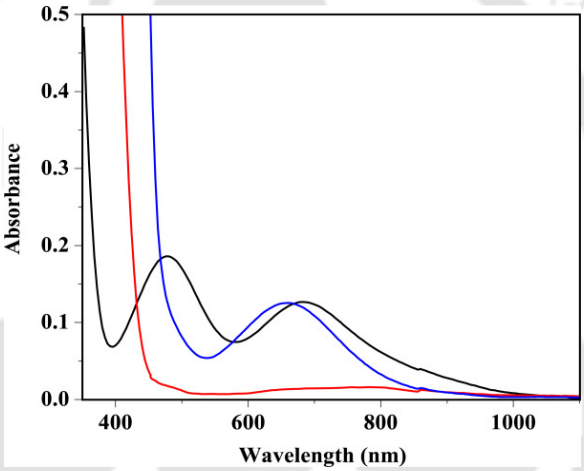

Figure A1.7. UV-visible spectra of complex **2.1** before (black), after purging 1 equivalent (red) and 2 equivalent of NO_2 (blue) in methanol.

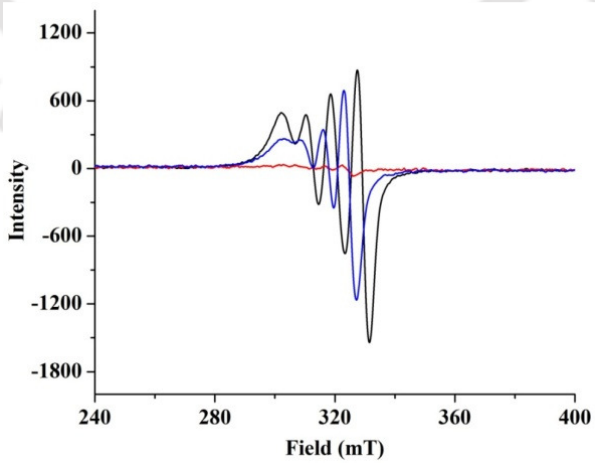

Figure A1.8. X-band EPR spectra of complex **2.1** before (black), after purging 1 equivalent (red) and 2 equivalent of NO_2 (blue) in methanol at 298 K.

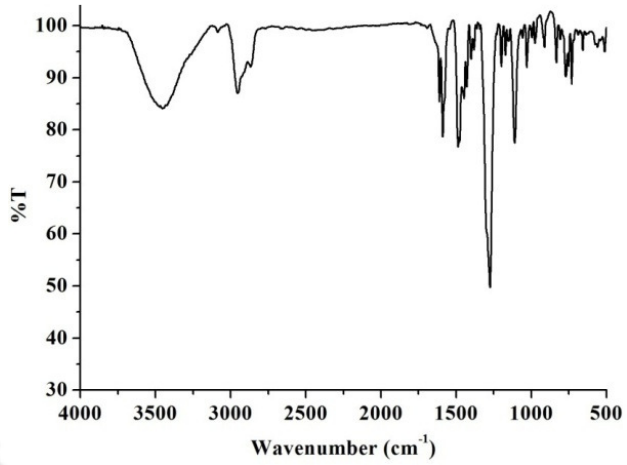

Figure A1.9. FT-IR spectrum of complex **2.2** in KBr pellet.

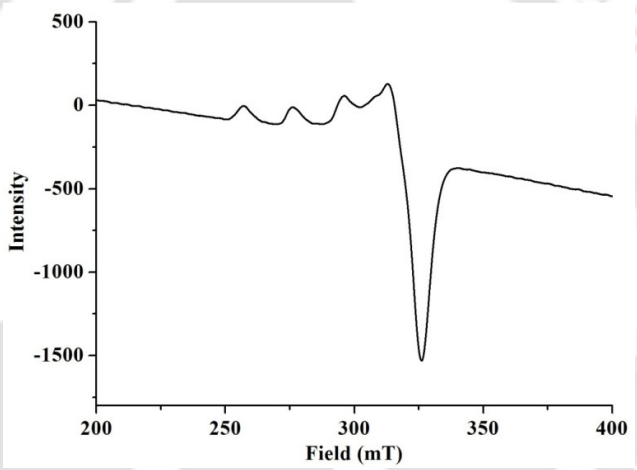

Figure A1.10. X-band EPR spectrum of complex **2.2** in methanol at 77 K.

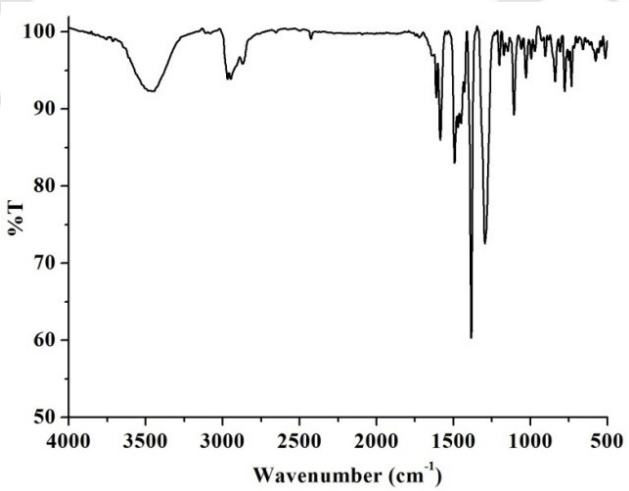

Figure A1.11. FT-IR spectrum of complex **2.3** in KBr pellet.

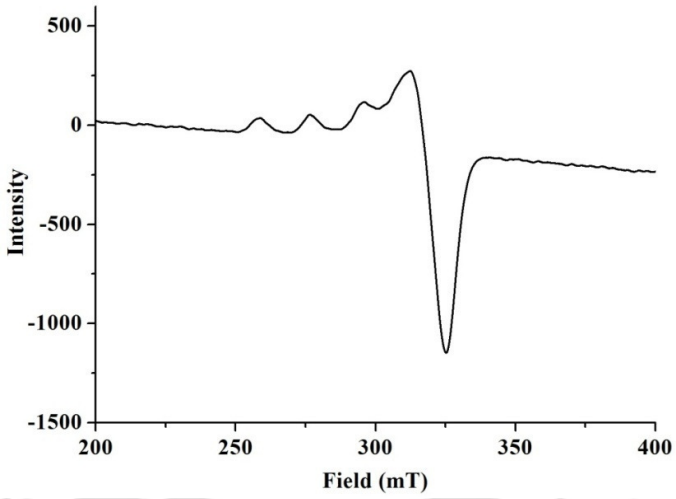

Figure A1.12. X-band EPR spectrum of complex **2.3** in methanol at 77 K.

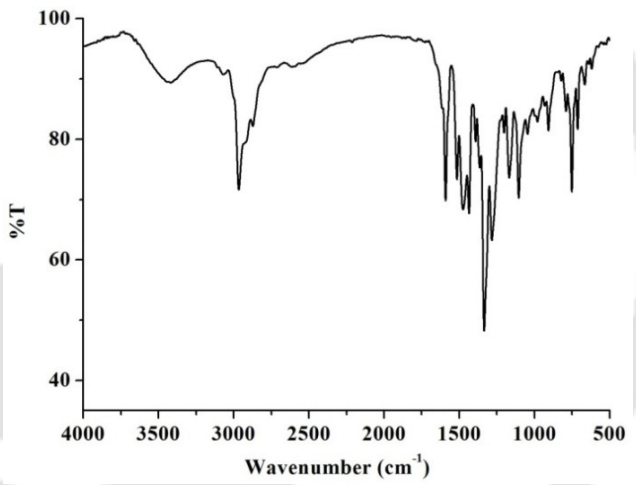

Figure A1.13. FT-IR spectrum of modified ligand **L1′H** in KBr pellet.

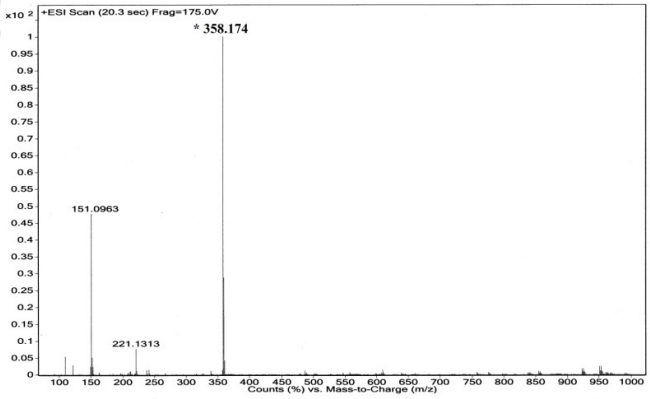

Figure A1.14. ESI-mass spectrum of modified ligand **L1′H** in methanol.

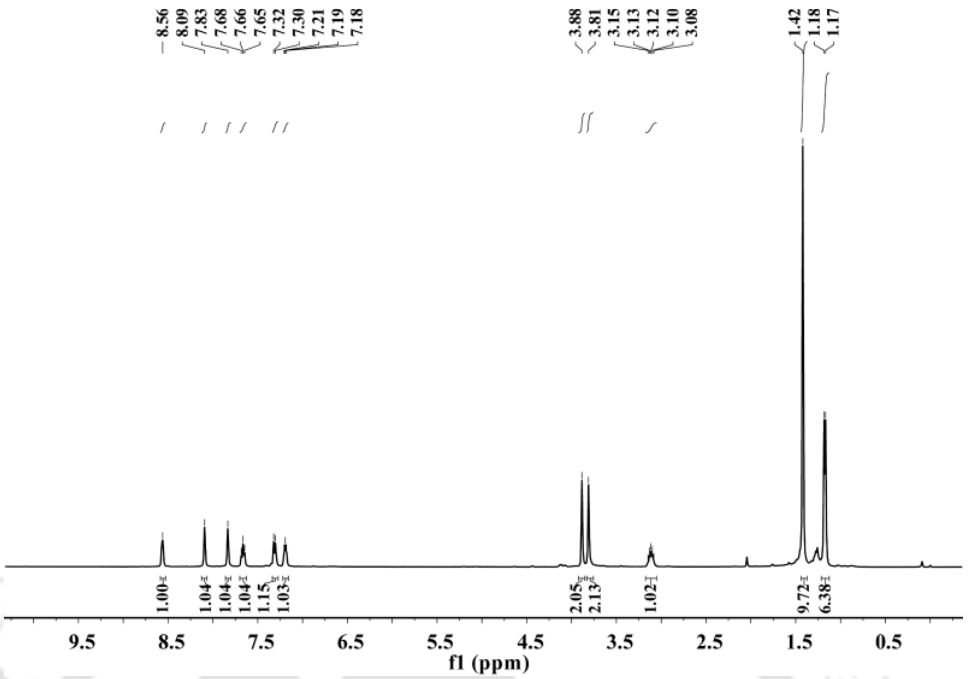

Figure A1.15. ^{1}H-NMR spectrum of modified ligand **L1′H** in $CDCl_3$.

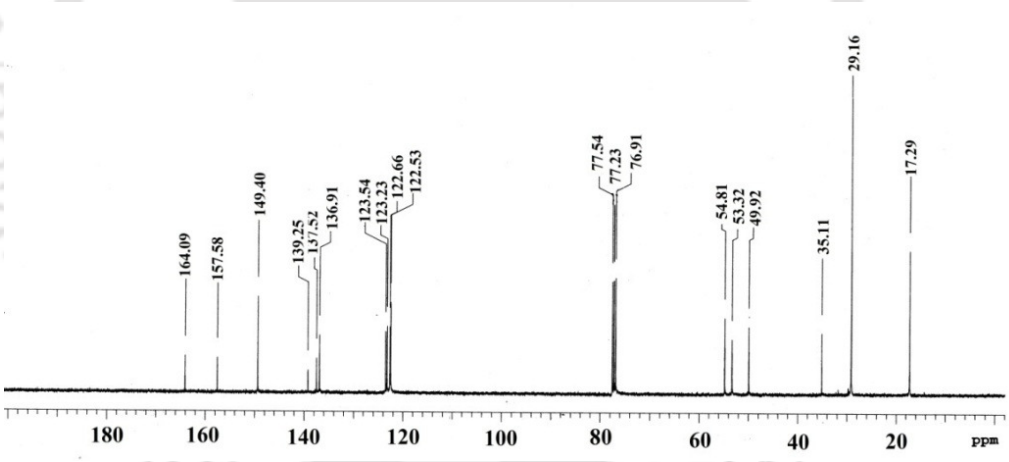

Figure A1.16. ^{13}C-NMR spectrum of modified ligand **L1′H** in $CDCl_3$.

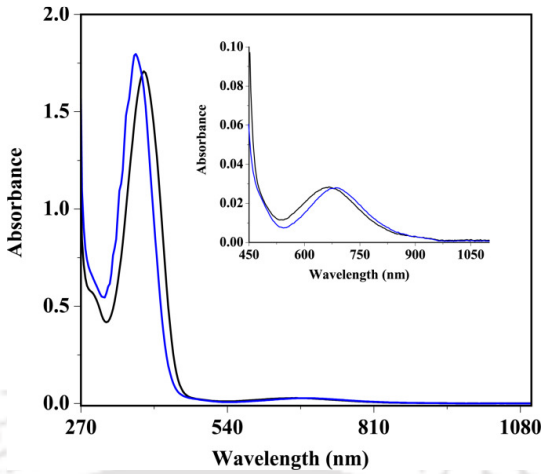

Figure A1.17. UV-visible spectra of complex **2.2** before (black) and after purging NO_2 (blue) in methanol.

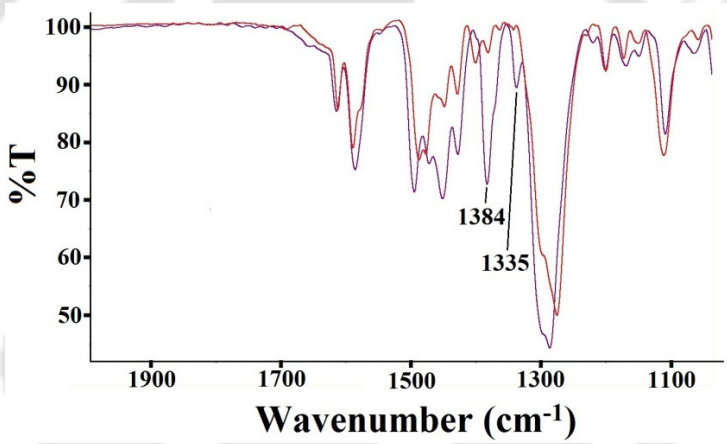

Figure A1.18. FT-IR spectra of complex **2.2** (red) and {**2.2** + ^{18}ONO} (violet) in KBr pellet.

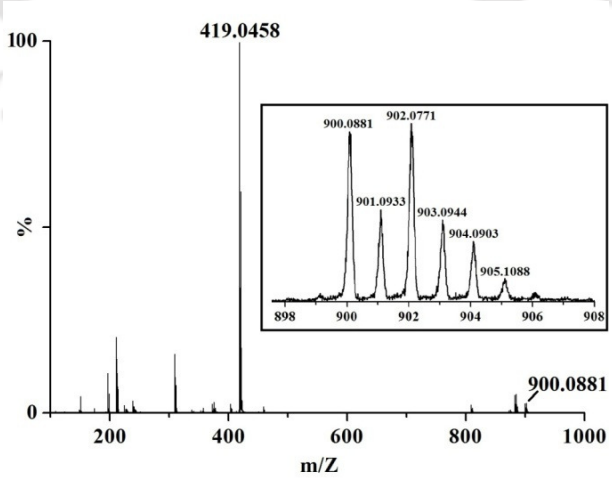

Figure A1.19. ESI-mass spectrum of complex **2.3** in methanol.

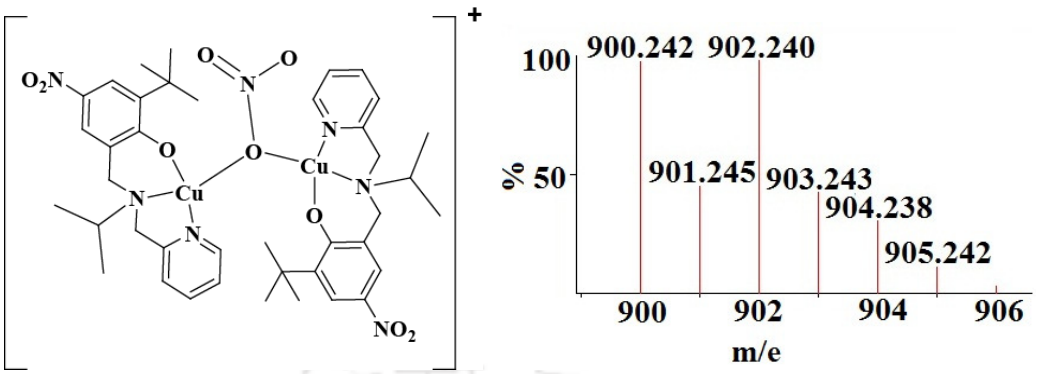

Figure A1.20. Simulated mass of $[\{Cu(L1')\}_2(NO_3)]^+$.

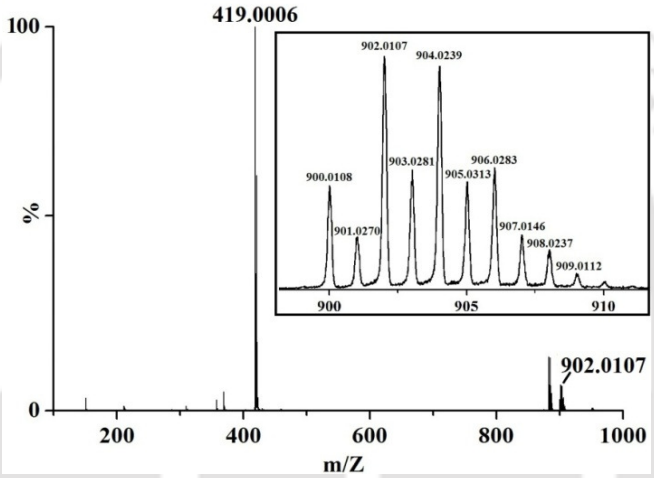

Figure A1.21. ESI-mass spectrum of [**2.2** + ^{18}ONO] in methanol.

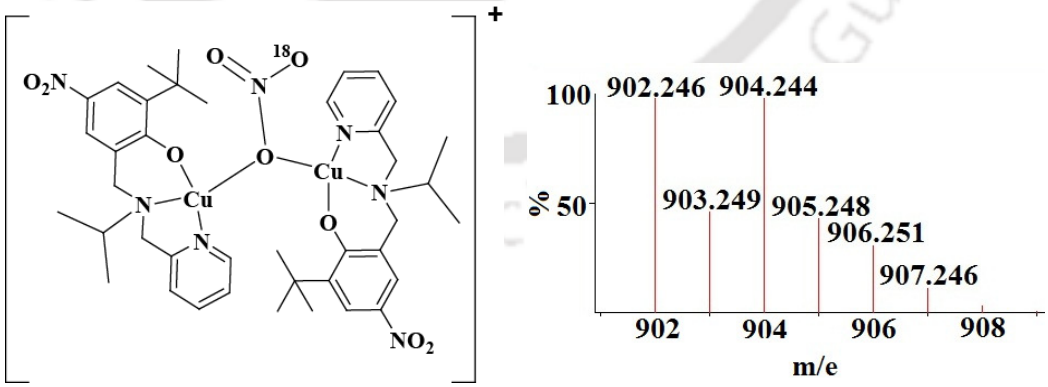

Figure A1.22. Simulated mass spectrum of $[\{Cu(L1')\}_2(^{18}ONO_2)]^+$.

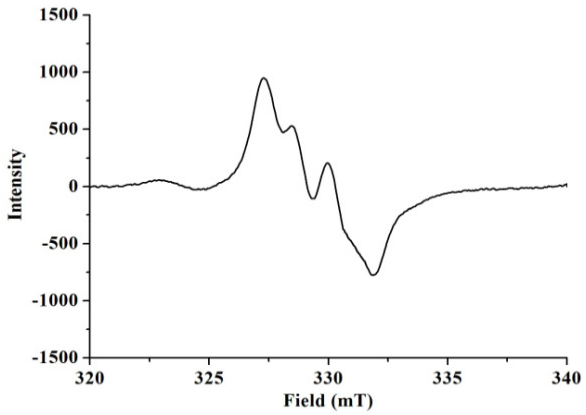

Figure A1.23. X-band EPR spectrum of $[(DTC)_2Fe^{II}]$ after reaction with NO released during the reaction of complex **2.2** with NO_2 in acetonitrile at 298 K.

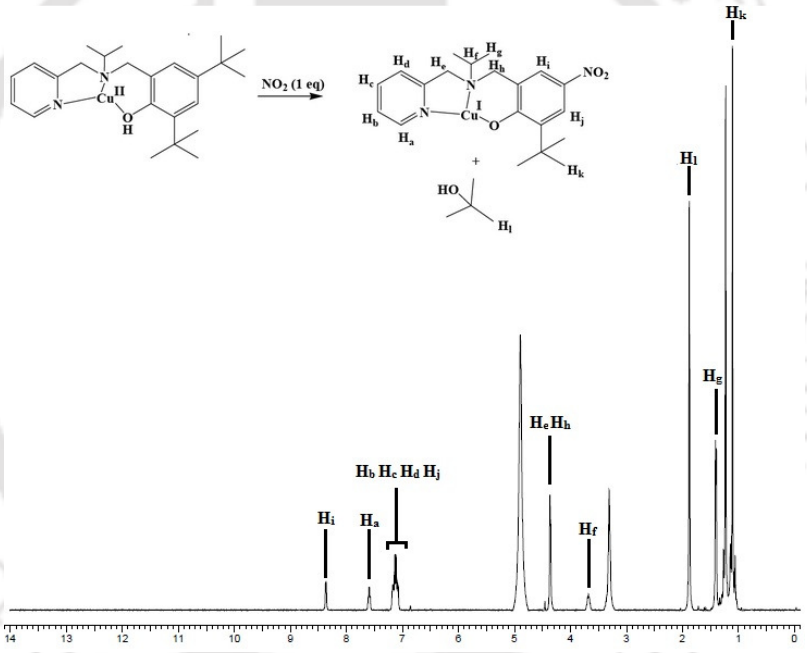

Figure A1.24. ^{1}H-NMR spectrum of complex **2.1** after purging 1 equivalent of NO_2 in CD_3OD.

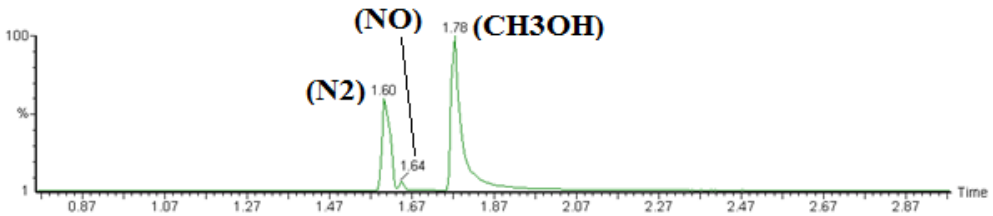

Figure A1.25. GC chromatogram of the head space gas from the reaction of complex **2.2** with NO_2 in methanol.

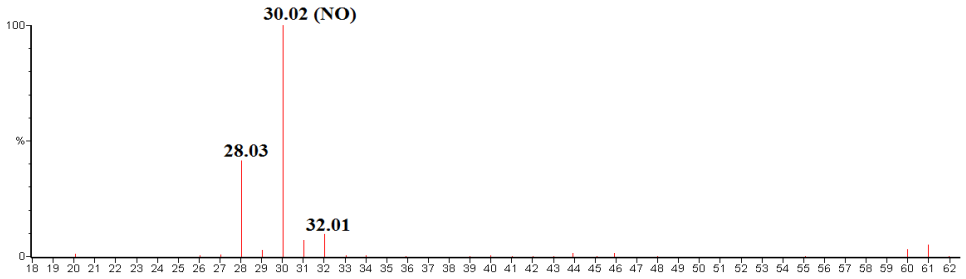

Figure A1.26. GC-mass spectrum of the head space gas from the reaction of complex **2.2** with NO_2 in methanol.

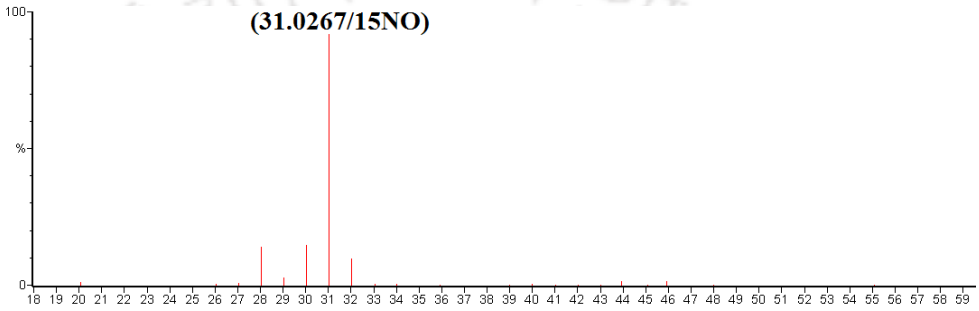

Figure A1.27. GC-mass spectrum of the head space gas from the reaction of complex **2.2** with $^{15}NO_2$ in methanol.

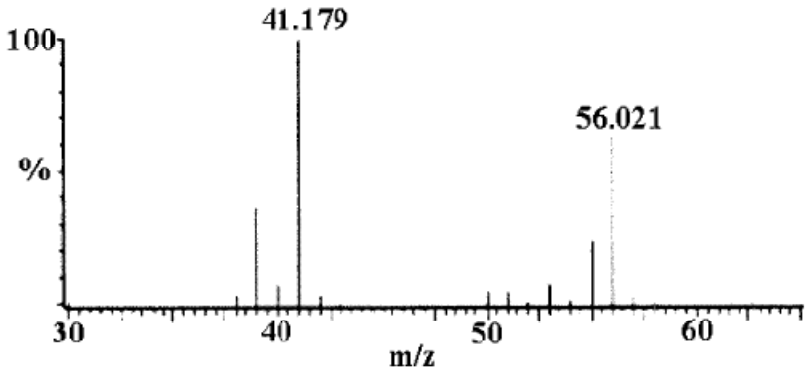

Figure A1.28. GC–mass spectrum of the head space gas from the reaction of complex **2.1** with 1 equivalent of NO_2 in dry methanol. The peak at m/z, 56.021 followed by 41.179 indicates the presence of isobutylene.

Appendix II

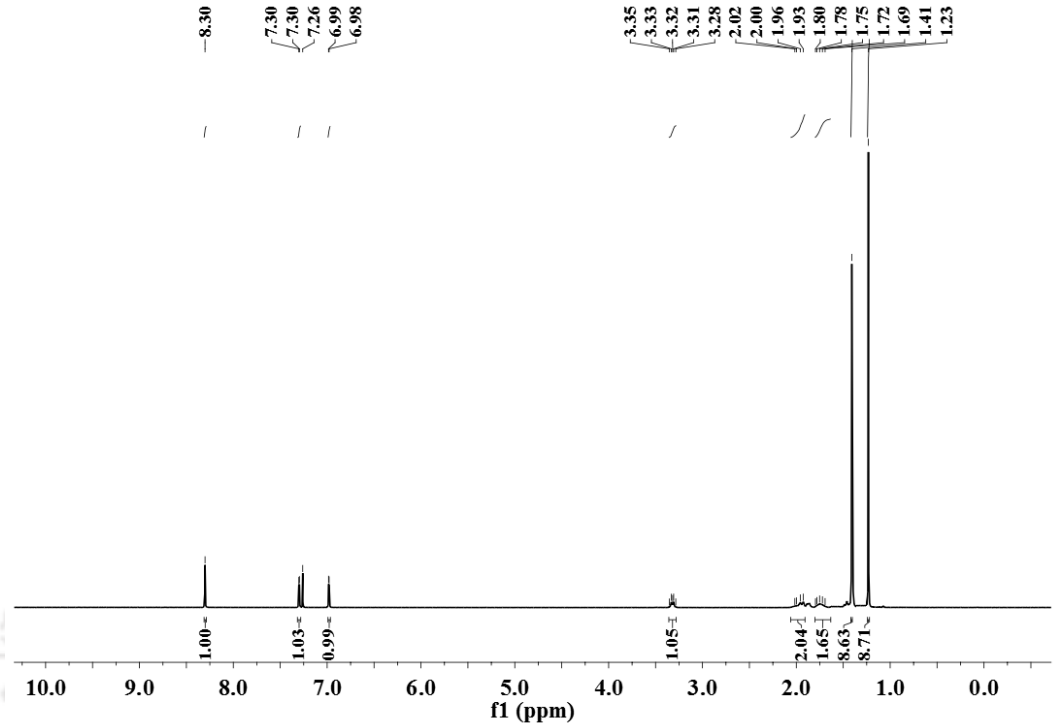

Figure A2.1. ^{1}H-NMR spectrum of ligand **L2H$_2$** in $CDCl_3$.

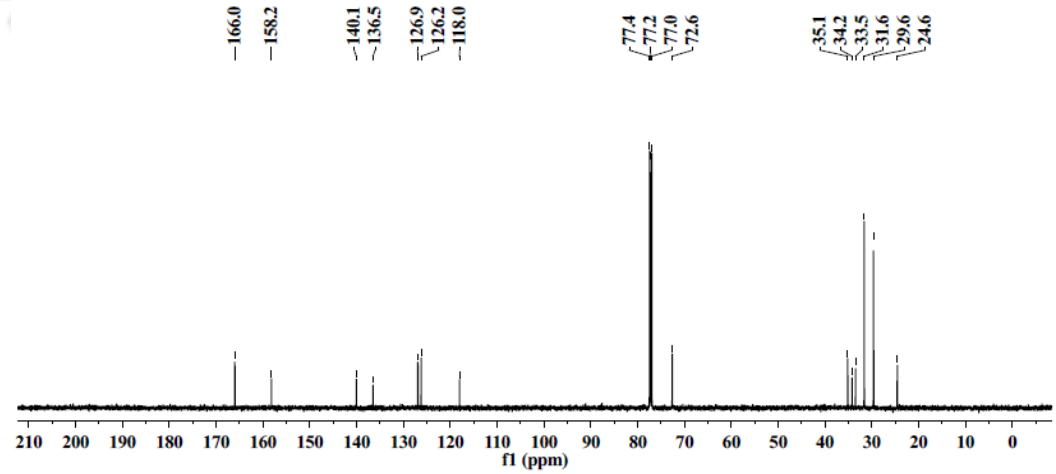

Figure A2.2. ^{13}C-NMR spectrum of ligand **L2H$_2$** in $CDCl_3$.

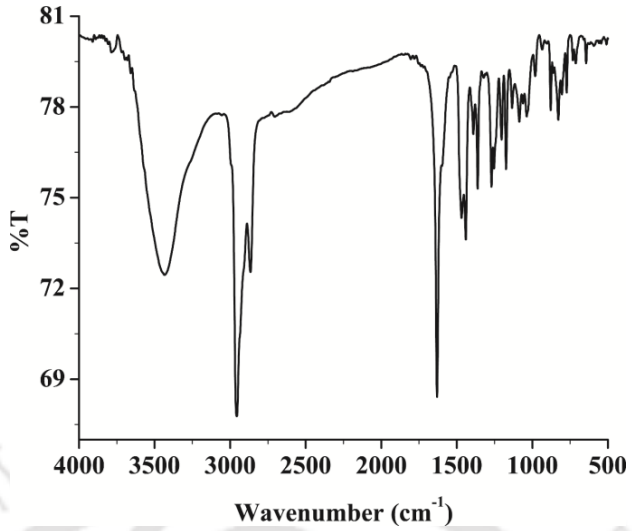

Figure A2.3. FT-IR spectrum of ligand **L2H$_2$** in KBr pellet.

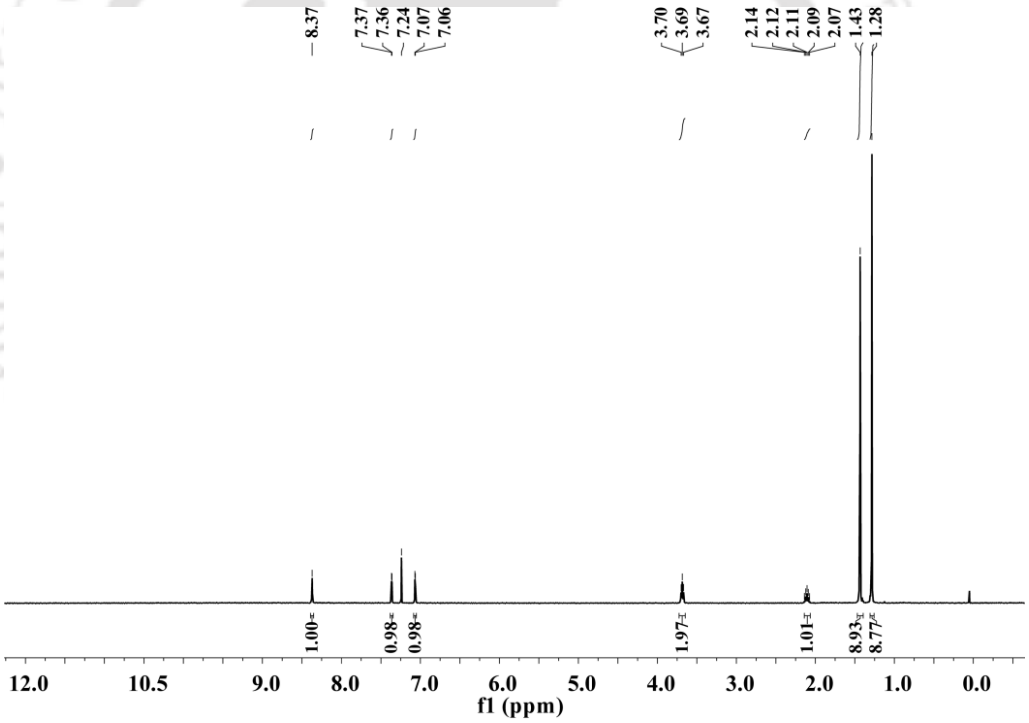

Figure A2.4. ^{1}H-NMR spectrum of ligand **L3H$_2$** in $CDCl_3$.

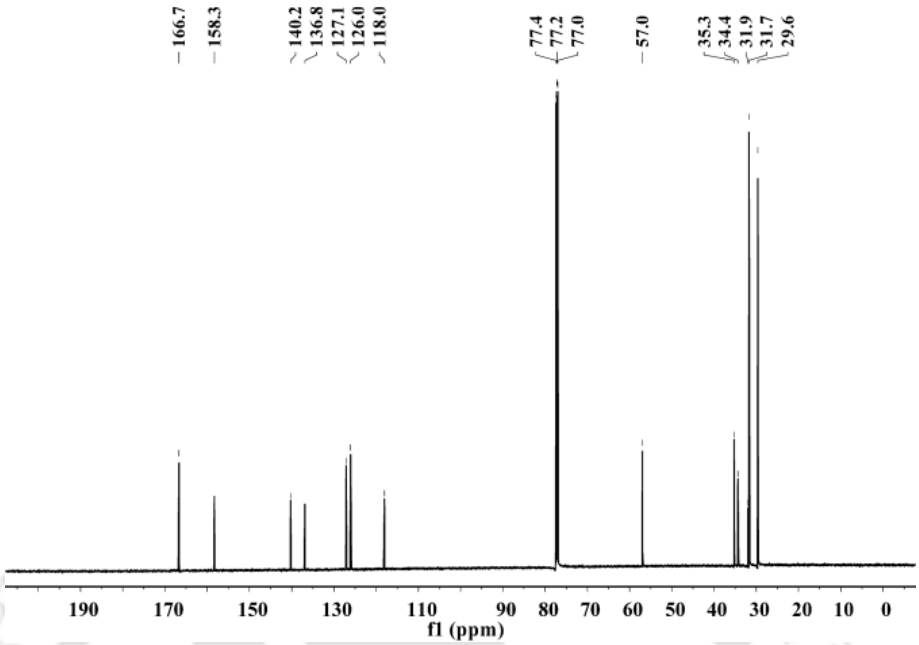

Figure A2.5. ^{13}C-NMR spectrum of ligand **L3H$_2$** in $CDCl_3$.

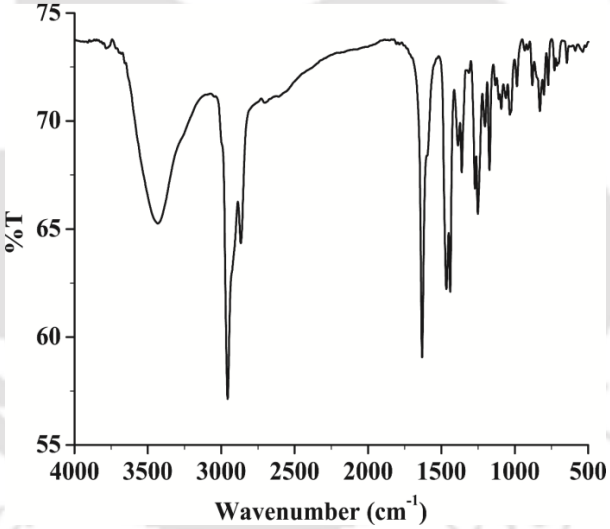

Figure A2.6. FT-IR spectrum of ligand **L3H$_2$** in KBr pellet.

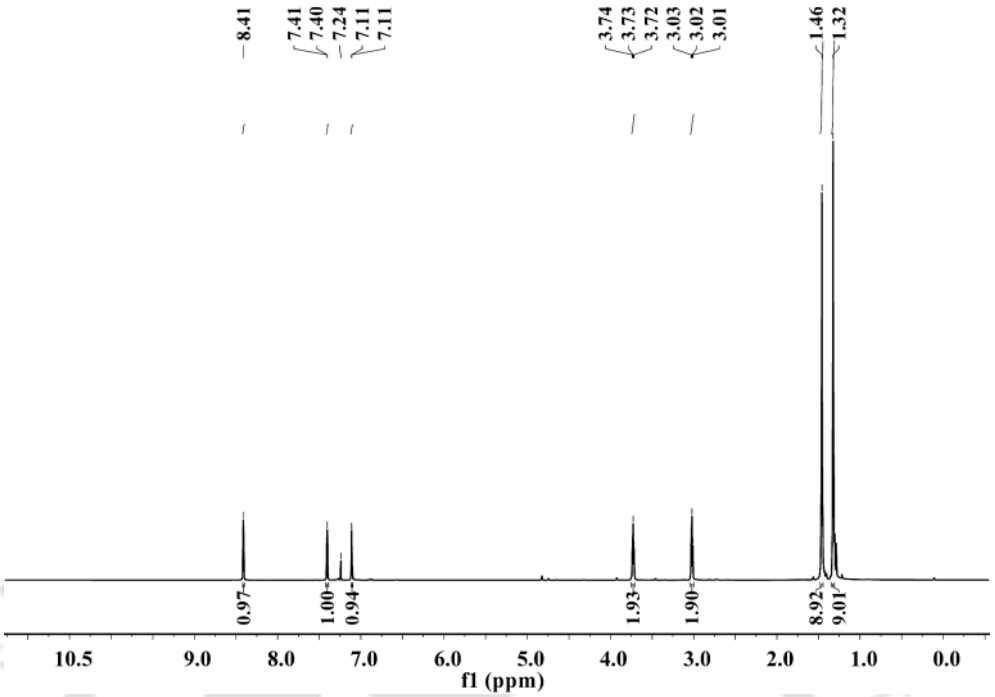

Figure A2.7. ^{1}H-NMR spectrum of ligand **L4H$_2$** in $CDCl_3$.

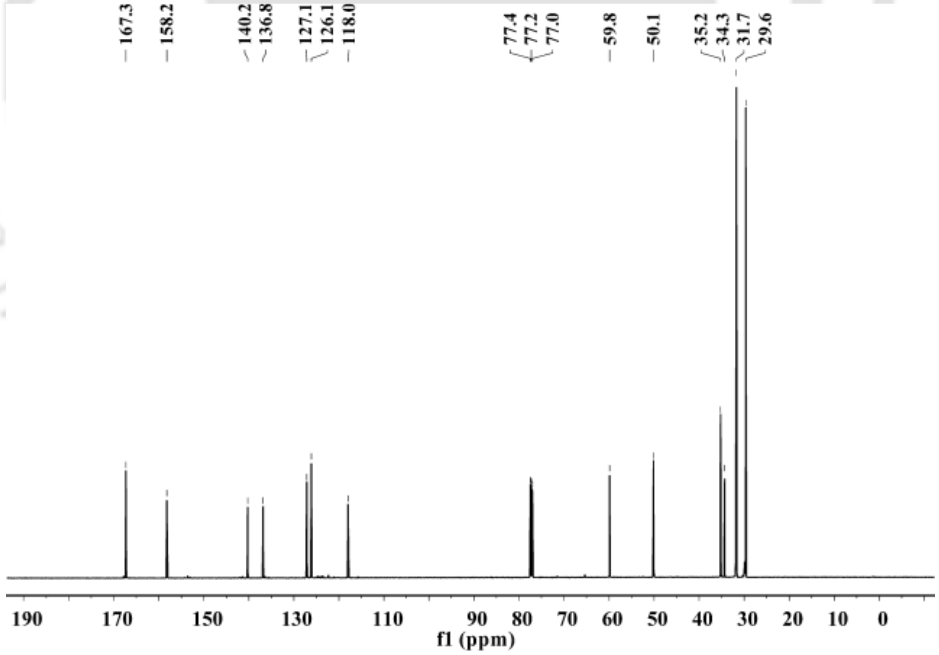

Figure A2.8. ^{13}C-NMR spectrum of ligand **L4H$_2$** in $CDCl_3$.

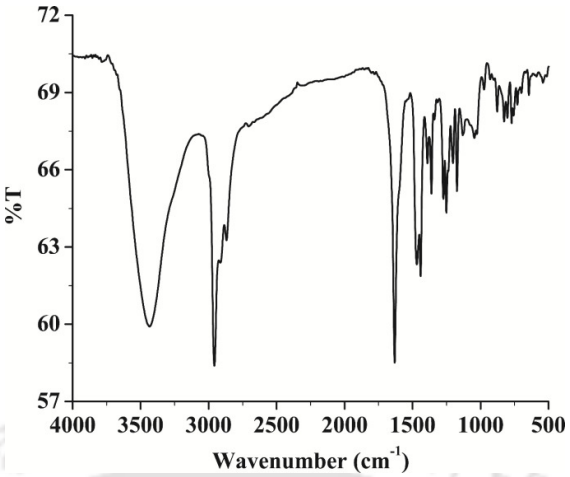

Figure A2.9. FT-IR spectrum of ligand $\mathbf{L4H_2}$ in KBr.

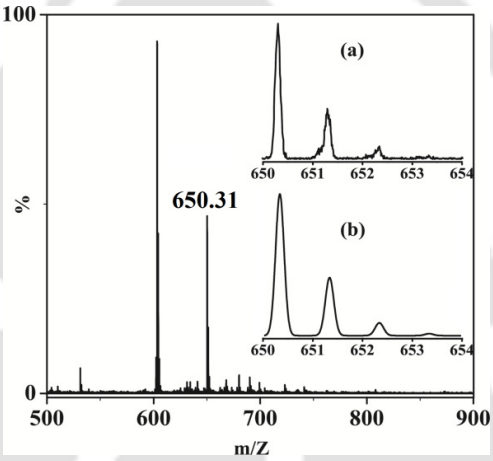

Figure A2.10. ESI-mass spectrum of complex **3.1** in methanol. Inset shows (a) experimental and (b) simulated isotopic distribution pattern.

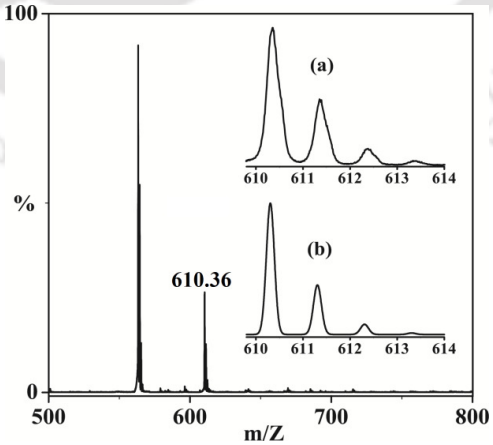

Figure A2.11. ESI-mass spectrum of complex **3.2** in methanol. Inset shows (a) experimental and (b) simulated isotopic distribution pattern.

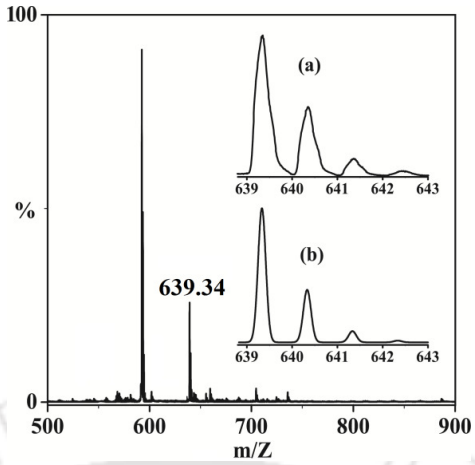

Figure A2.12. ESI-mass spectrum of complex **3.3** in methanol. Inset shows (a) experimental and (b) simulated isotopic distribution pattern.

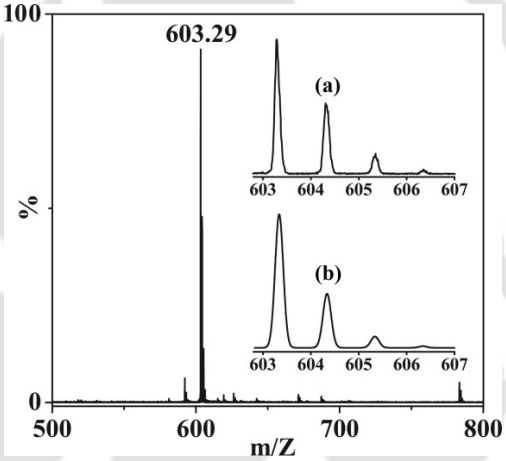

Figure A2.13. ESI-mass spectrum of complex **3.4** in methanol. Inset shows (a) experimental and (b) simulated isotopic distribution pattern.

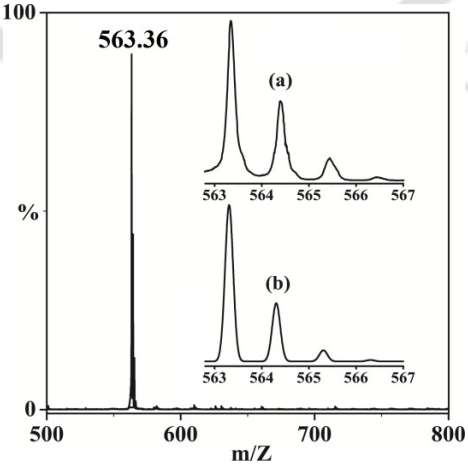

Figure A2.14. ESI-mass spectrum of complex **3.5** in methanol. Inset shows (a) experimental and (b) simulated isotopic distribution pattern.

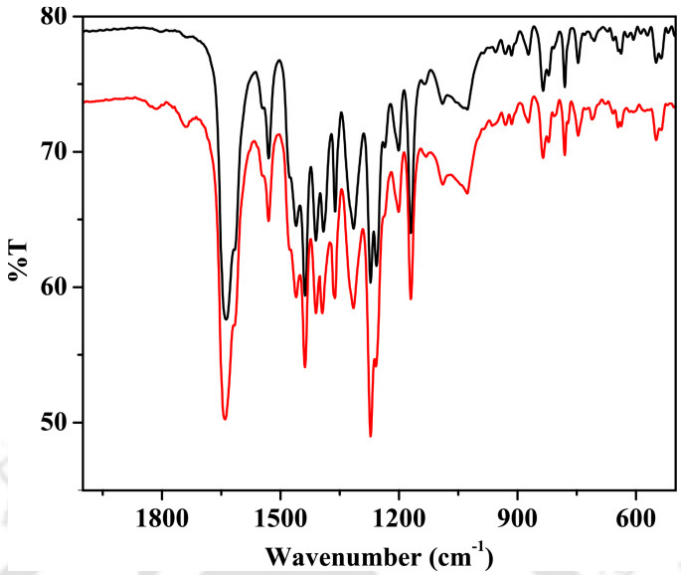

Figure A2.15. FT-IR spectra of complex **3.3** (black) and after reaction with DMS (red) in CH_3OH.

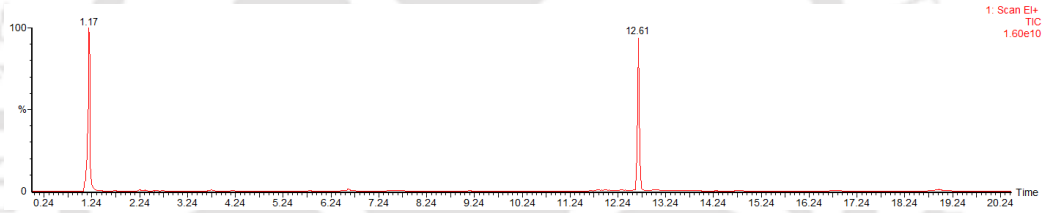

Figure A2.16. GC chromatograph of hexane wash of the reaction mixture of complexes **3.1/3.2** with DMS.

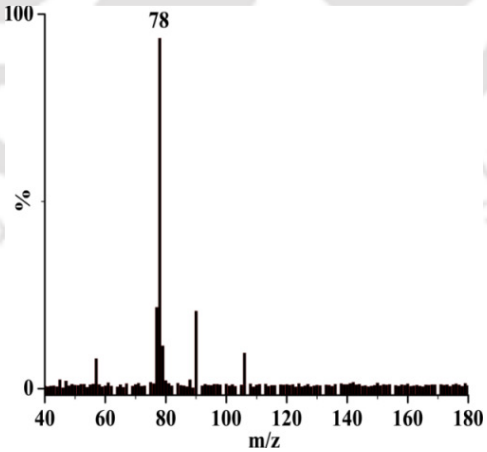

Figure A2.17. GC-mass spectrum of hexane wash of the reaction mixture of complexes **3.1/3.2** with DMS (retention time= 12.61 min).

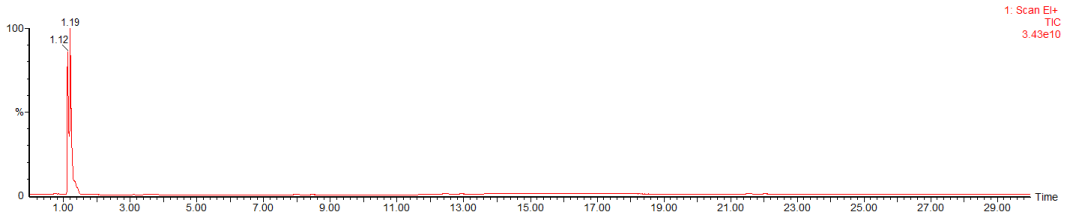

Figure A2.18. GC chromatograph of headspace gas of the reaction mixture of complexes **3.1/3.2** with DMS.

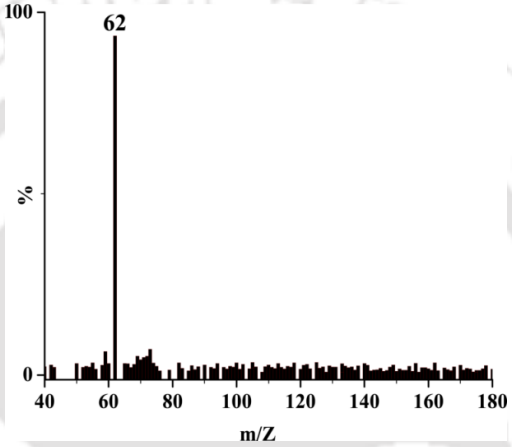

Figure A2.19. GC-mass spectrum of headspace gas of the reaction mixture of complexes **3.1/3.2** with DMS (retention time= 1.12 min).

Appendix III

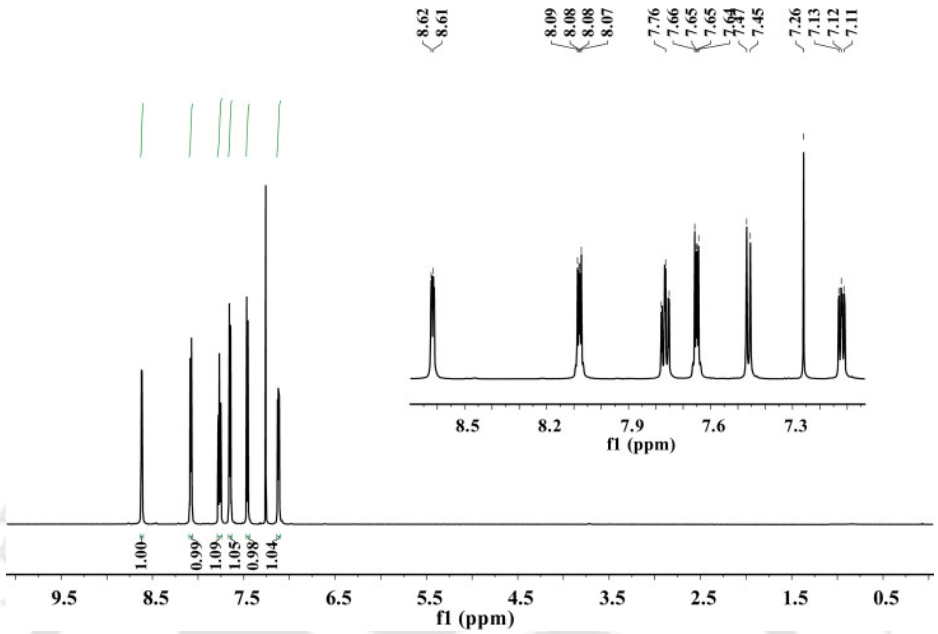

Figure A3.1. ^{1}H-NMR spectrum of ligand **L5H** in $CDCl_3$.

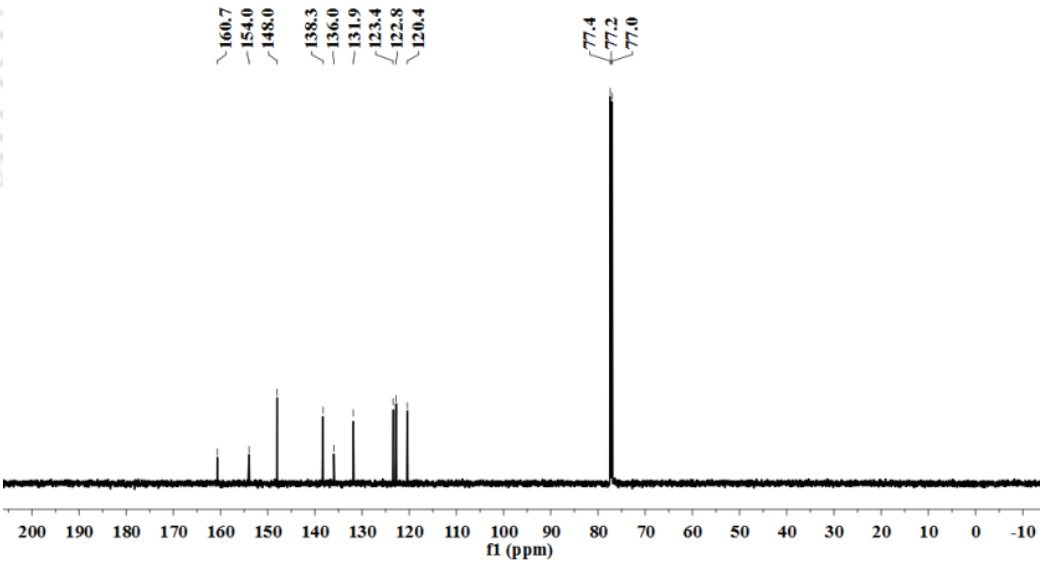

Figure A3.2. ^{13}C-NMR spectrum of ligand **L5H** in $CDCl_3$.

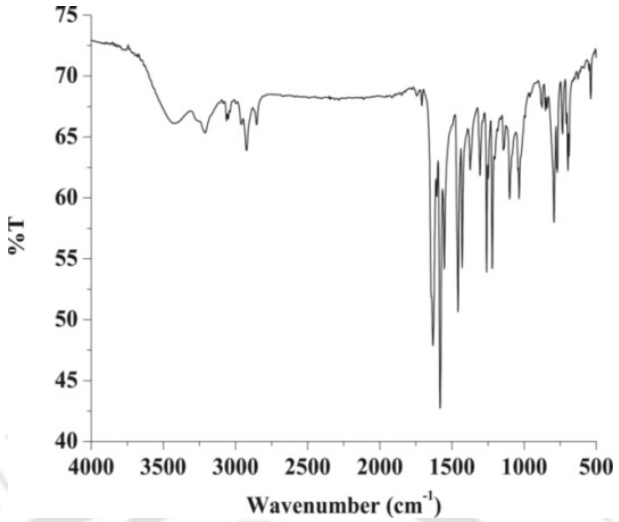

Figure A3.3. FT-IR spectrum of ligand **L5H** in KBr Pellet.

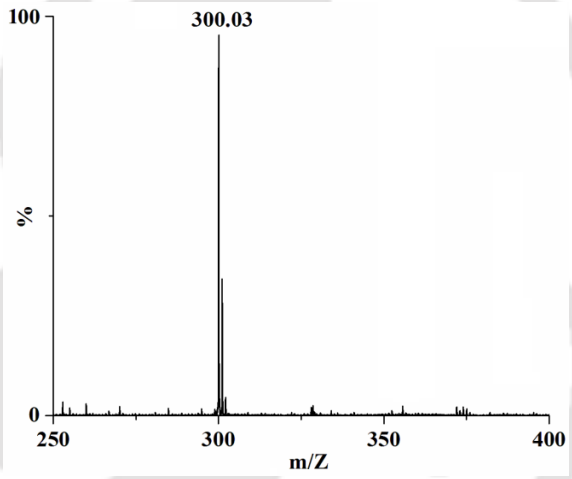

Figure A3.4. ESI-mass spectrum of ligand **L5H** in acetonitrile.

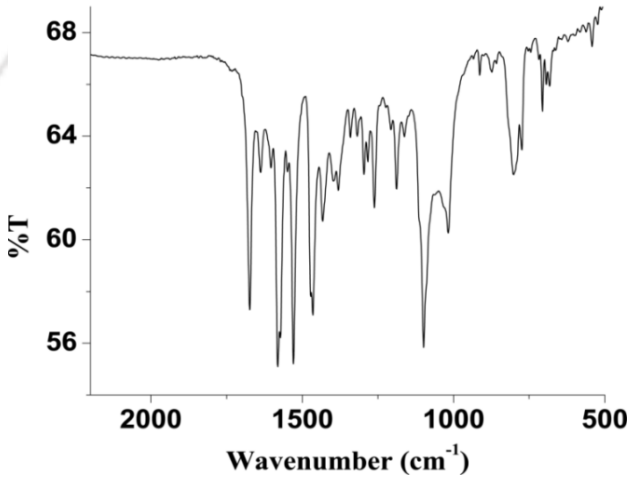

Figure A3.5. FT-IR spectrum of complex **4.1** in KBr pellet.

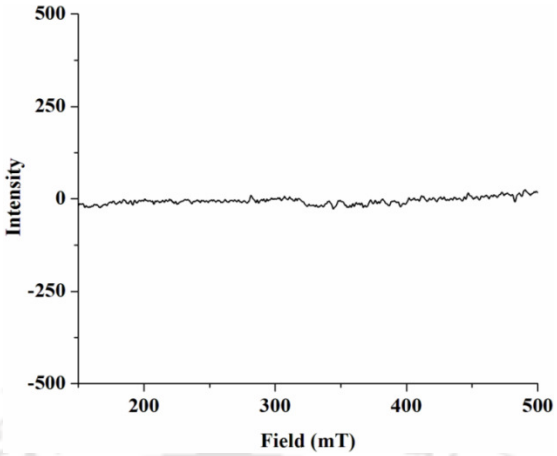

Figure A3.6. X-band EPR spectrum of complex **4.1** in CH_2Cl_2 at 77 K.

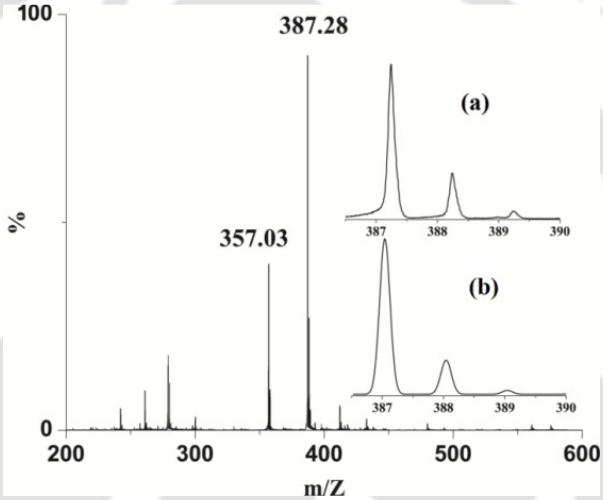

Figure A3.7. ESI-mass spectrum of complex **4.1** in acetonitrile. Inset (a) experimental and (b) simulated isotopic distribution pattern.

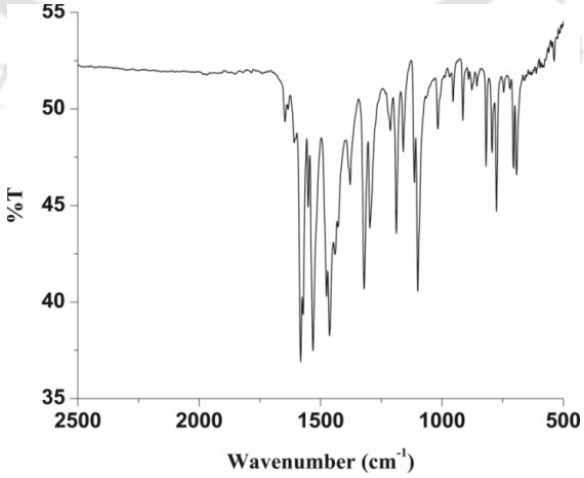

Figure A3.8. FT-IR spectrum of complex **4.2** in KBr pellet.

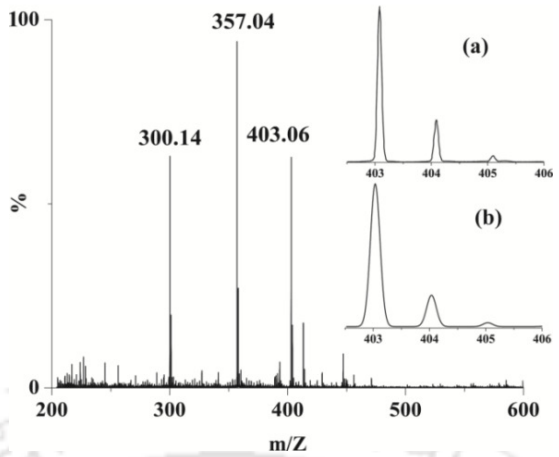

Figure A3.9. ESI-mass spectrum of complex **4.2** in acetonitrile. Inset (a) experimental and (b) simulated isotopic distribution pattern.

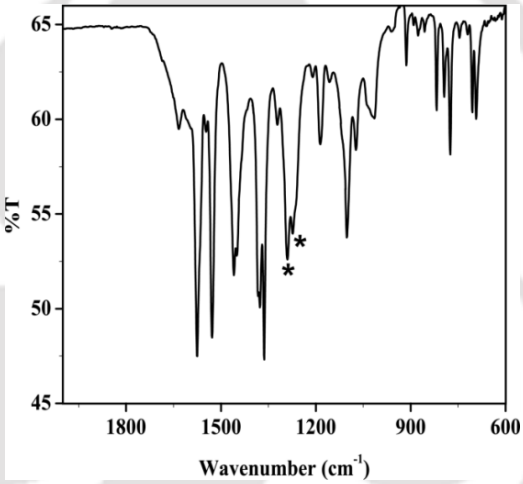

Figure A3.10. FT-IR spectrum of complex **4.1** after reaction with $^{18}O_2$ in KBr pellet (*N-O stretching frequencies for nitro group shifted to 1290 cm^{-1} and 1271 cm^{-1} from 1320 cm^{-1} and 1296 cm^{-1}).

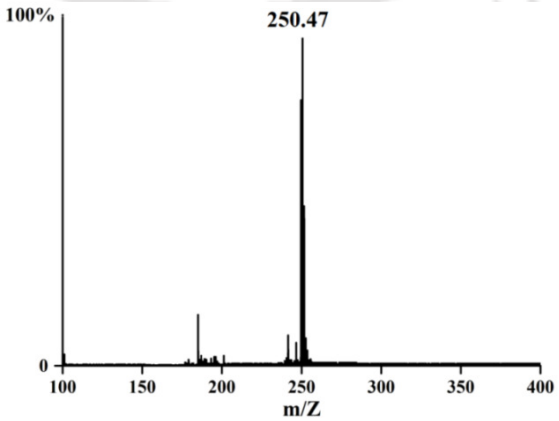

Figure A3.11. ESI-mass spectrum of 2,4-di-*tert*-butyl-6-nitrophenol in methanol.

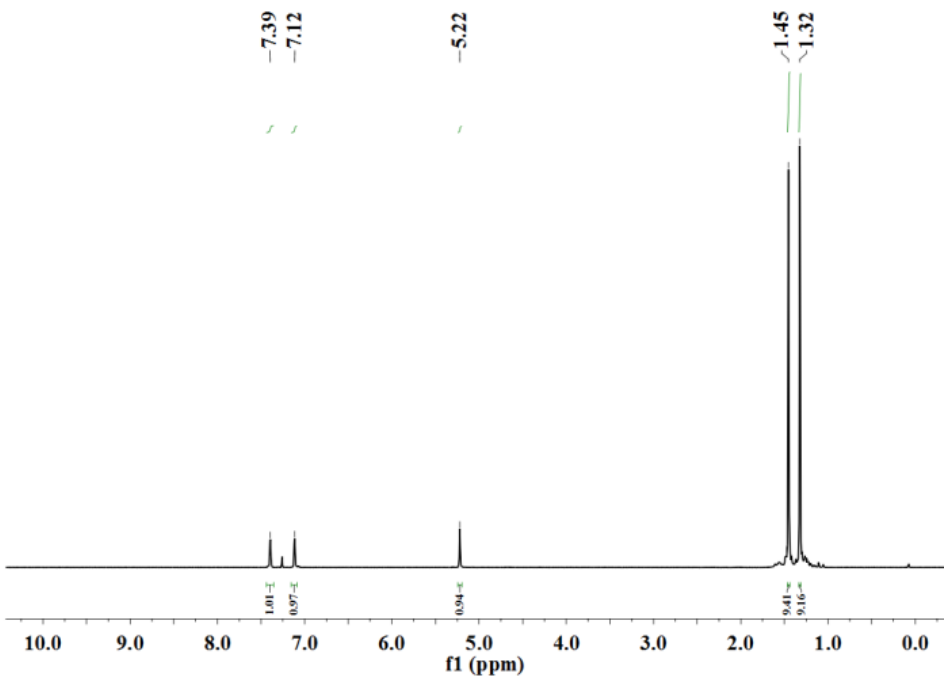

Figure A3.12. [1]H-NMR spectrum of 2,4-di-*tert*-butyl-6-nitrophenol in $CDCl_3$.

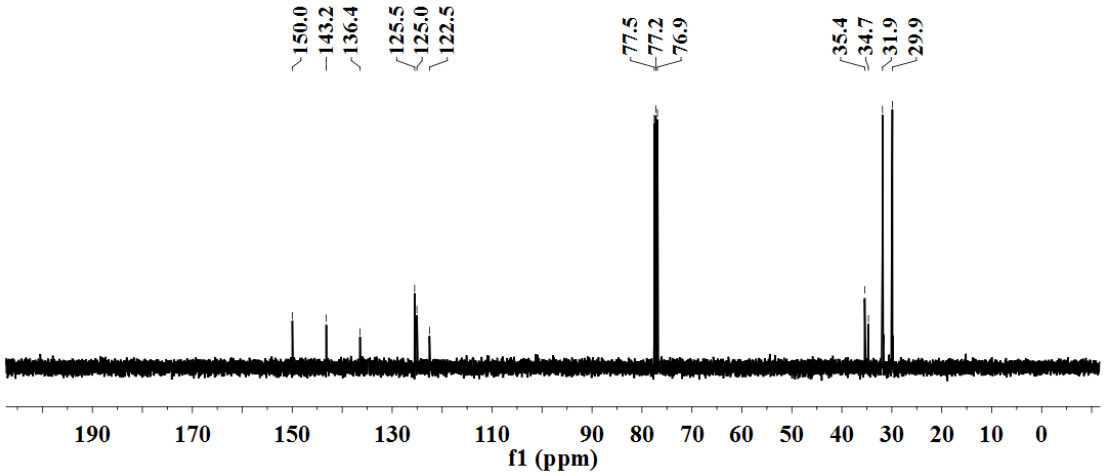

Figure A3.13. [13]C-NMR spectrum of 2,4-di-*tert*-butyl-6-nitrophenol in $CDCl_3$.

Appendix IV

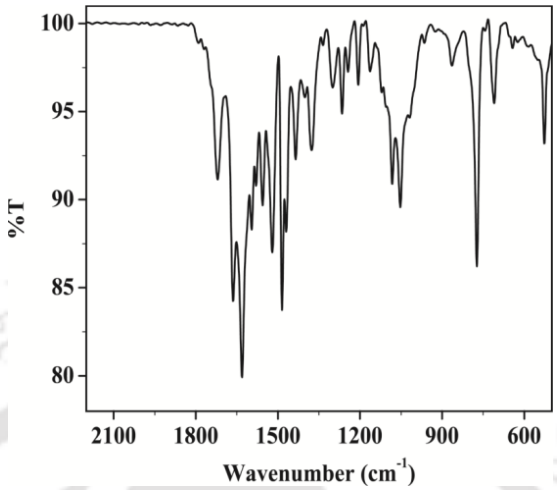

Figure A4.1. FT-IR spectrum of complex **5.1** in KBr pellet.

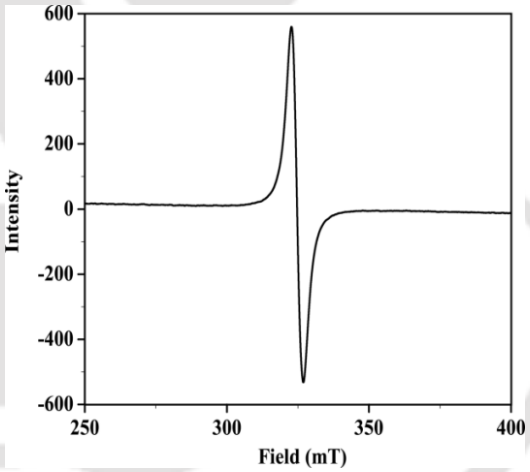

Figure A4.2. X-band EPR spectrum of complex **5.1** in CH_3CN/DMF at 77 K.

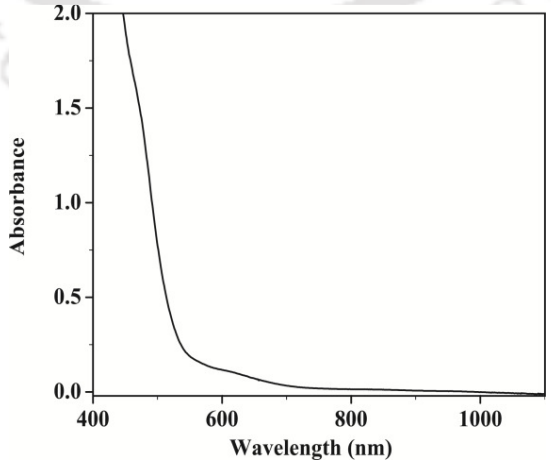

Figure A4.3. UV-visible spectrum of complex **5.1** in acetonitrile.

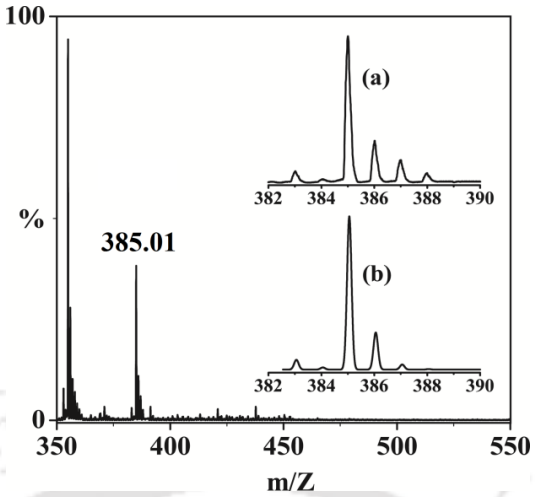

Fiugure A4.4. ESI-mass spectrum of complex **5.1** in CH_3OH. Inset shows (a) experimental and (b) simulated isotopic distribution patterns.

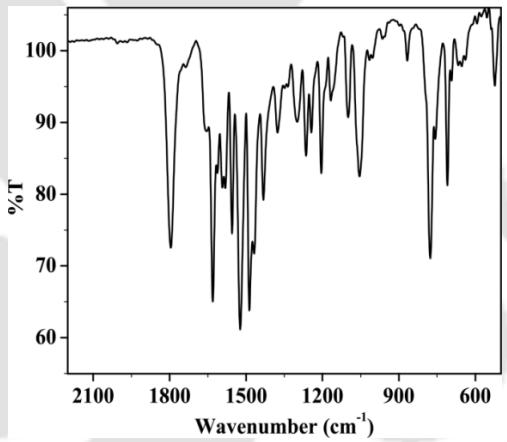

Figure A4.5. FT-IR spectrum of complex **5.2** in KBr pellet.

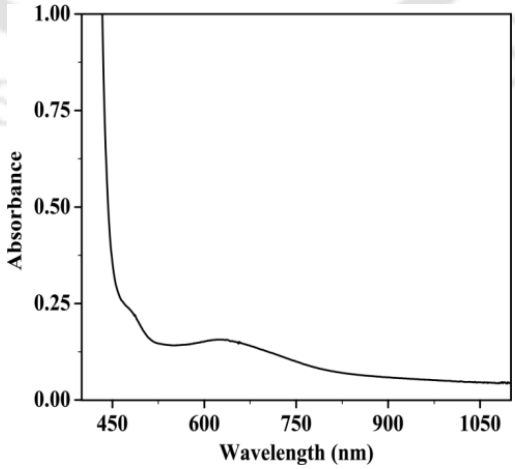

Figure A4.6. UV-visible spectrum of complex **5.2** in acetonitrile at -40 °C.

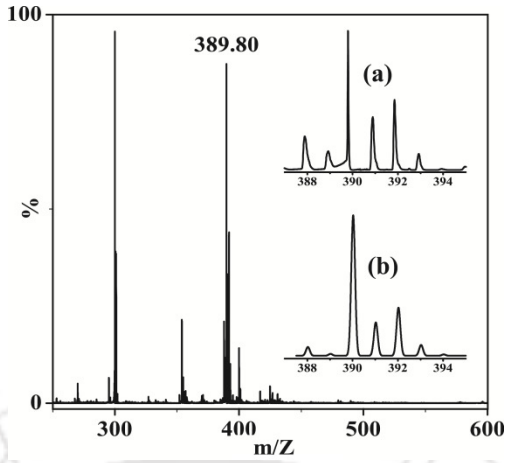

Fiugure A4.7. ESI-mass spectrum of complex **5.2** in $CH_3OH/CHCl_3$. Inset shows (a) experimental and (b) simulated isotopic distribution patterns.

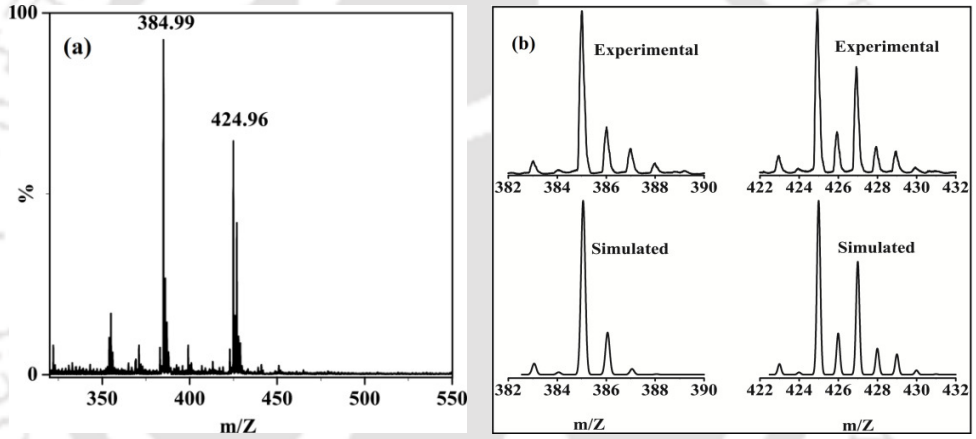

Fiugure A4.8. (a) ESI-mass spectrum of complex **5.2** after disproportionation in CH_3OH/CH_3CN. (b) Experimental and simulated isotopic distribution patterns.

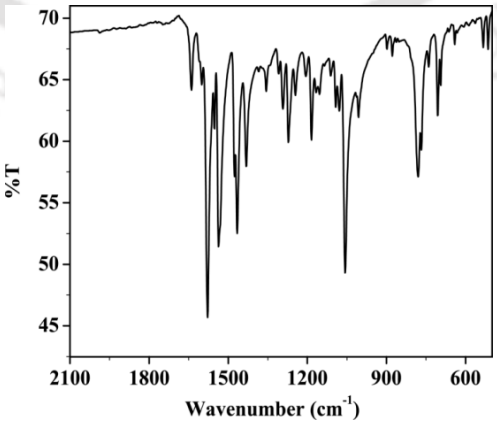

Figure A4.9. FT-IR spectrum of complex **5.3** in KBr pellet.

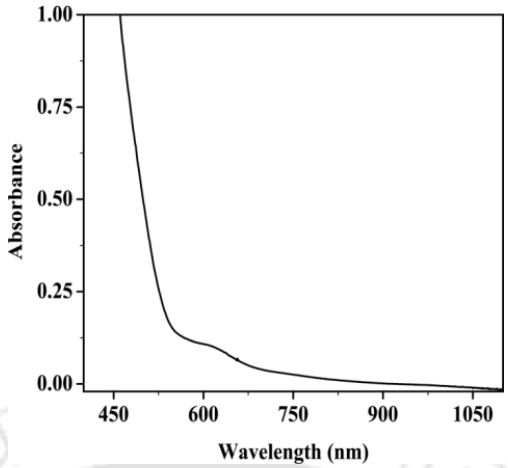

Figure A4.10. UV-visible spectrum of complex **5.3** in CH_3CN.

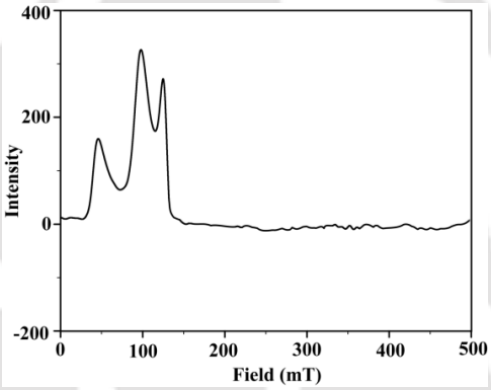

Figure A4.11. X-band EPR spectrum of complex **5.3** in CH_3CN/DMF at 77 K.

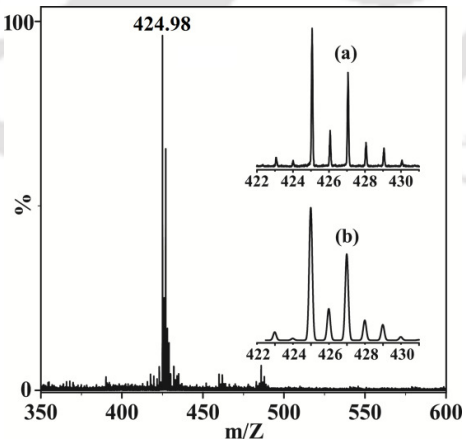

Fiugure A4.12. ESI-mass spectrum of complex **5.3** in $CH_3OH/CHCl_3$. Inset shows (a) experimental and (b) simulated isotopic distribution patterns.

List of Publications

(1) "Oxo transfer from nitrogen dioxide to nitrito group in a copper(II) complex"

Gogoi, K.; Deka, H.; Kumar, V.; Mondal, B. *Inorg. Chem*. **2015**, *54*, 4799.

(2) "Reductive nitrosylation of nickel(II) complex by nitric oxide followed by nitrous oxide release"

Ghosh, S.; Deka, H.; Dangat, Y. B.; Saha, S.; Gogoi, K.; Vanka, K.; Mondal, B. *Dalton Trans.* **2016**, *45*, 10200.

(3) "Effect of ligand denticity on the nitric oxide reactivity of cobalt(II) complexes"

Deka, H.; Ghosh, S.; Saha, S.; Gogoi, K.; Mondal, B. *Dalton Trans.* **2016**, *45*, 10979.

(4) **"**Nitric oxide reactivity of a Cu(II) complex of an imidazole based ligand: Aromatic C-nitrosation followed by the formation of N-nitrosohydroxylaminato complex"

Deka, H.; Ghosh, S.; Gogoi, K.; Saha, S.; Mondal, B. *Inorg. Chem.* **2017**, *56*, 5034.

(5) "Reaction of a nitrosyl complex of cobalt-porphyrin with hydrogen peroxide: Putative formation of peroxynitrite intermediate"

Saha, S.; Gogoi, K.; Mondal, B.; Ghosh, S.; Deka, H.; Mondal, B. *Inorg. Chem.* **2017**, *56,* 7781.

(6) "Reaction of a Co(III)-peroxo complex and NO: Formation of a putative peroxynitrite intermediate"

Saha, S.; Ghosh, S.; Gogoi, K.; Deka, H.; Mondal, B.; Mondal, B. *Inorg. Chem.* **2017**, *56*, 10932.

(7) "Dioxygenation reaction of a cobalt-nitrosyl: Putative formation of a cobalt–peroxynitrite via a $\{Co^{III}(NO)(O_2^-)\}$ intermediate"

Gogoi, K.; Saha, S.; Ghosh, S.; Deka, H.; Mondal, B.; Mondal, B. *Inorg. Chem.* **2017**, *56*, 14438.

(8) "Nitric oxide reactivity of Cu(II) complex of N- donor ligand: Formation of a stable nitrous oxide complex"

Deka, H.; Dangat, Y. B.; Saha, S.; Gogoi, K.; Vanka, K.; Mondal, B. *Inorg. Chem.* (Under revision).

(9) "Disproportionation of a $\{FeNO\}^7$ species into $\{Fe(NO)_2\}^9$ and ferric complex"

Gogoi, K.; Boro, M.; Saha, S.; Mondal, B. (Communicated).

(10) "Oxo Transfer Reaction in Cobalt(III)-nitro Complexes"

Gogoi, K.; Saha, S.; Mondal, B. (Communicated).

(11) "Reductive nitrosylation of cobalt(II) complex by nitric oxide followed by release of nitrous oxide"

Saha, S.; Gogoi, K.; Mondal, B. (Communicated)